

Probing H_0 and resolving AGN disks with ultrafast photon counters



Marios Galanis

Perimeter Institute

Based on [PhysRevD.109.123029](#), arXiv:[2403.15903](#)

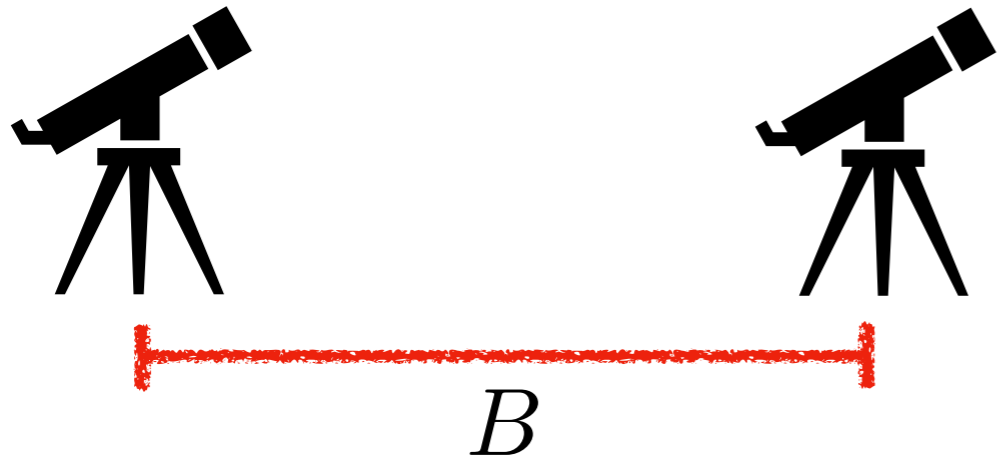
with Neal Dalal (PI),

Charles Gammie (UIUC), Sam Gralla (University of Arizona), Norm Murray (CITA)

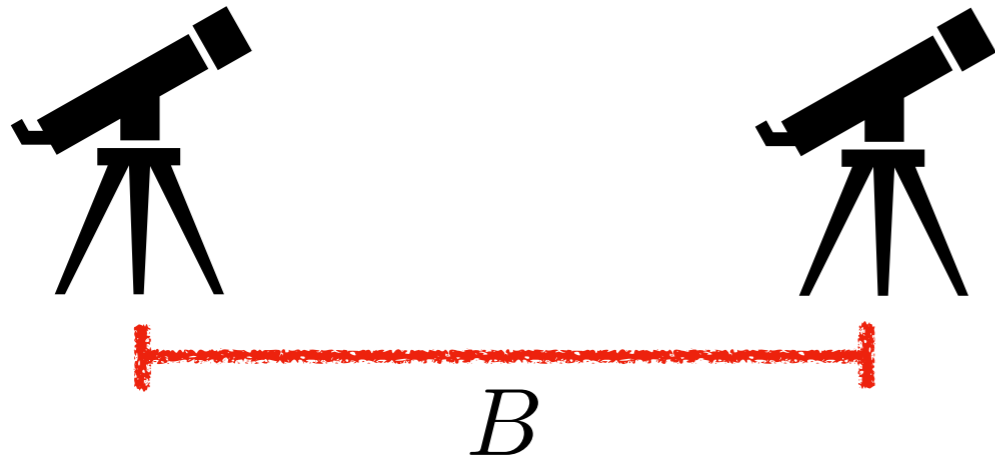
Xmas Theoretical Physics Workshop @Athens - December 18, 2024

Michelson Interferometry

Michelson Interferometry

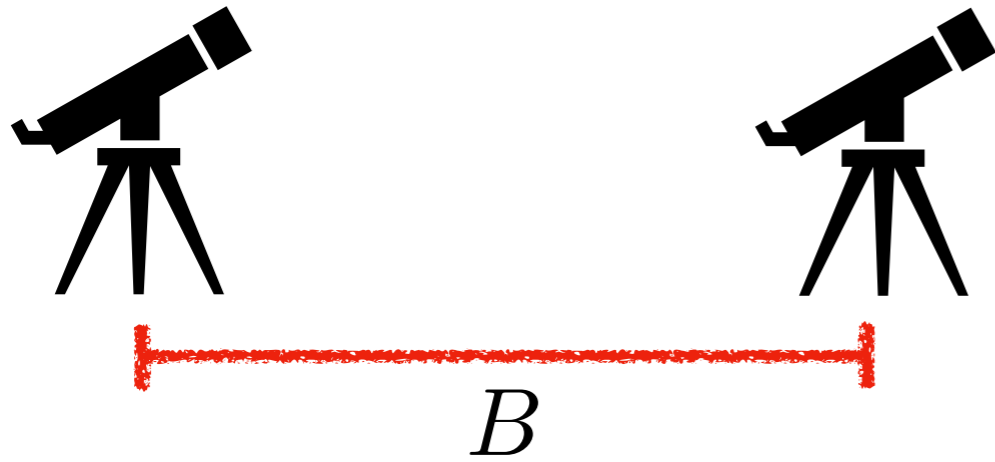


Michelson Interferometry

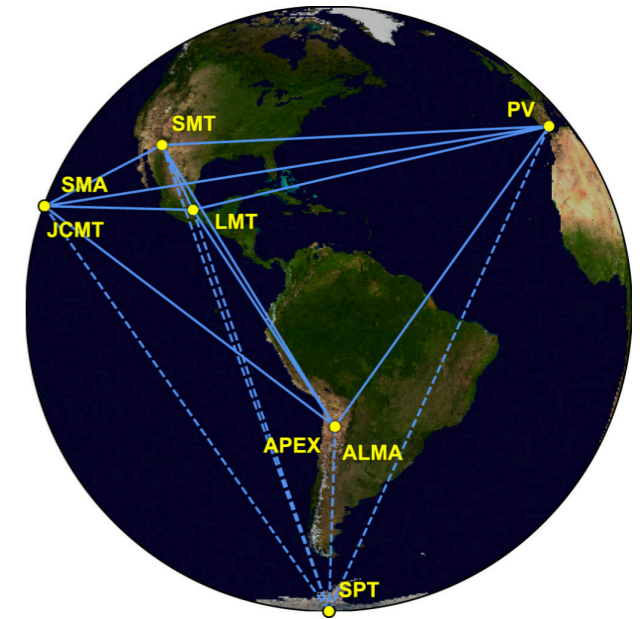


$$\text{Resolution} \approx \frac{\lambda}{B}$$

Michelson Interferometry



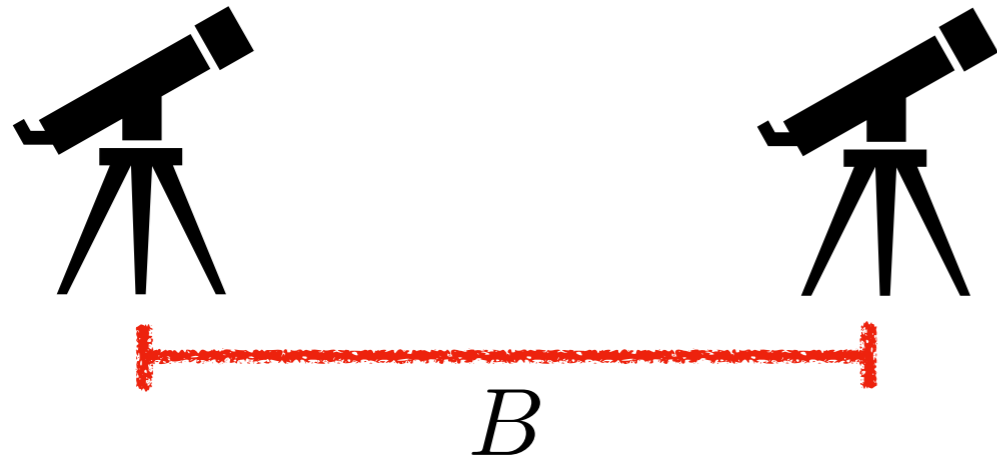
$$\text{Resolution} \approx \frac{\lambda}{B} \approx \frac{3\text{mm}}{25,000\text{km}}$$



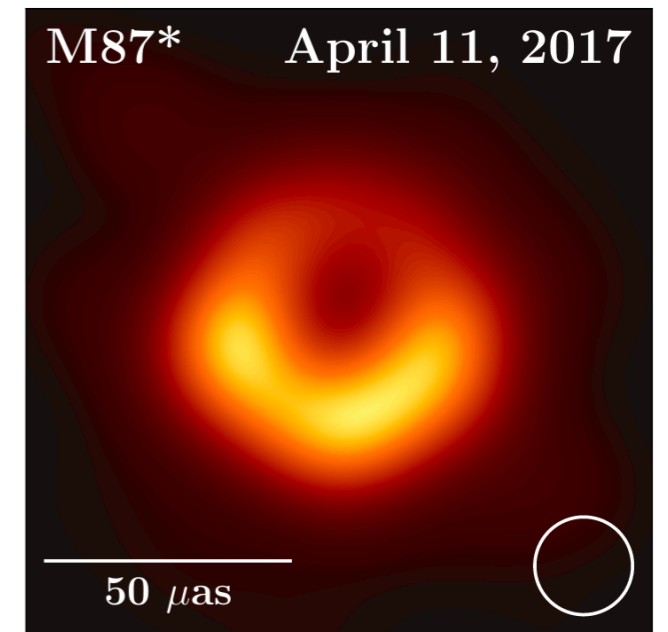
Event Horizon Telescope

$$\sigma_{\theta_{\text{res}}} \approx 30 \mu\text{as}$$

Michelson Interferometry



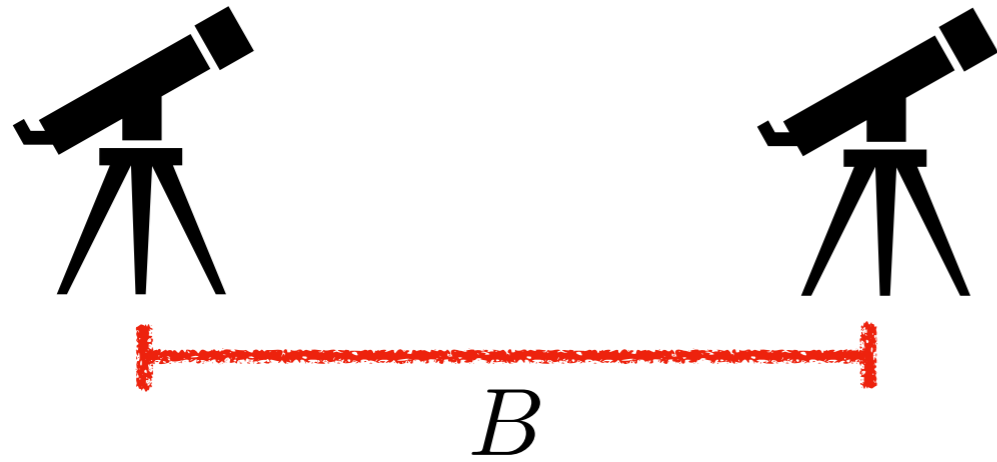
$$\text{Resolution} \approx \frac{\lambda}{B} \approx \frac{3\text{mm}}{25,000\text{km}}$$



Event Horizon Telescope

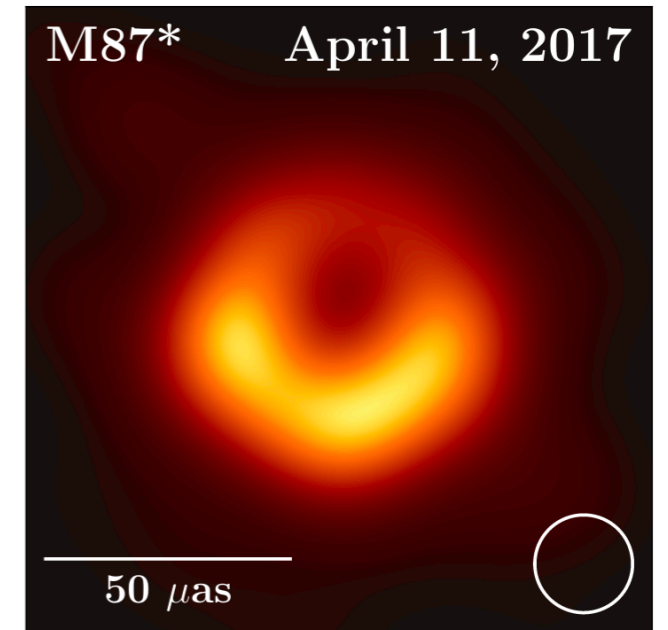
$$\sigma_{\theta_{\text{res}}} \approx 30 \mu\text{as}$$

Michelson Interferometry



$$\text{Resolution} \approx \frac{\lambda}{B} \approx \frac{3\text{mm}}{25,000\text{km}}$$

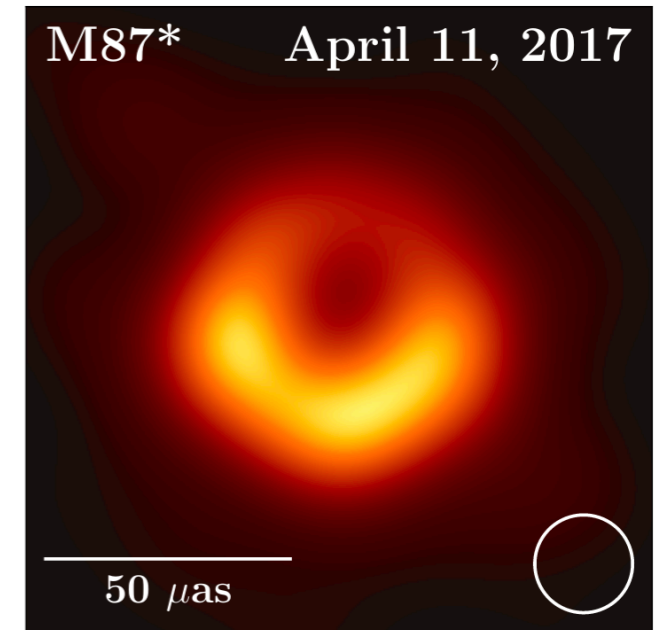
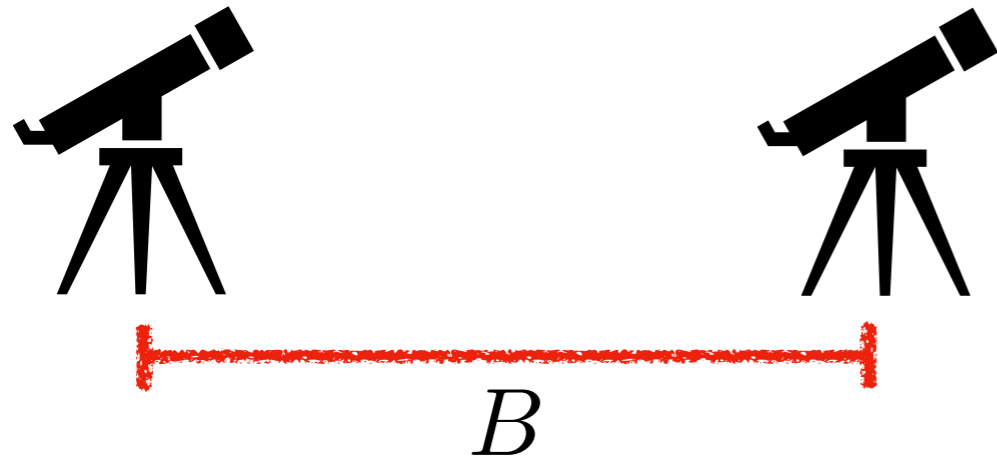
$$\text{Visibility} \sim \langle E_1 E_2^* \rangle \sim \text{FT} \left[\text{Image} \right]$$



Event Horizon Telescope

$$\sigma_{\theta_{\text{res}}} \approx 30 \mu\text{as}$$

Michelson Interferometry



Event Horizon Telescope

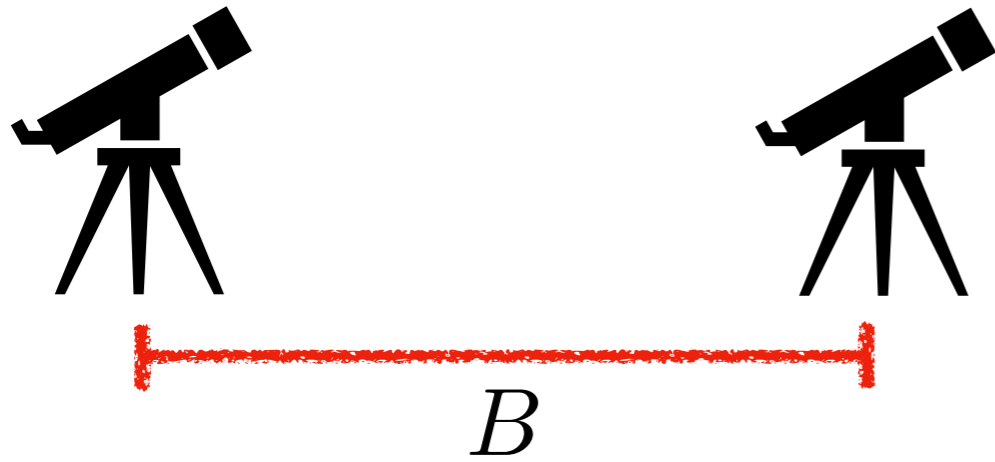
$$\sigma_{\theta_{\text{res}}} \approx 30 \mu\text{as}$$

$$\text{Resolution} \approx \frac{\lambda}{B} \approx \frac{3\text{mm}}{25,000\text{km}}$$

$$\text{Visibility} \sim \langle E_1 E_2^* \rangle \sim \text{FT} \left[\text{Image} \right]$$

Van Cittert-Zernike Theorem

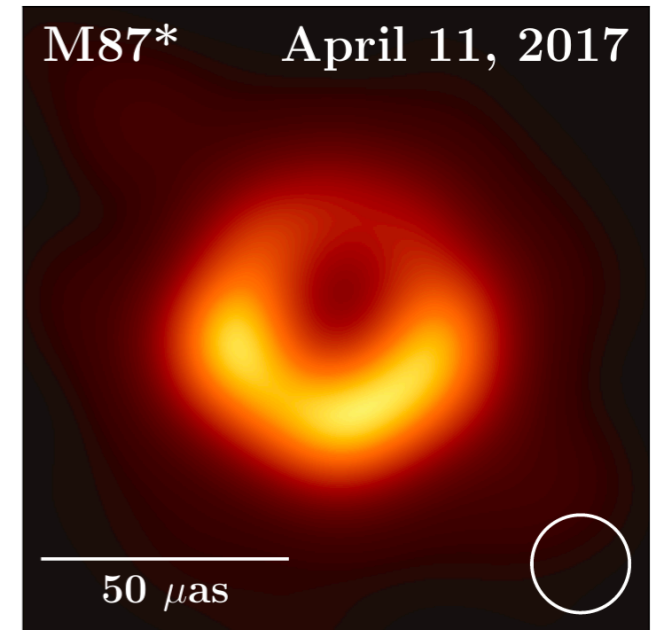
Michelson Interferometry



$$\text{Resolution} \approx \frac{\lambda}{B} \approx \frac{0.5 \mu\text{m}}{300\text{m}}$$

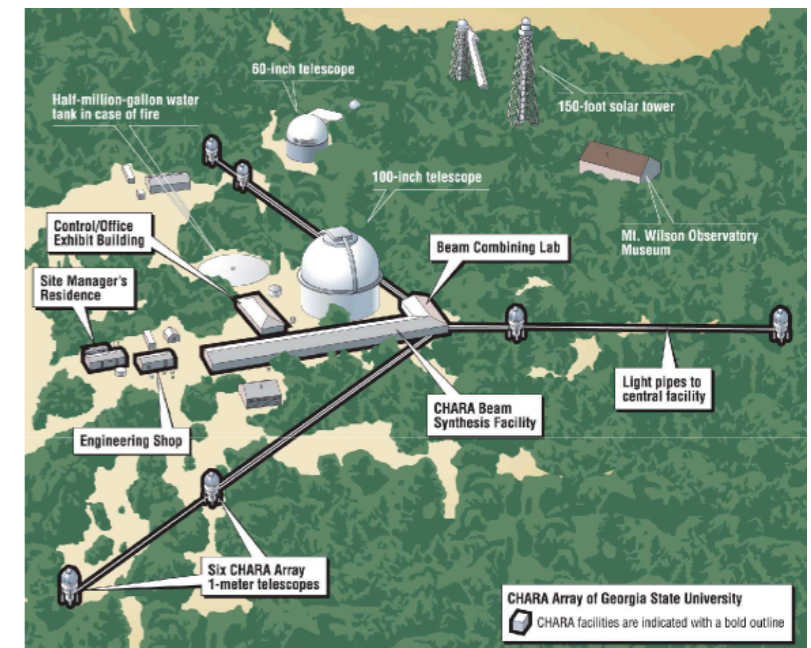
$$\text{Visibility} \sim \langle E_1 E_2^* \rangle \sim \text{FT} \left[\text{Image} \right]$$

Van Cittert-Zernike Theorem



Event Horizon Telescope

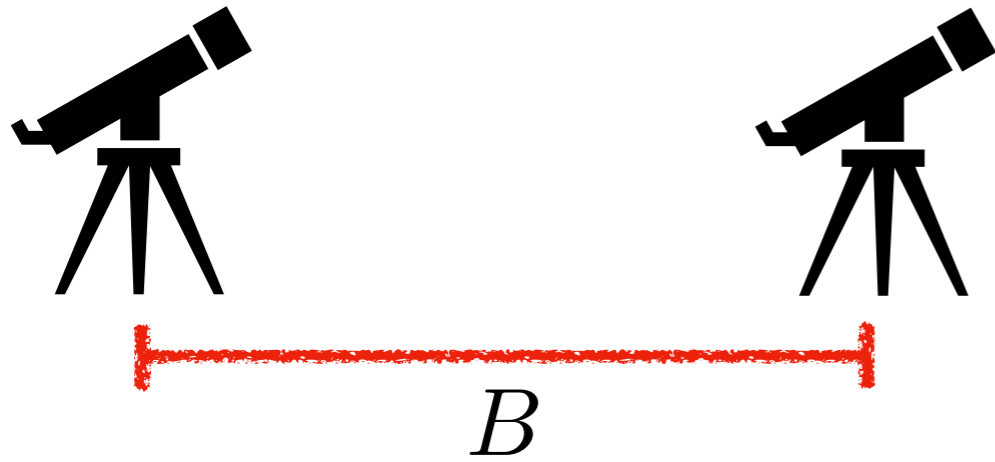
$$\sigma_{\theta_{\text{res}}} \approx 30 \mu\text{as}$$



CHARA array

$$\sigma_{\theta_{\text{res}}} \approx 200 \mu\text{as}$$

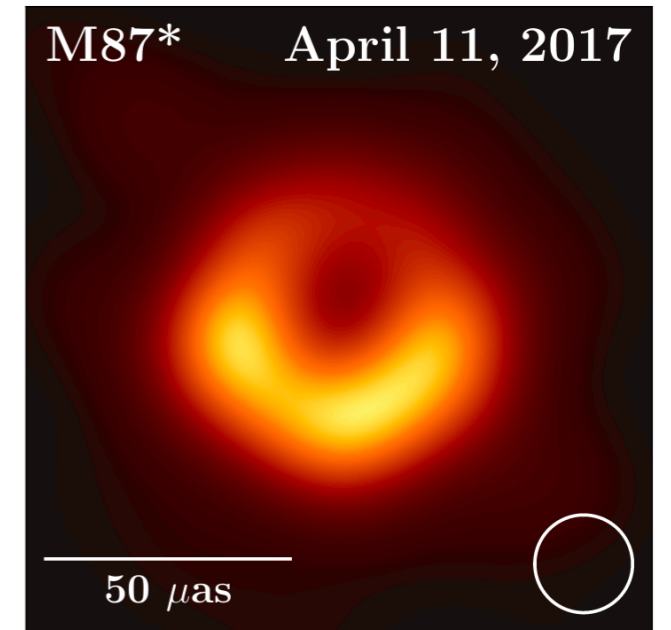
Michelson Interferometry



$$\text{Resolution} \approx \frac{\lambda}{B} \approx \frac{0.5 \mu\text{m}}{300\text{m}}$$

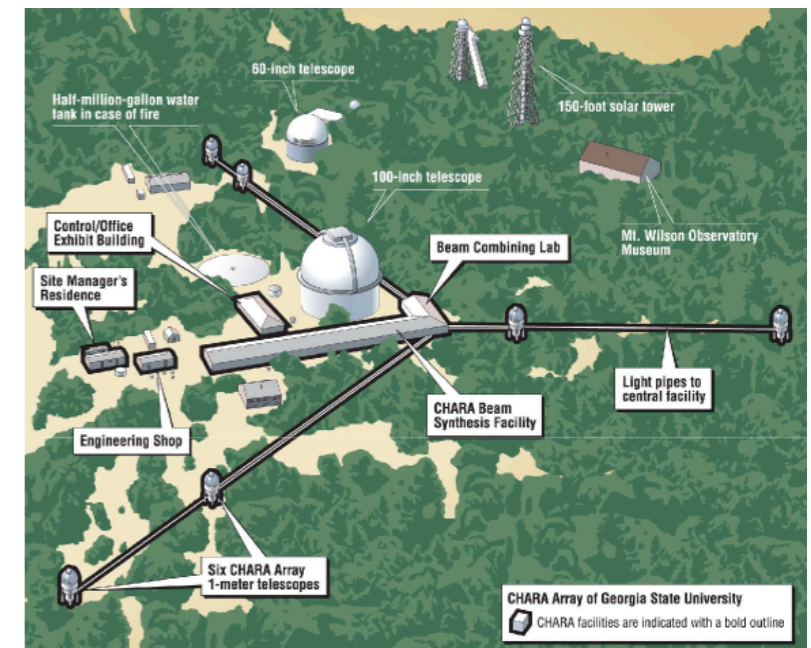
$$\text{Visibility} \sim \langle E_1 E_2^* \rangle \sim \text{FT} \left[\text{Image} \right]$$

Van Cittert-Zernike Theorem



Event Horizon Telescope

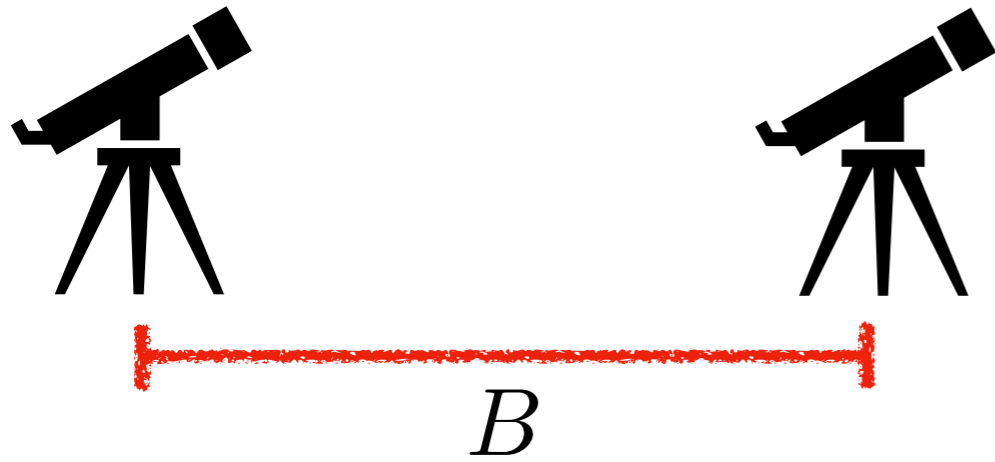
$$\sigma_{\theta_{\text{res}}} \approx 30 \mu\text{as}$$



CHARA array

$$\sigma_{\theta_{\text{res}}} \approx 200 \mu\text{as}$$

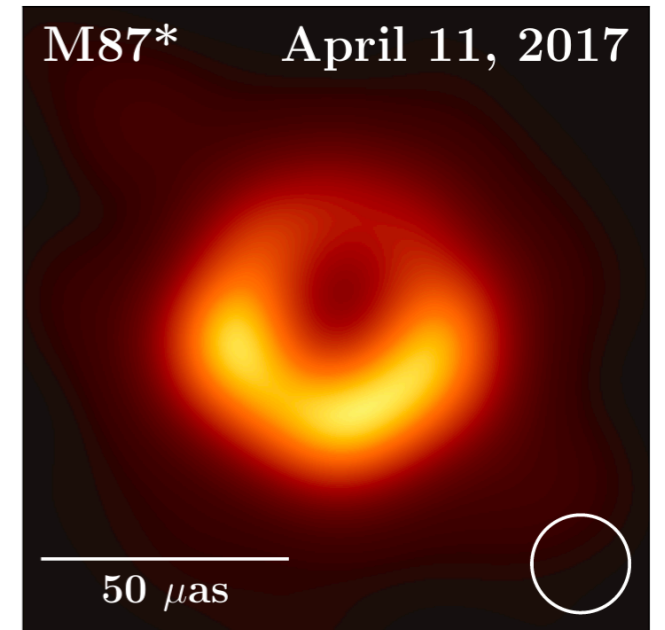
Michelson Interferometry



$$\text{Resolution} \approx \frac{\lambda}{B} \approx \frac{0.5 \mu\text{m}}{25,000 \text{km}} ?$$

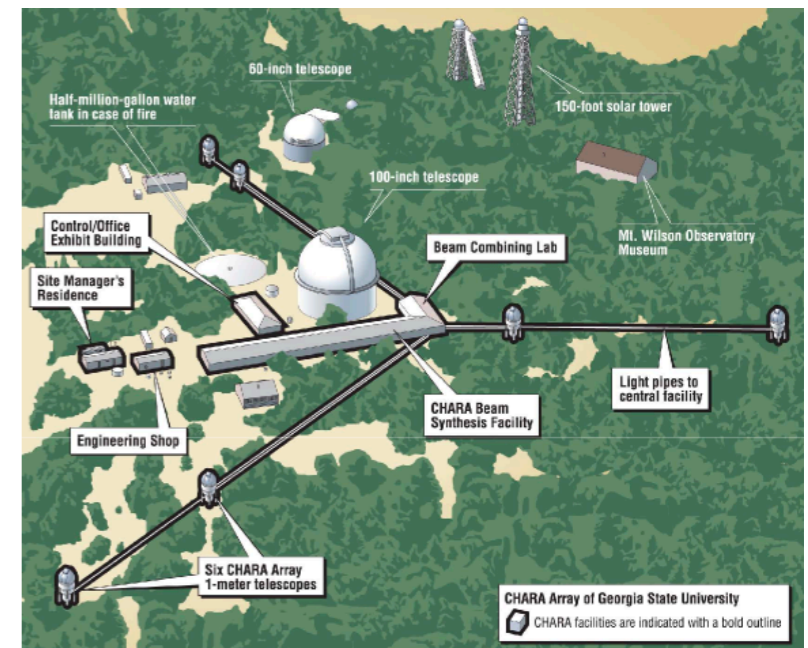
$$\text{Visibility} \sim \langle E_1 E_2^* \rangle \sim \text{FT} \left[\text{Image} \right]$$

Van Cittert-Zernike Theorem



Event Horizon Telescope

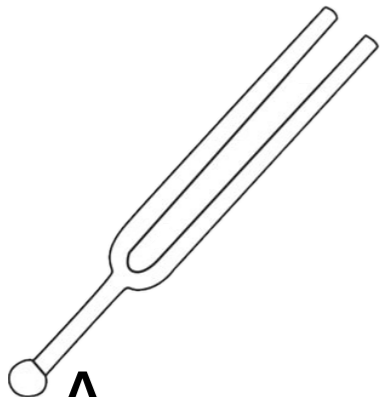
$$\sigma_{\theta_{\text{res}}} \approx 30 \mu\text{as}$$



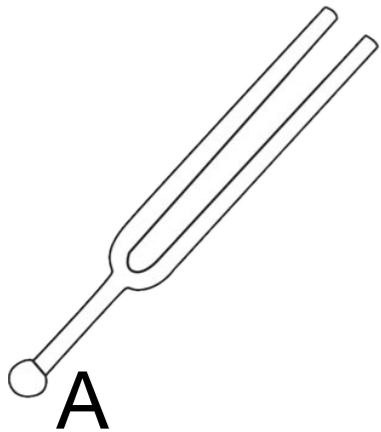
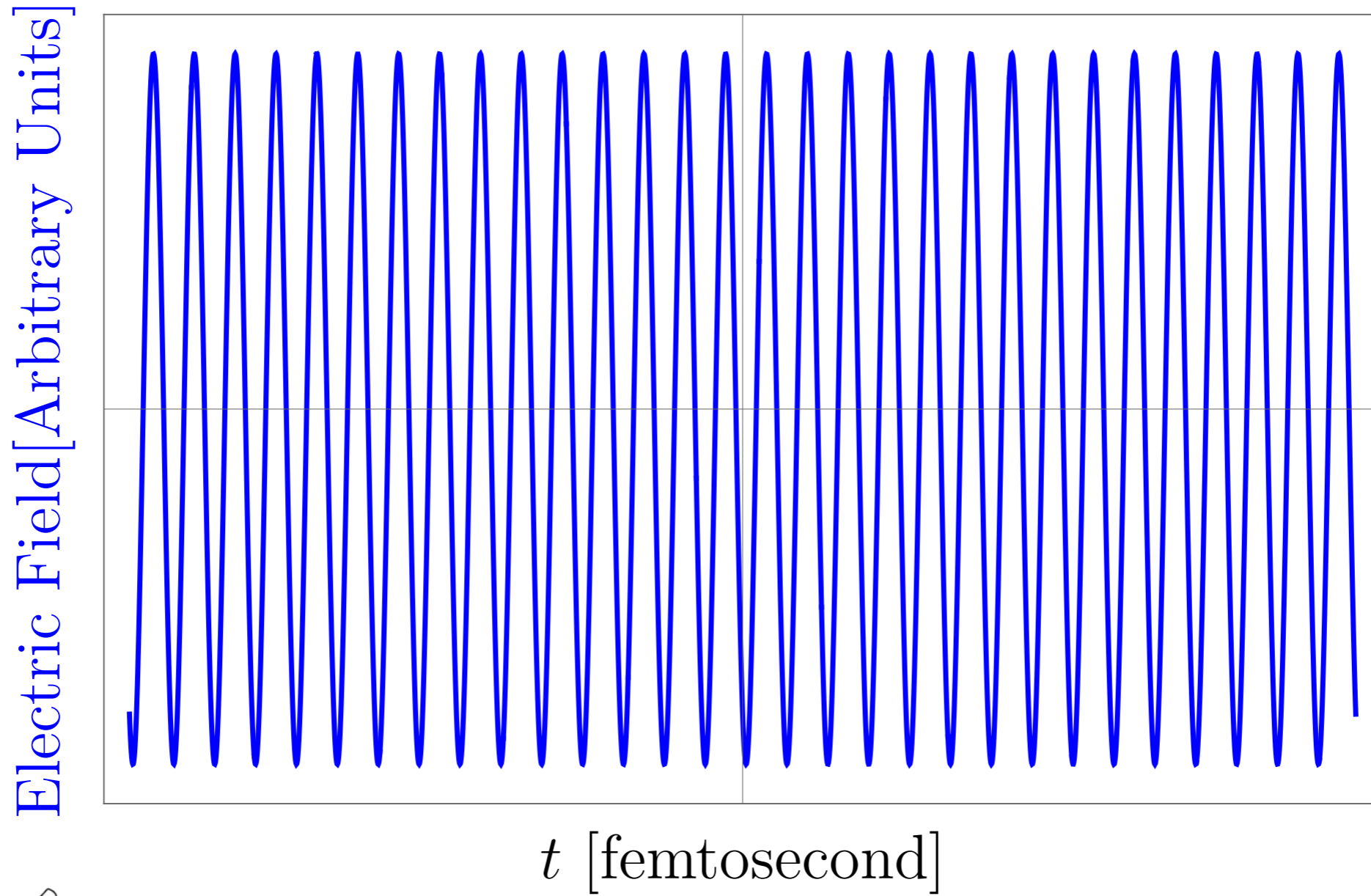
CHARA array

$$\sigma_{\theta_{\text{res}}} \approx 200 \mu\text{as}$$

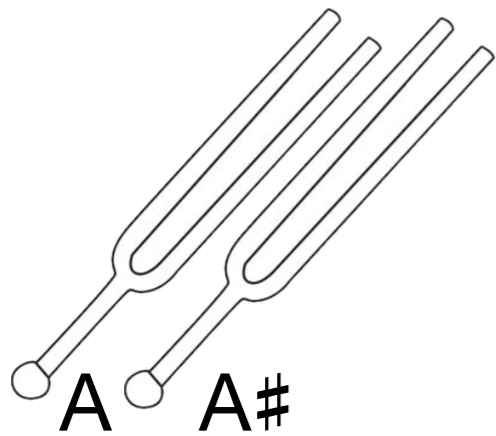
Hanbury Brown and Twiss effect



Hanbury Brown and Twiss effect

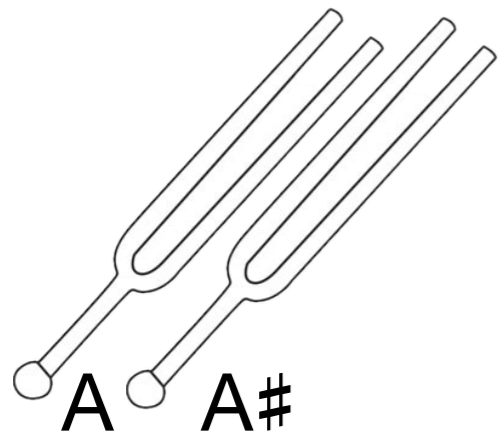
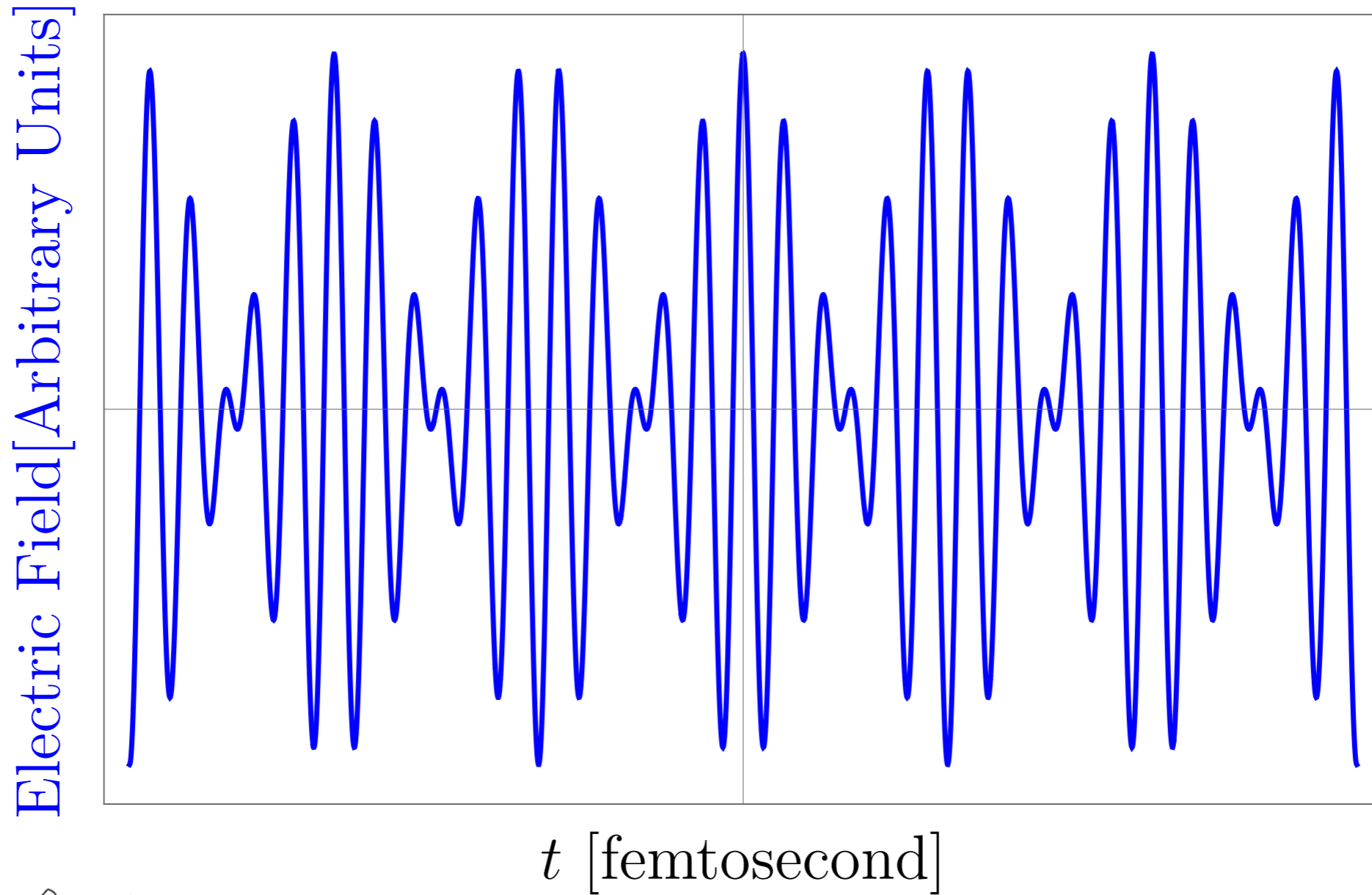


Hanbury Brown and Twiss effect



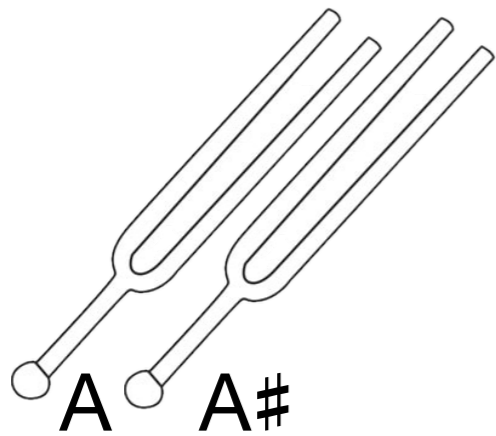
Two sine waves, slightly detuned

Hanbury Brown and Twiss effect

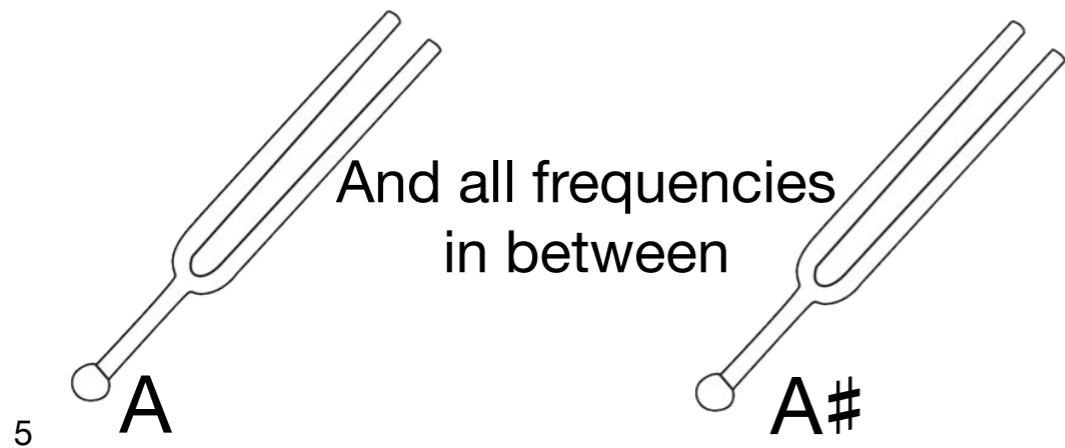


Two sine waves, slightly detuned

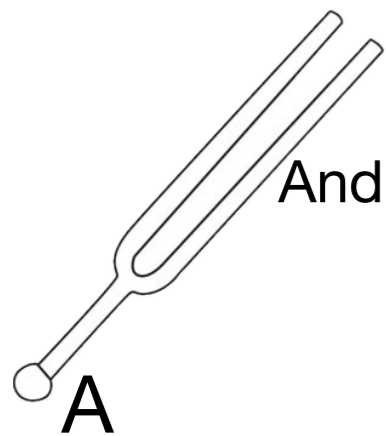
Hanbury Brown and Twiss effect



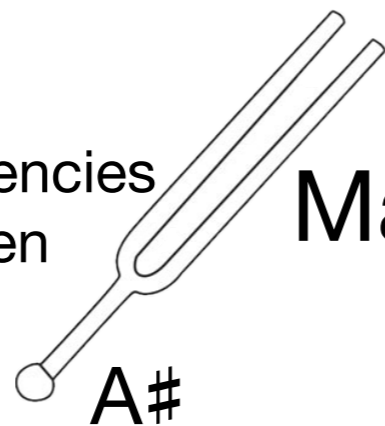
Hanbury Brown and Twiss effect



Hanbury Brown and Twiss effect

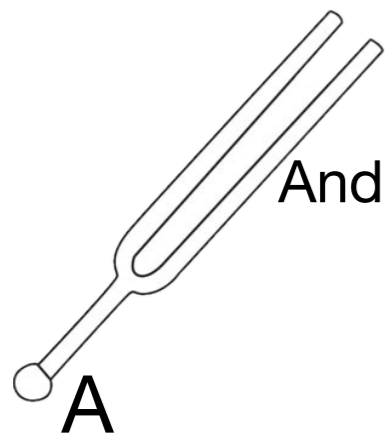
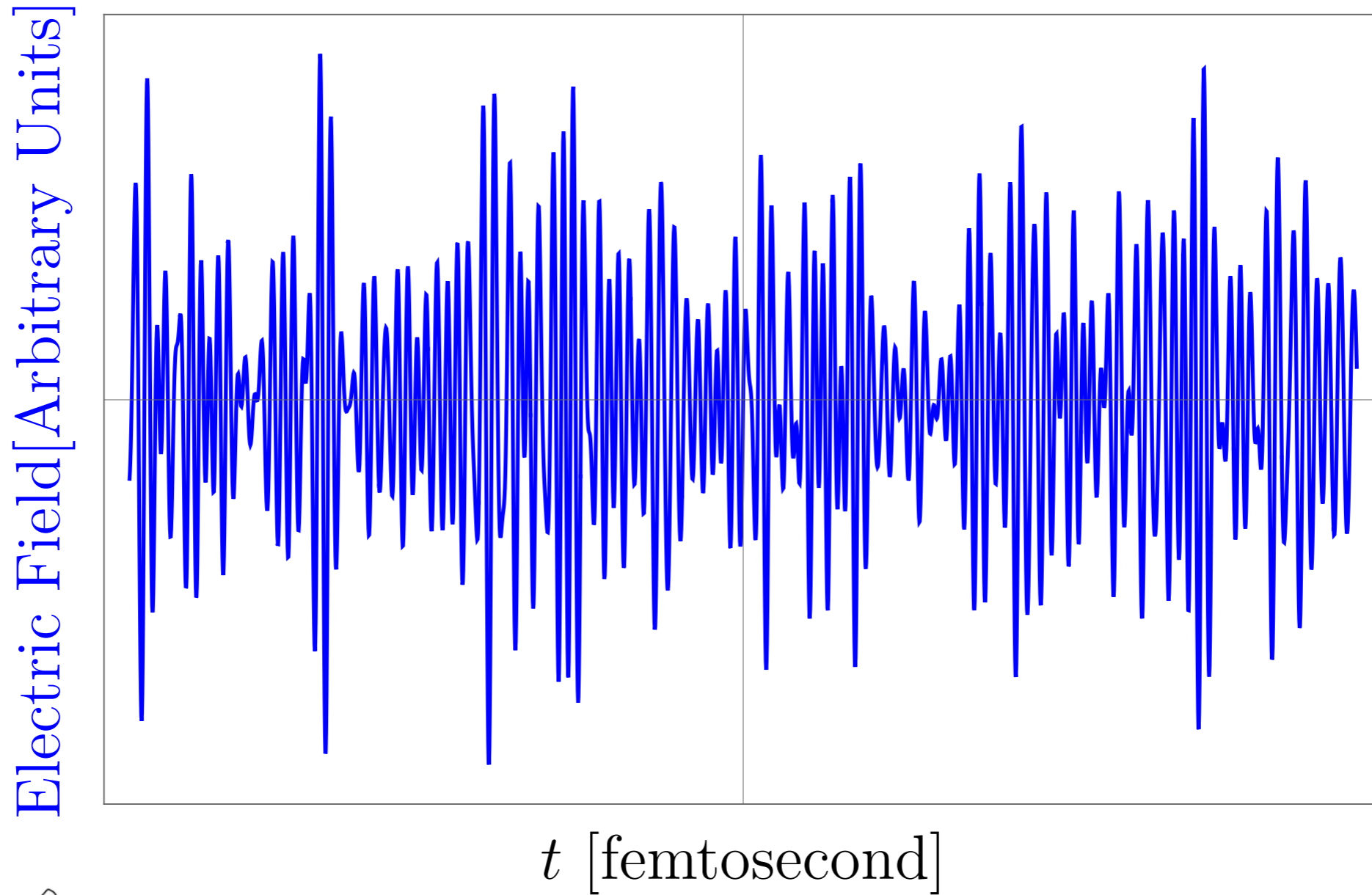


And all frequencies
in between

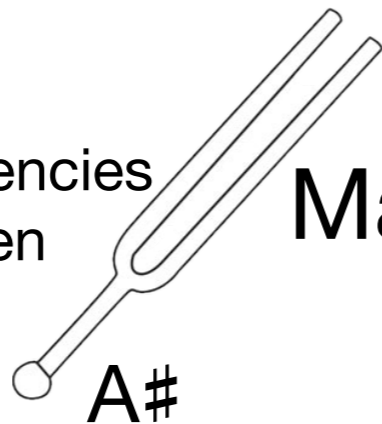


Many sine waves

Hanbury Brown and Twiss effect

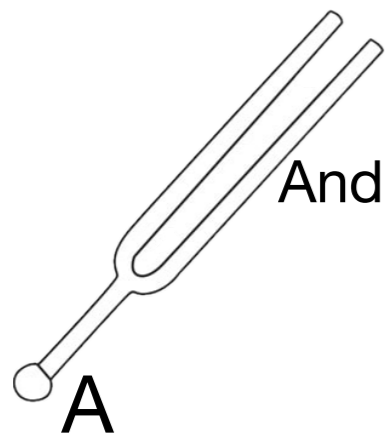
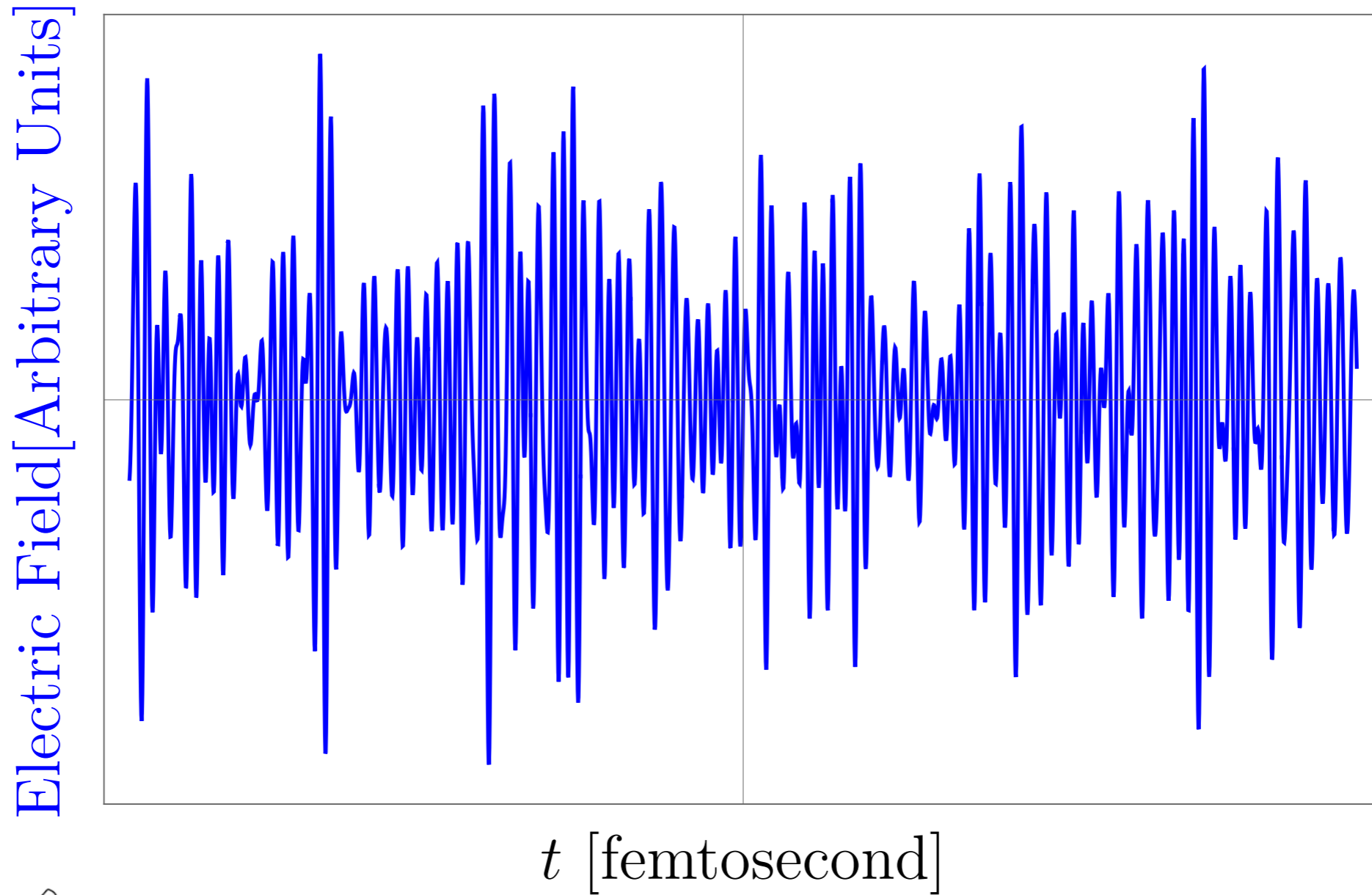


And all frequencies
in between

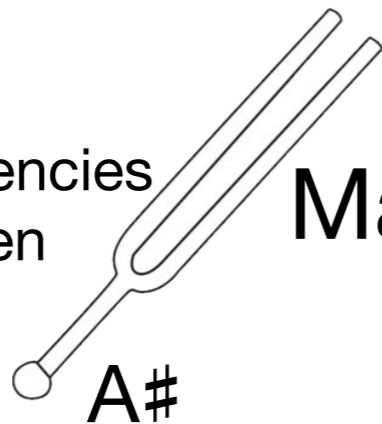


Many sine waves

Hanbury Brown and Twiss effect



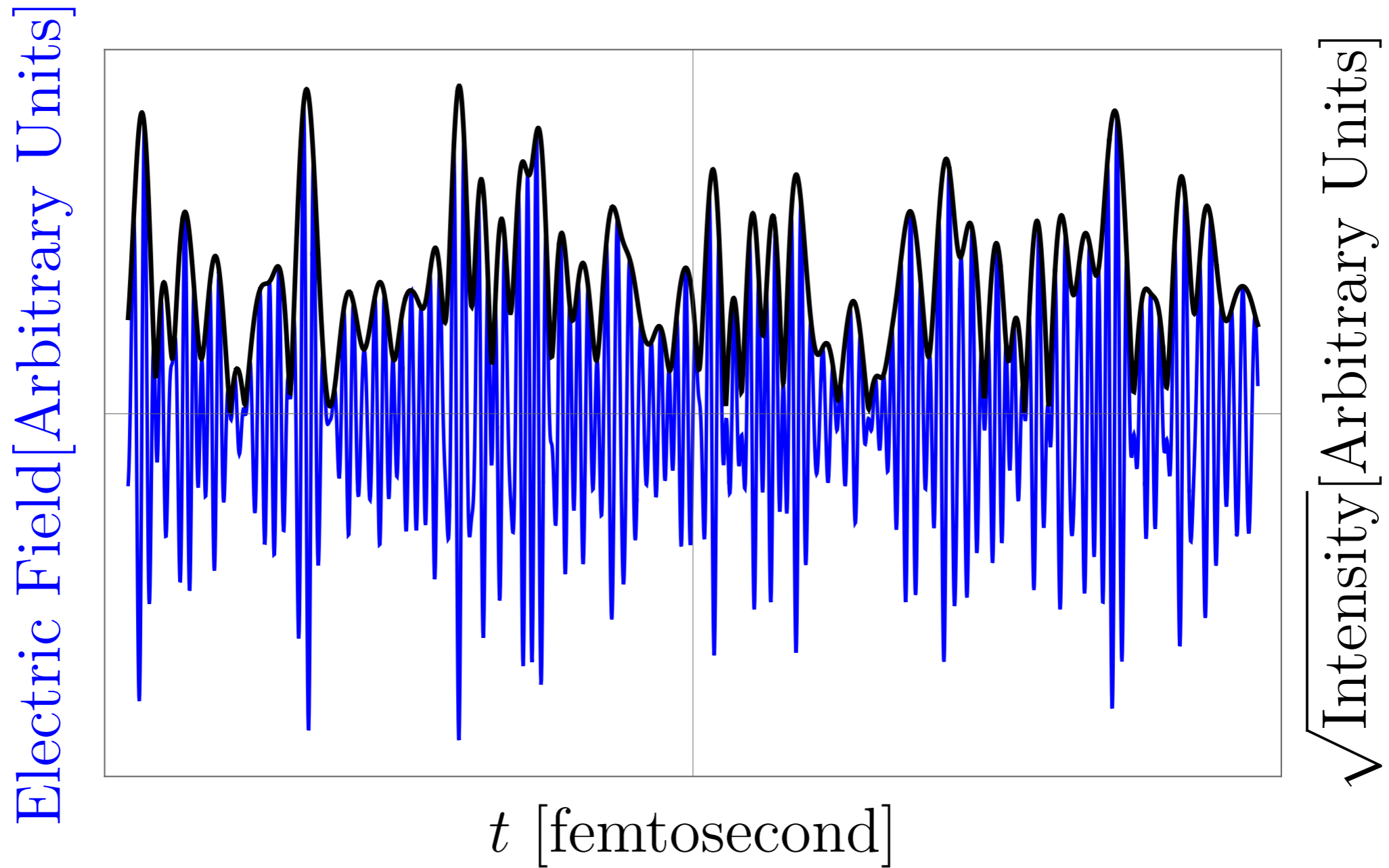
And all frequencies
in between



Many sine waves

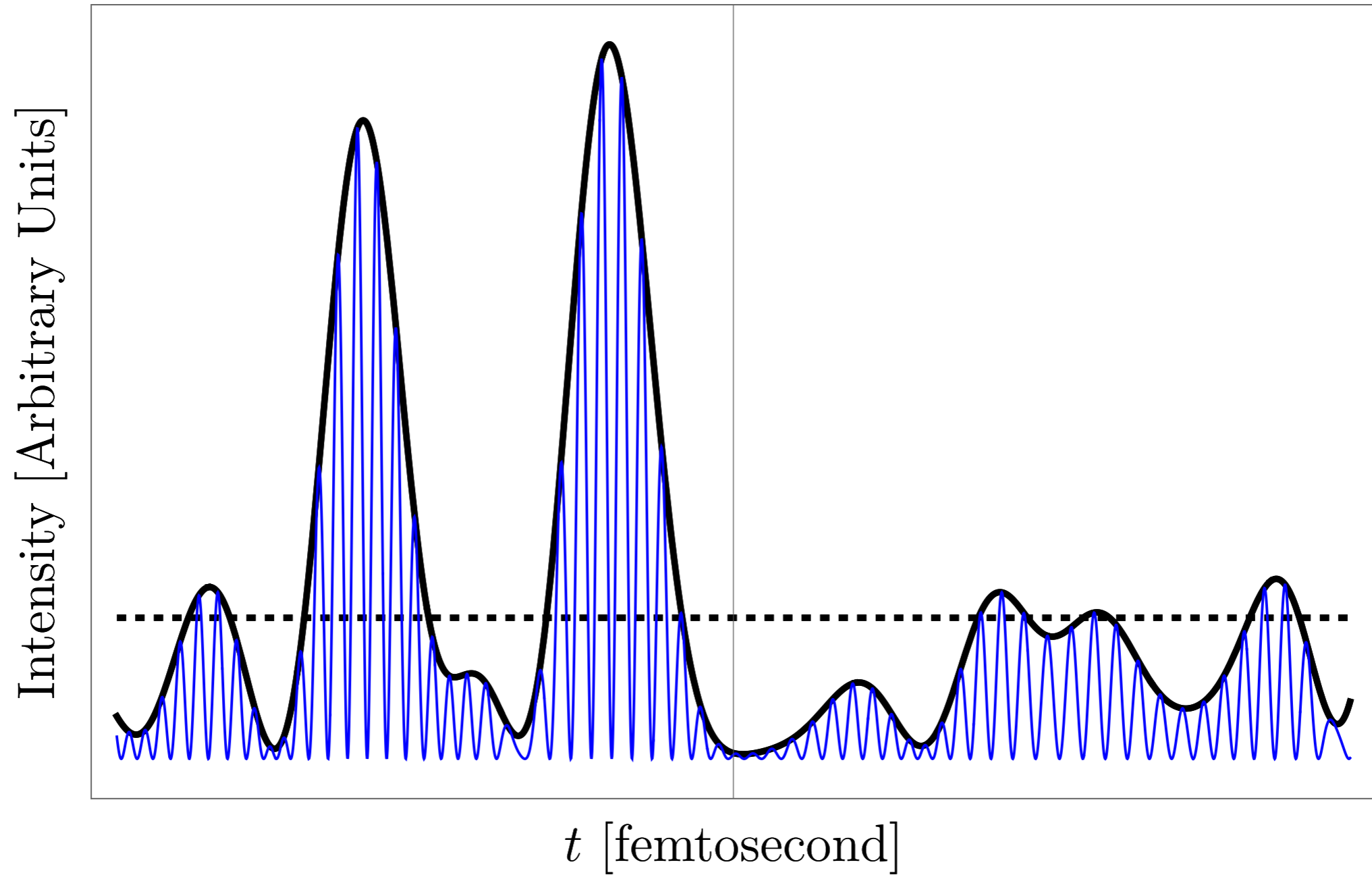
$$E = \sum_i \exp[i(\omega + \delta\omega)t + i\phi_i], \quad \frac{\delta\omega}{\omega} < 1$$

Hanbury Brown and Twiss effect



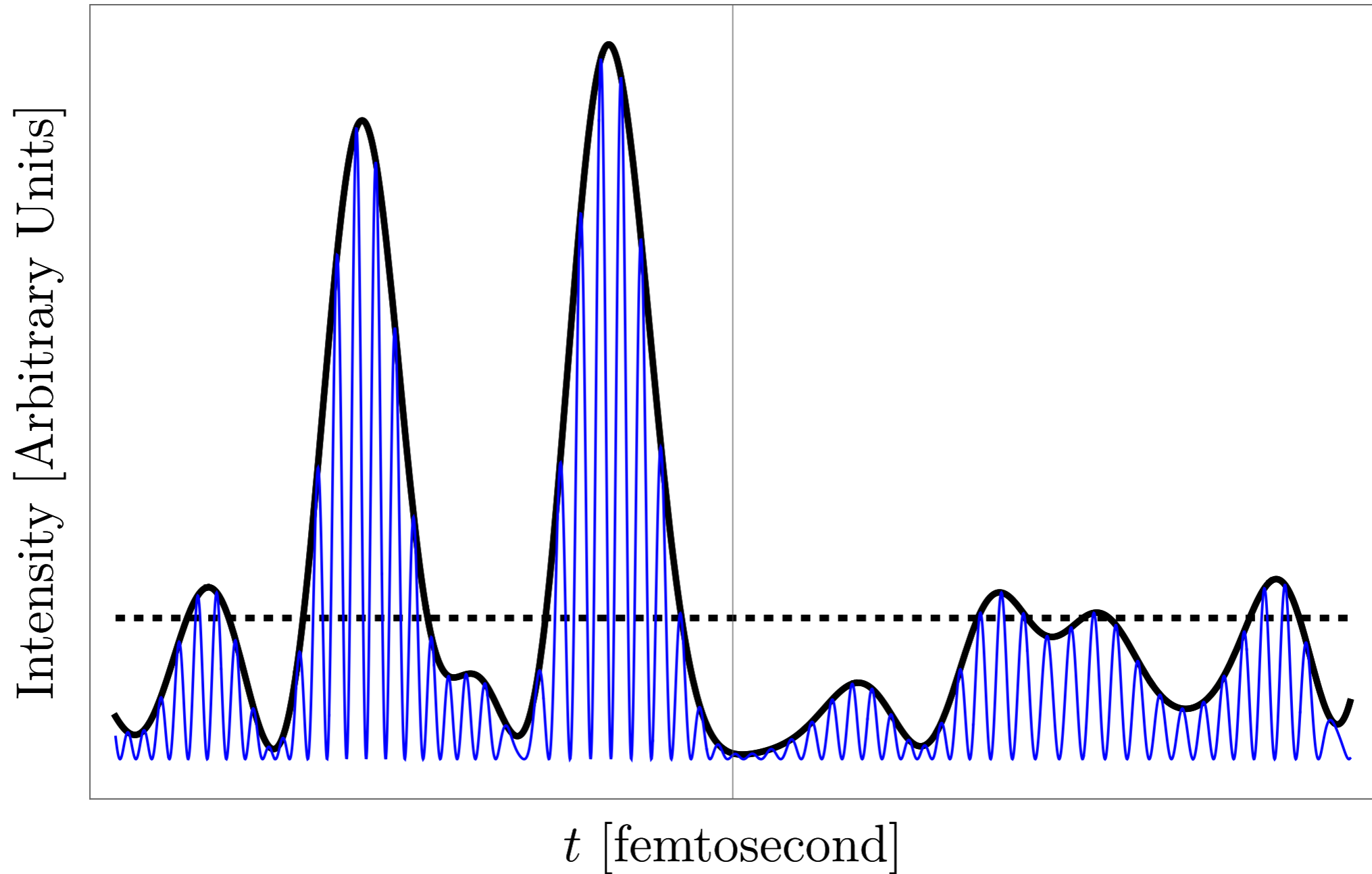
Many sine waves

Hanbury Brown and Twiss effect



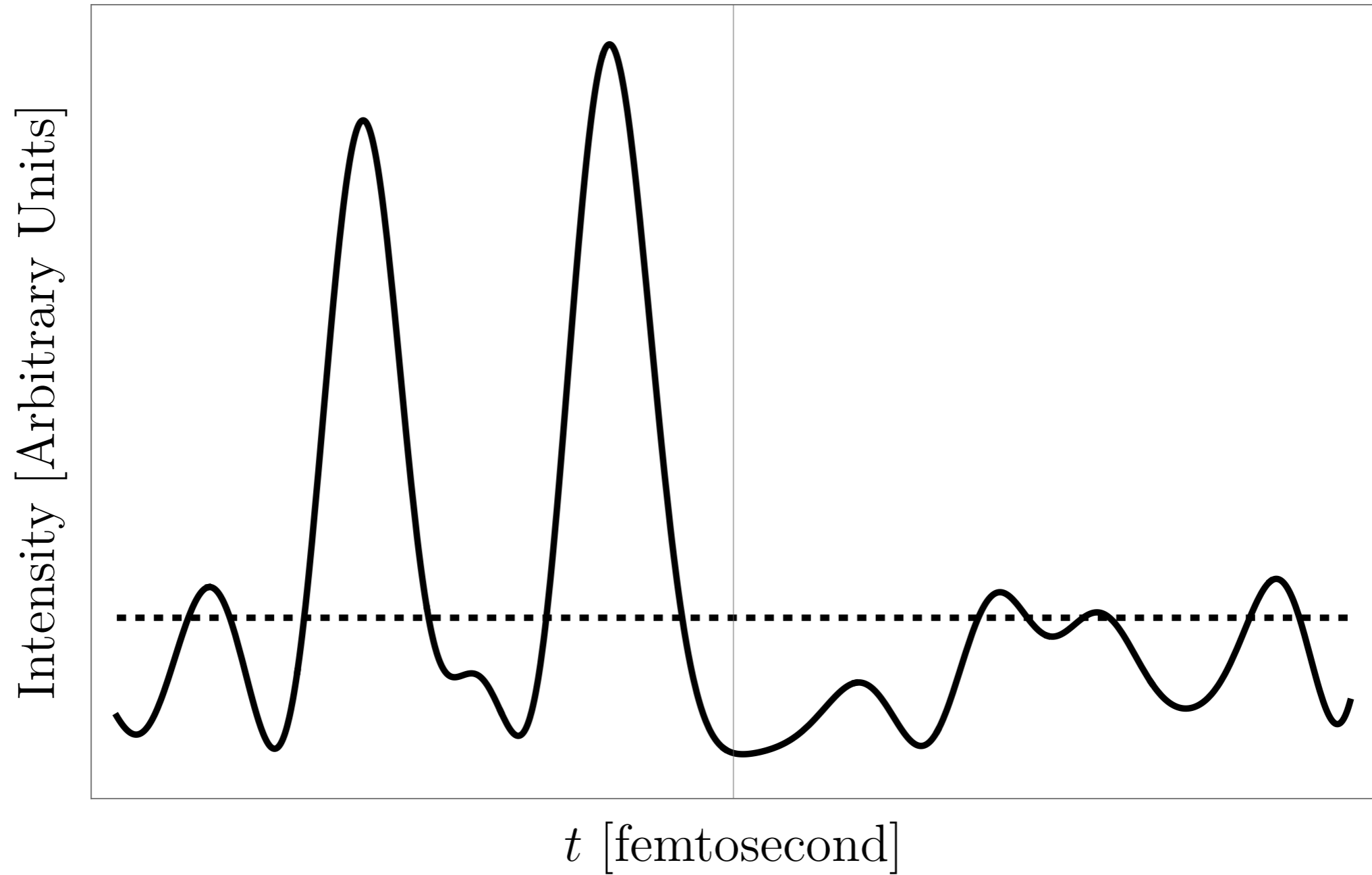
Many sine waves

Hanbury Brown and Twiss effect

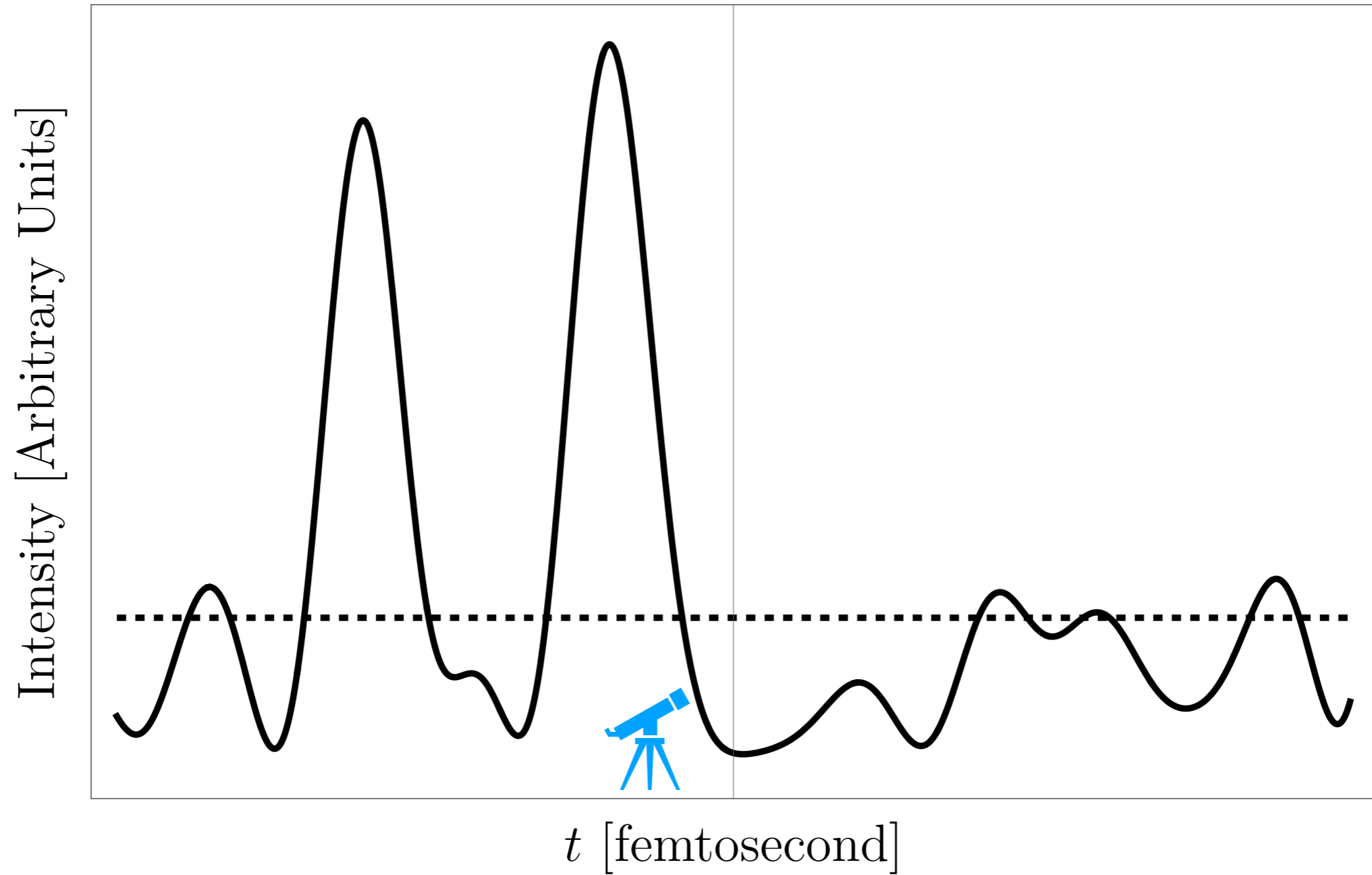


$$E = \sum_i \exp[i(\omega + \delta\omega)t + i\phi_i], \quad \frac{\delta\omega}{\omega} < 1$$

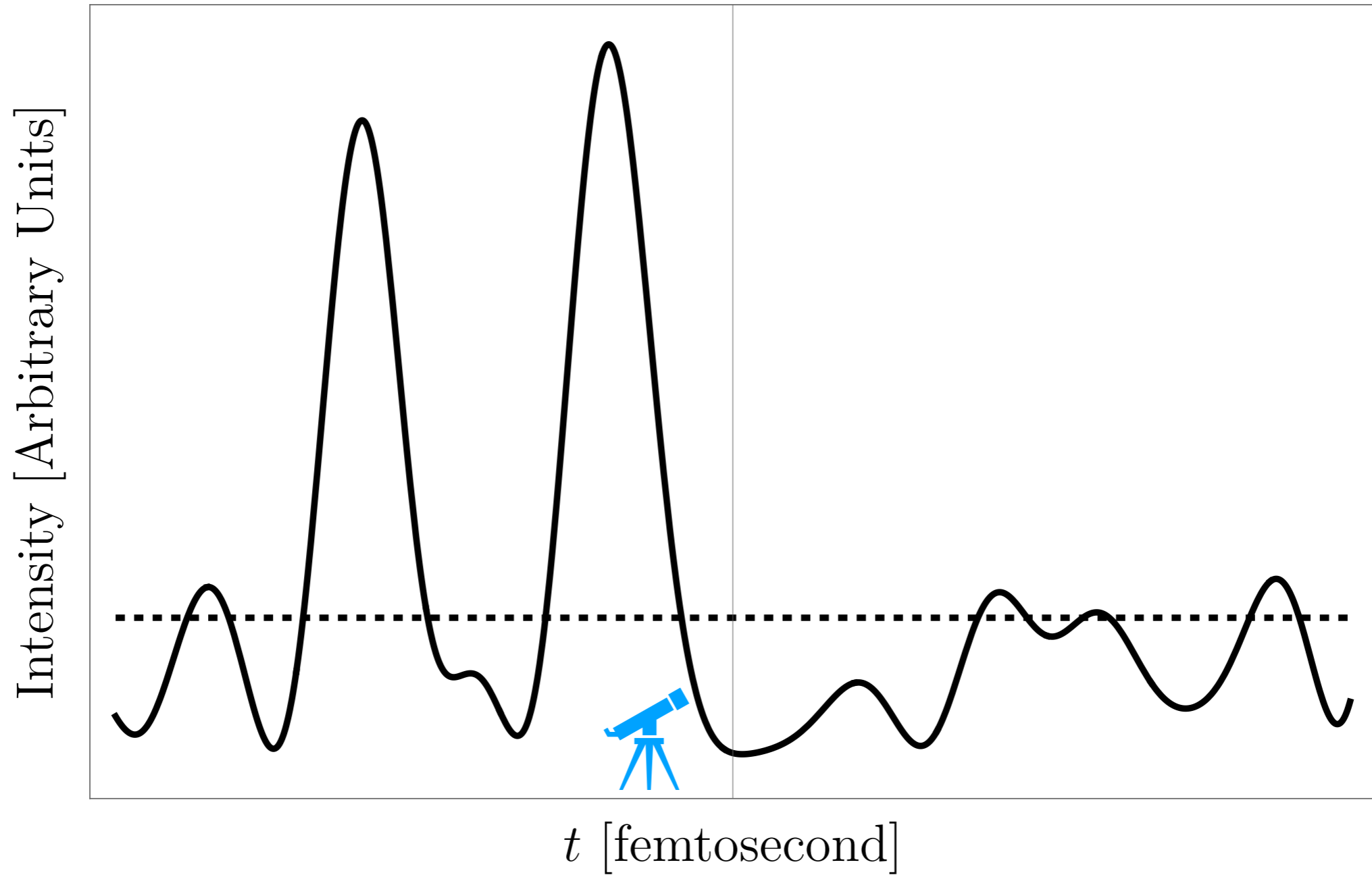
Hanbury Brown and Twiss effect



Hanbury Brown and Twiss effect

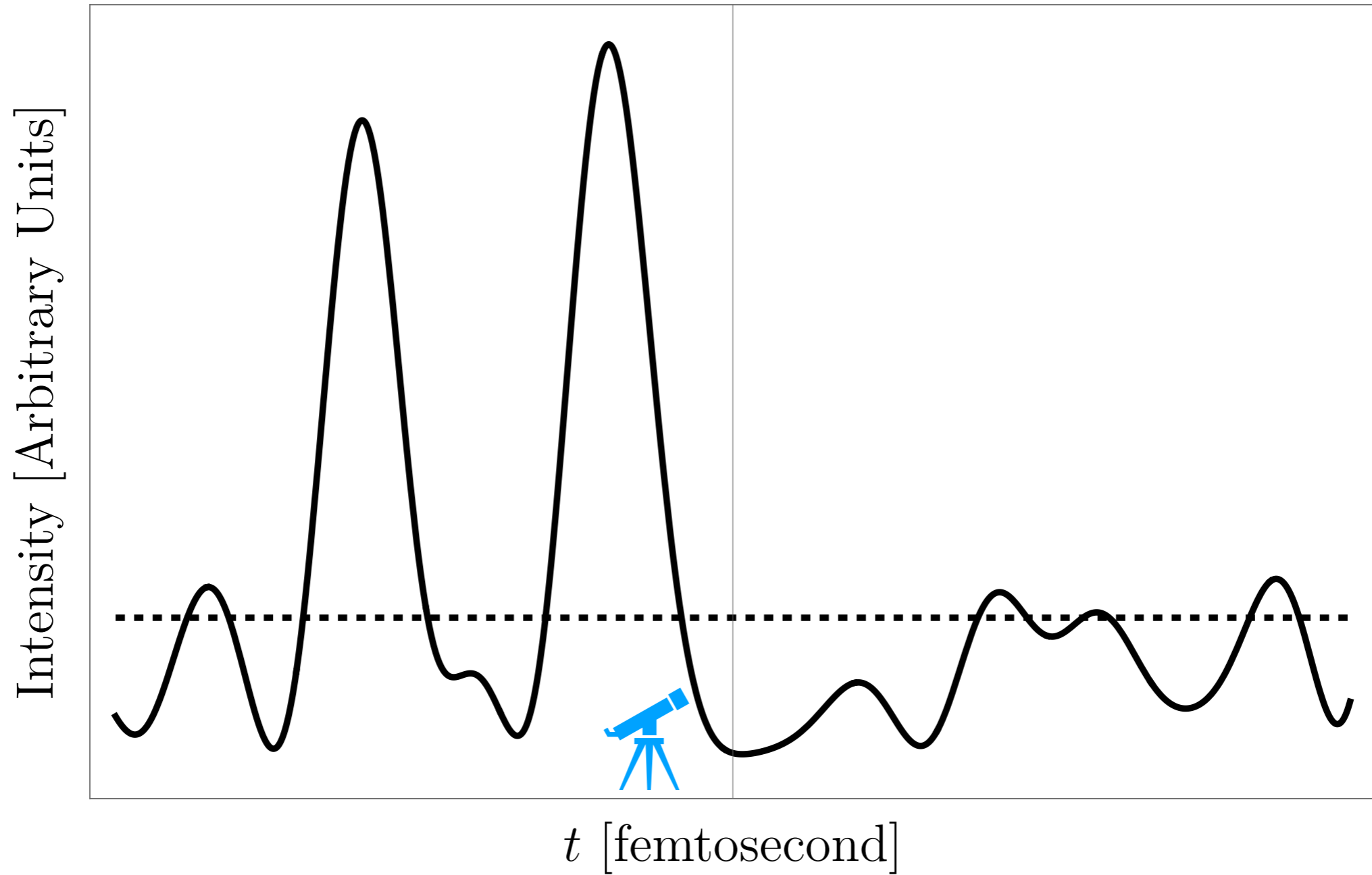


Hanbury Brown and Twiss effect



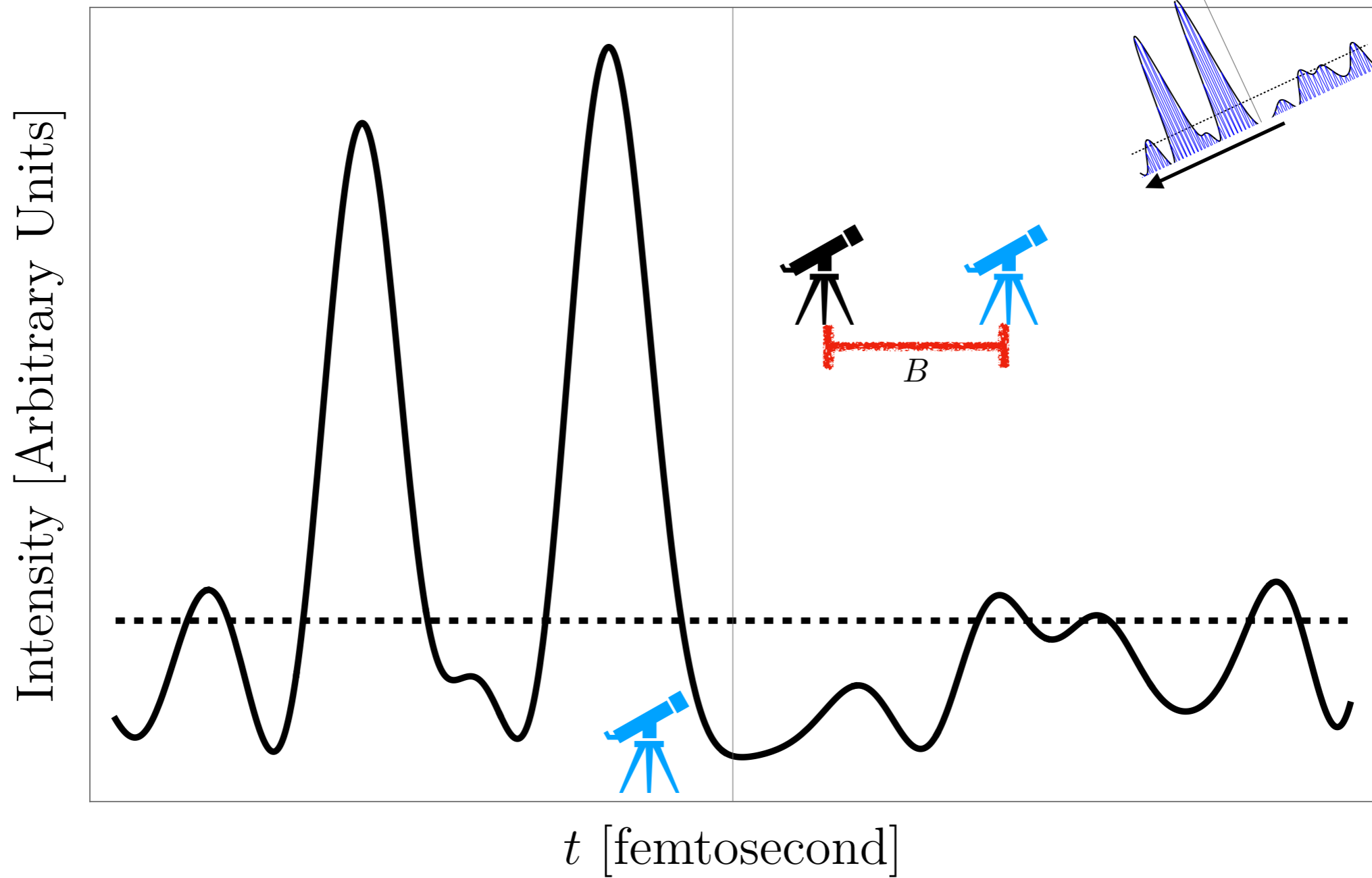
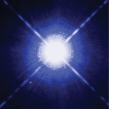
$$\langle (n - \bar{n})^2 \rangle = \bar{n}$$

Hanbury Brown and Twiss effect



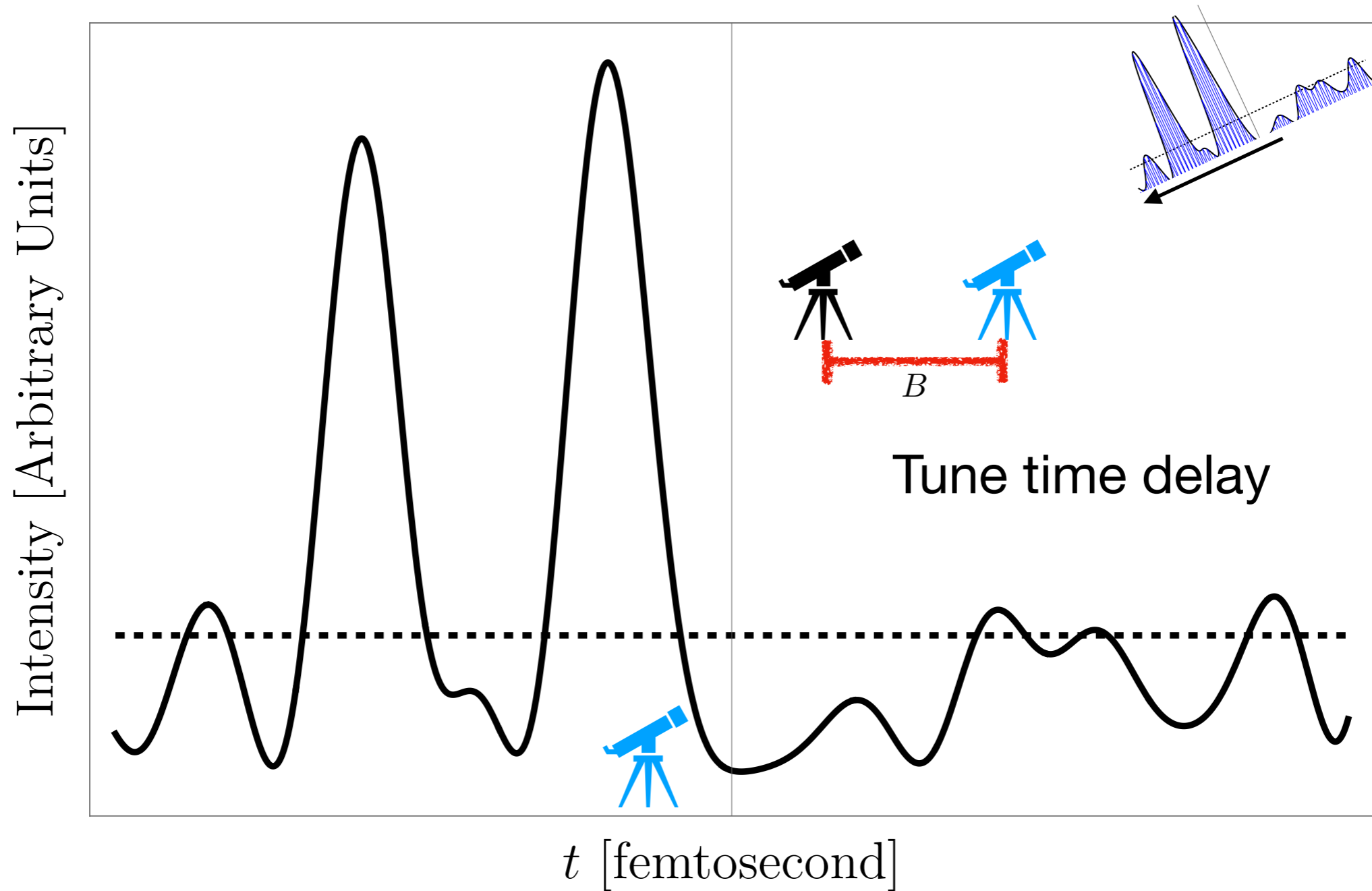
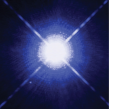
$$\langle (n - \bar{n})^2 \rangle = \bar{n} + \bar{n}^2$$

Hanbury Brown and Twiss effect



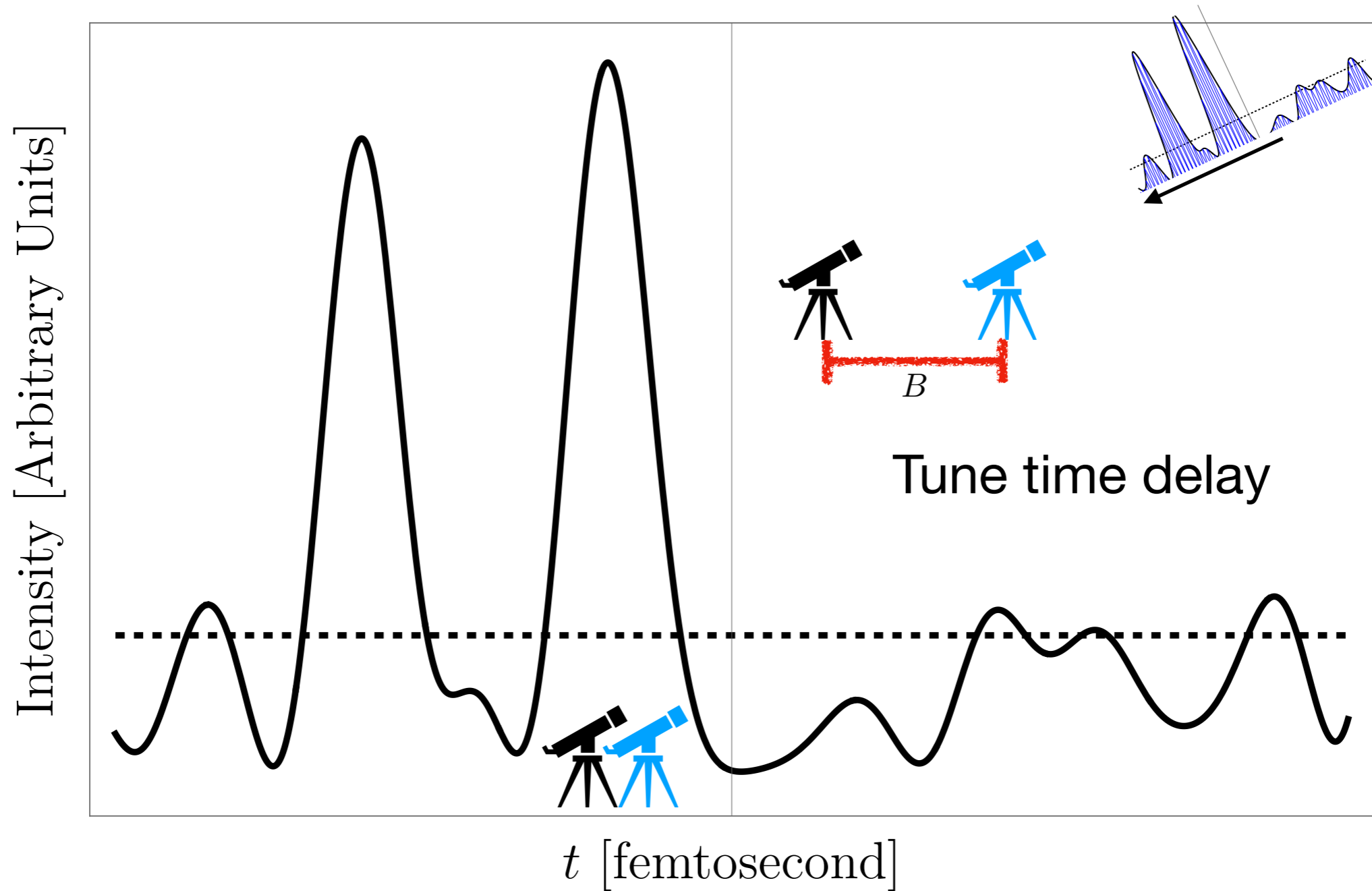
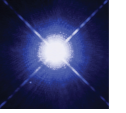
$$\langle (n - \bar{n})^2 \rangle = \bar{n} + \bar{n}^2$$

Hanbury Brown and Twiss effect



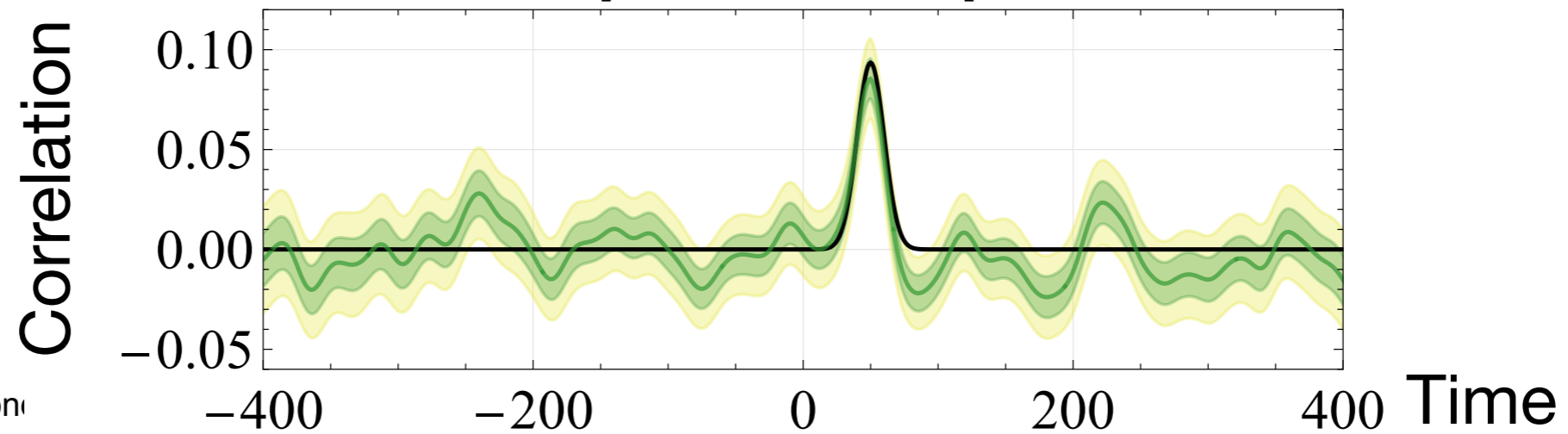
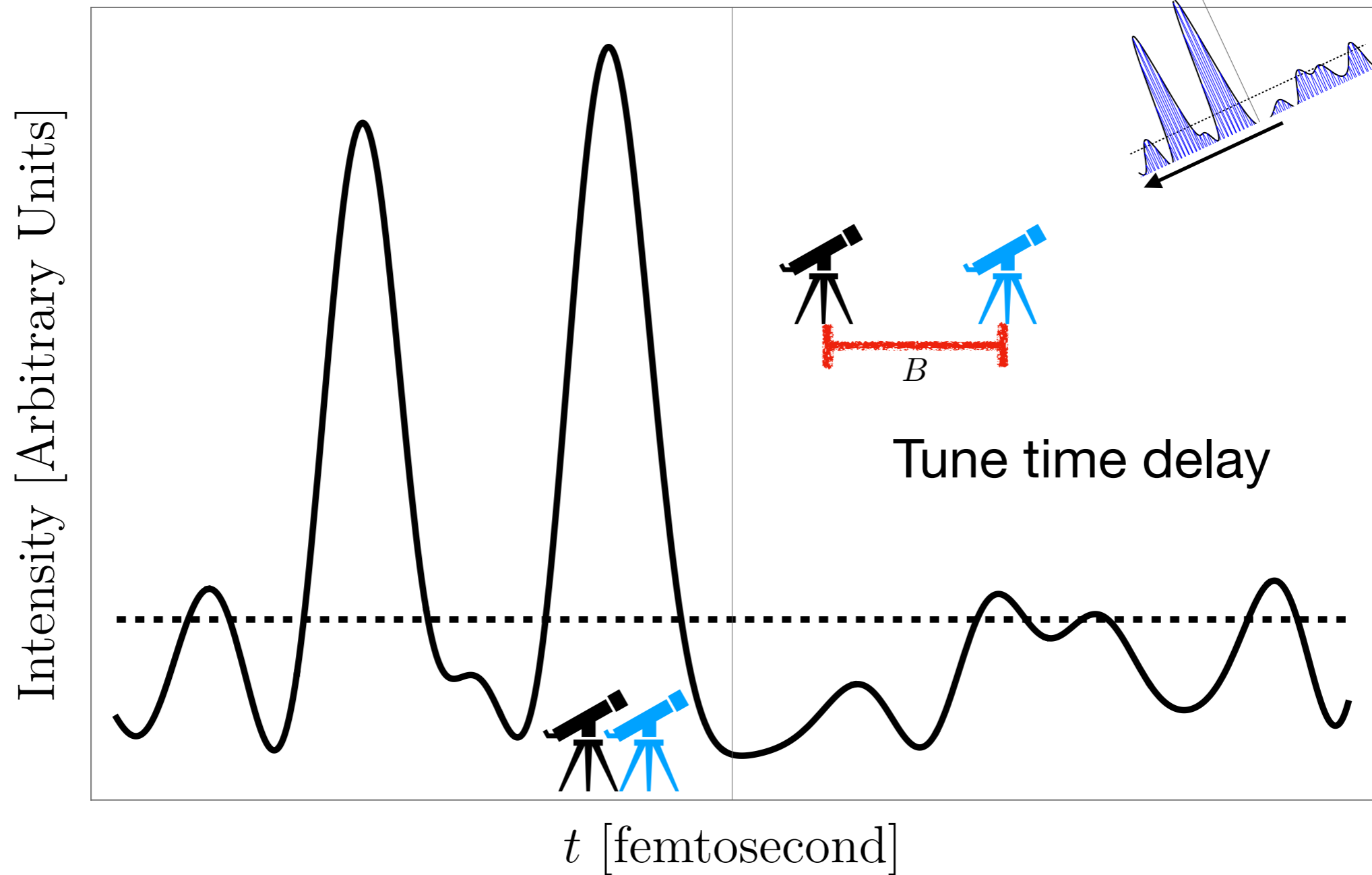
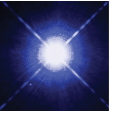
$$\langle (n - \bar{n})^2 \rangle = \bar{n} + \bar{n}^2$$

Hanbury Brown and Twiss effect

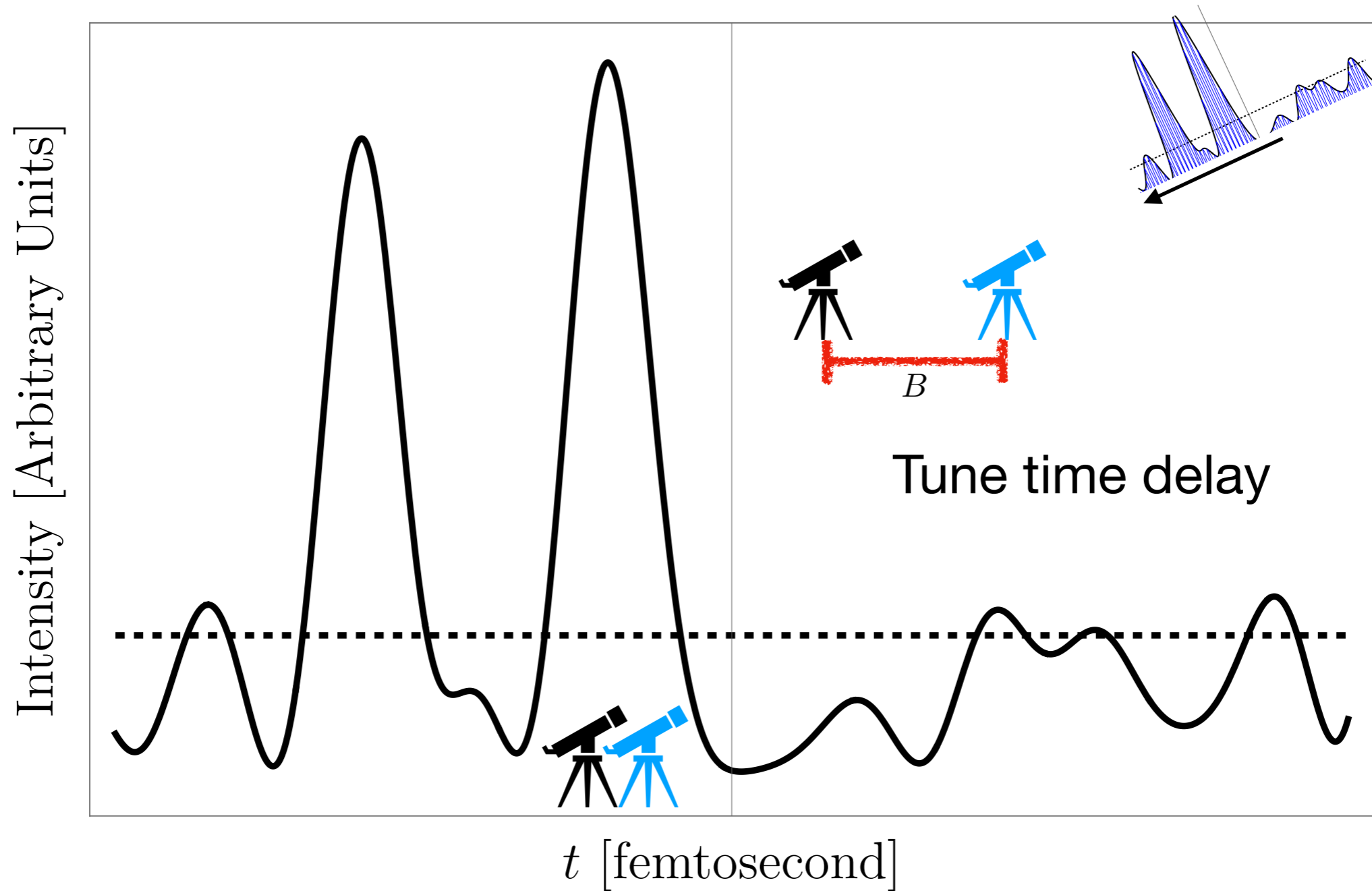
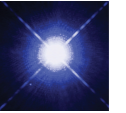


$$\langle (n_1 - \bar{n})(n_2 - \bar{n}) \rangle = \bar{n} + \bar{n}^2$$

Hanbury Brown and Twiss effect

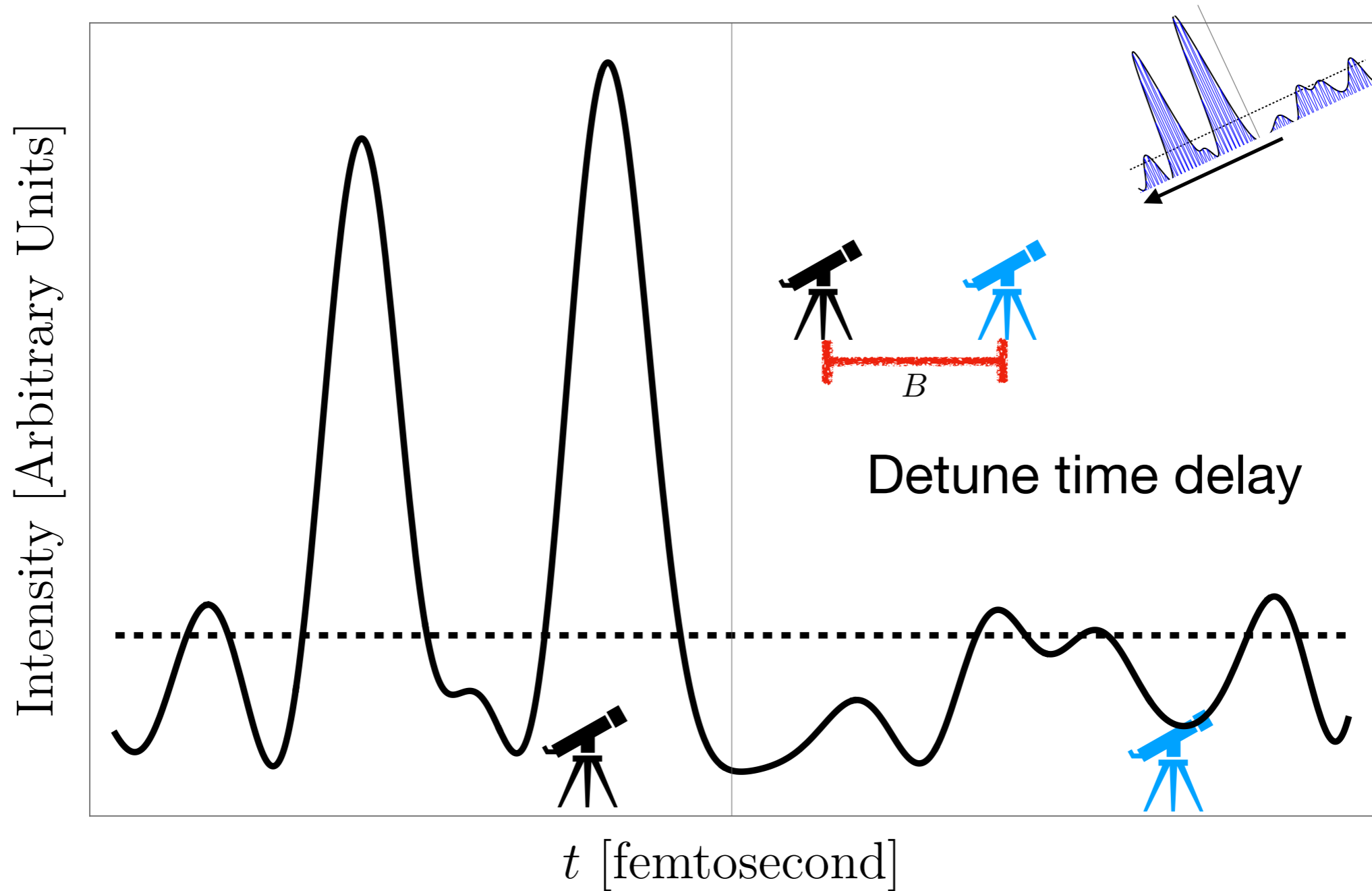
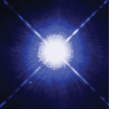


Hanbury Brown and Twiss effect



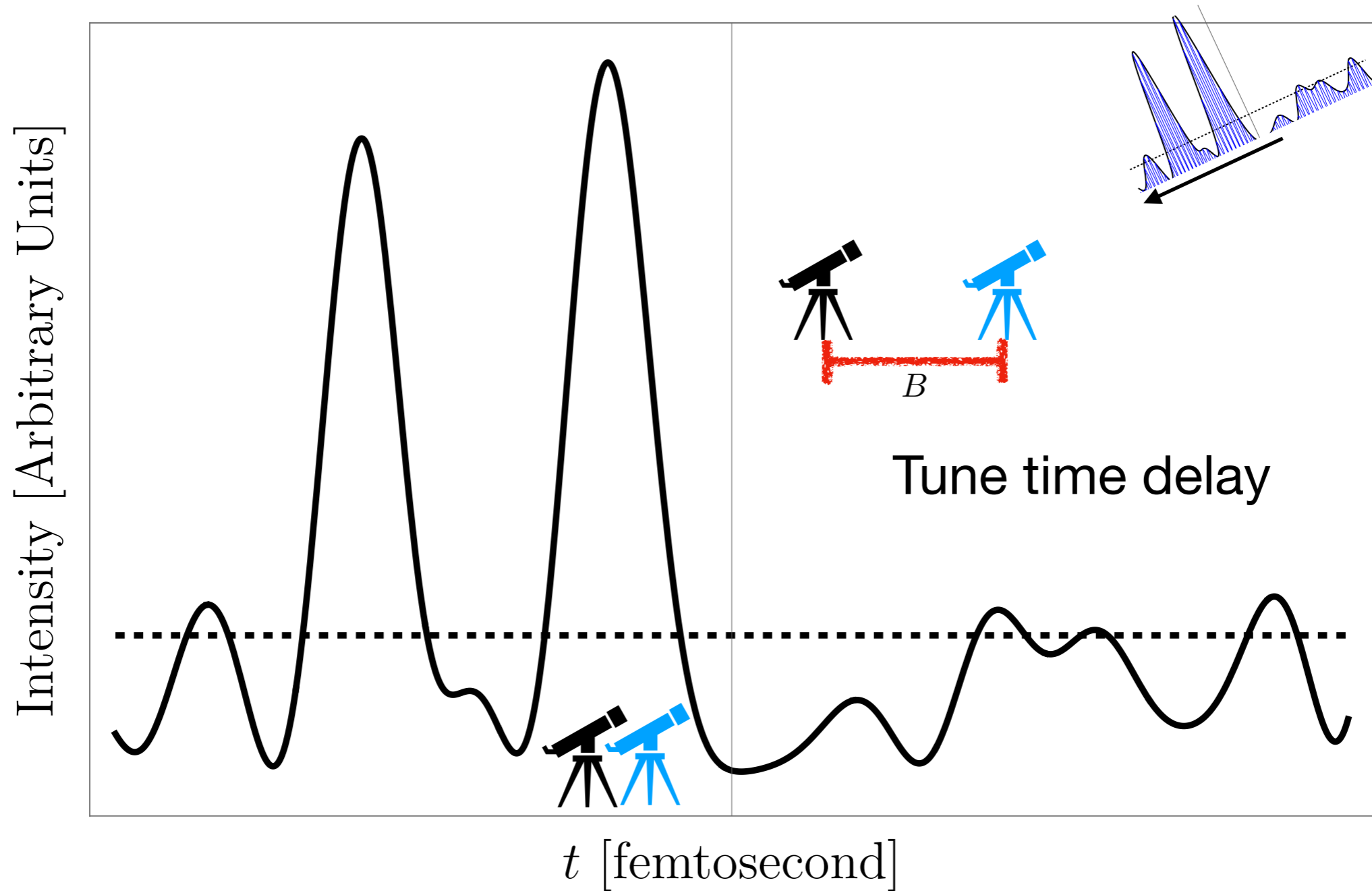
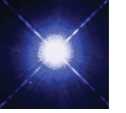
$$\langle (n_1 - \bar{n})(n_2 - \bar{n}) \rangle = \bar{n} + \bar{n}^2$$

Hanbury Brown and Twiss effect

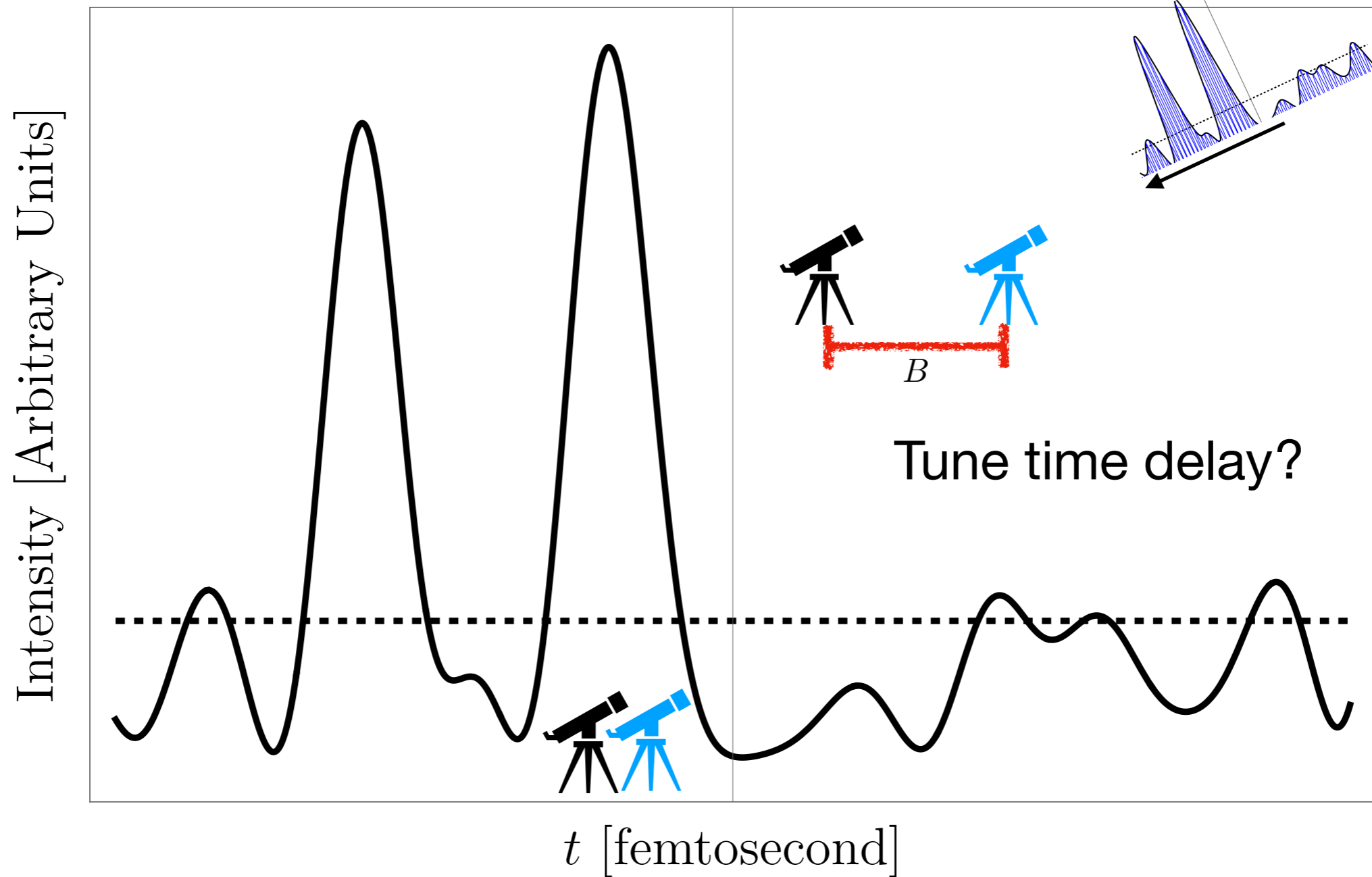
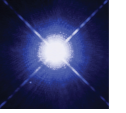


$$\langle (n_1 - \bar{n})(n_2 - \bar{n}) \rangle = \bar{n}$$

Hanbury Brown and Twiss effect

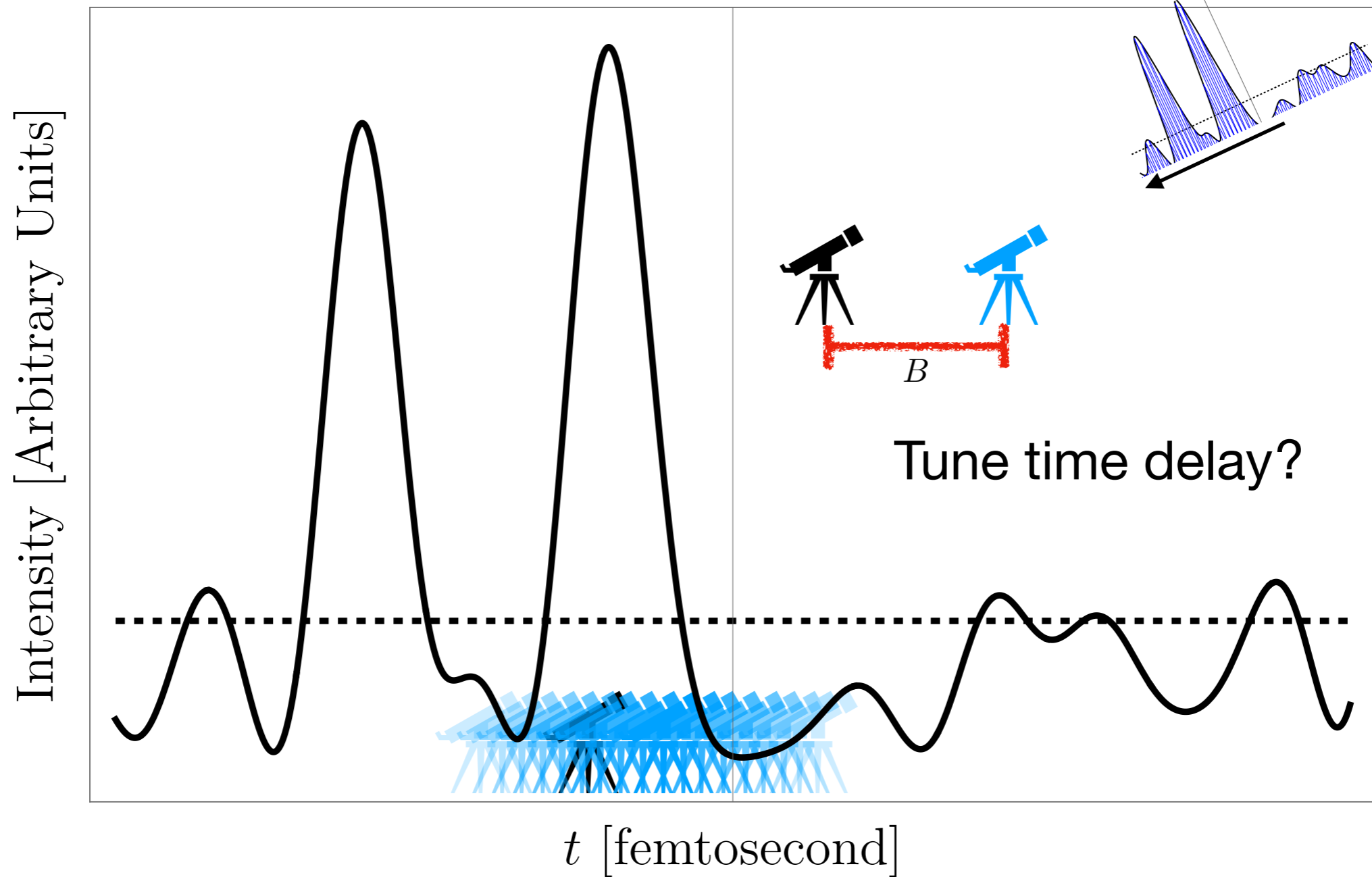
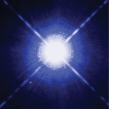


Hanbury Brown and Twiss effect



$$\langle (n_1 - \bar{n})(n_2 - \bar{n}) \rangle = \bar{n} + \bar{n}^2$$

Hanbury Brown and Twiss effect



$$\langle (n_1 - \bar{n})(n_2 - \bar{n}) \rangle = \bar{n} + \bar{n}^2 \frac{\tau_c}{\sigma_t}$$

Observable

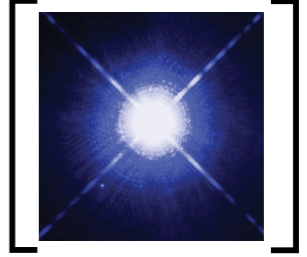
$$\langle I_1 I_2 \rangle \sim \langle E_1 E_1^* E_2 E_2^* \rangle$$

Observable

$$\langle I_1 I_2 \rangle \sim \langle E_1 E_1^* E_2 E_2^* \rangle \sim |\text{Visibility}|^2$$

Observable

$$\langle I_1 I_2 \rangle \sim \langle E_1 E_1^* E_2 E_2^* \rangle \sim |\text{Visibility}|^2 \sim \left| \text{FT} \left[\text{img} \right] \right|^2$$



Observable

$$\langle I_1 I_2 \rangle \sim \langle E_1 E_1^* E_2 E_2^* \rangle \sim |\text{Visibility}|^2 \sim \left| \text{FT} \left[\text{img} \right] \right|^2$$

$$\text{Signal} \sim N_{\text{photon}}^2$$

Observable

$$\langle I_1 I_2 \rangle \sim \langle E_1 E_1^* E_2 E_2^* \rangle \sim |\text{Visibility}|^2 \sim \left| \text{FT} \left[\text{img} \right] \right|^2$$

$$\text{Signal} \sim N_{\text{photon}}^2 |\mathcal{V}(\text{B, sky})|^2$$

Observable

$$\langle I_1 I_2 \rangle \sim \langle E_1 E_1^* E_2 E_2^* \rangle \sim |\text{Visibility}|^2 \sim \left| \text{FT} \left[\text{img} \right] \right|^2$$

$$\text{Signal} \sim N_{\text{photon}}^2 |\mathcal{V}(\text{B, sky})|^2 \frac{\tau_c}{\sigma_t}$$

Observable

$$\langle I_1 I_2 \rangle \sim \langle E_1 E_1^* E_2 E_2^* \rangle \sim |\text{Visibility}|^2 \sim \left| \text{FT} \left[\text{img} \right] \right|^2$$

$$\text{Signal} \sim N_{\text{photon}}^2 |\mathcal{V}(\mathbf{B}, \text{sky})|^2 \frac{\tau_c}{\sigma_t}$$

$$\text{Noise} \sim N_{\text{photon}}$$

Observable

$$\langle I_1 I_2 \rangle \sim \langle E_1 E_1^* E_2 E_2^* \rangle \sim |\text{Visibility}|^2 \sim \left| \text{FT} \left[\text{img} \right] \right|^2$$

$$\text{Signal} \sim N_{\text{photon}}^2 |\mathcal{V}(\text{B, sky})|^2 \frac{\tau_c}{\sigma_t} \quad \text{Noise} \sim N_{\text{photon}}$$

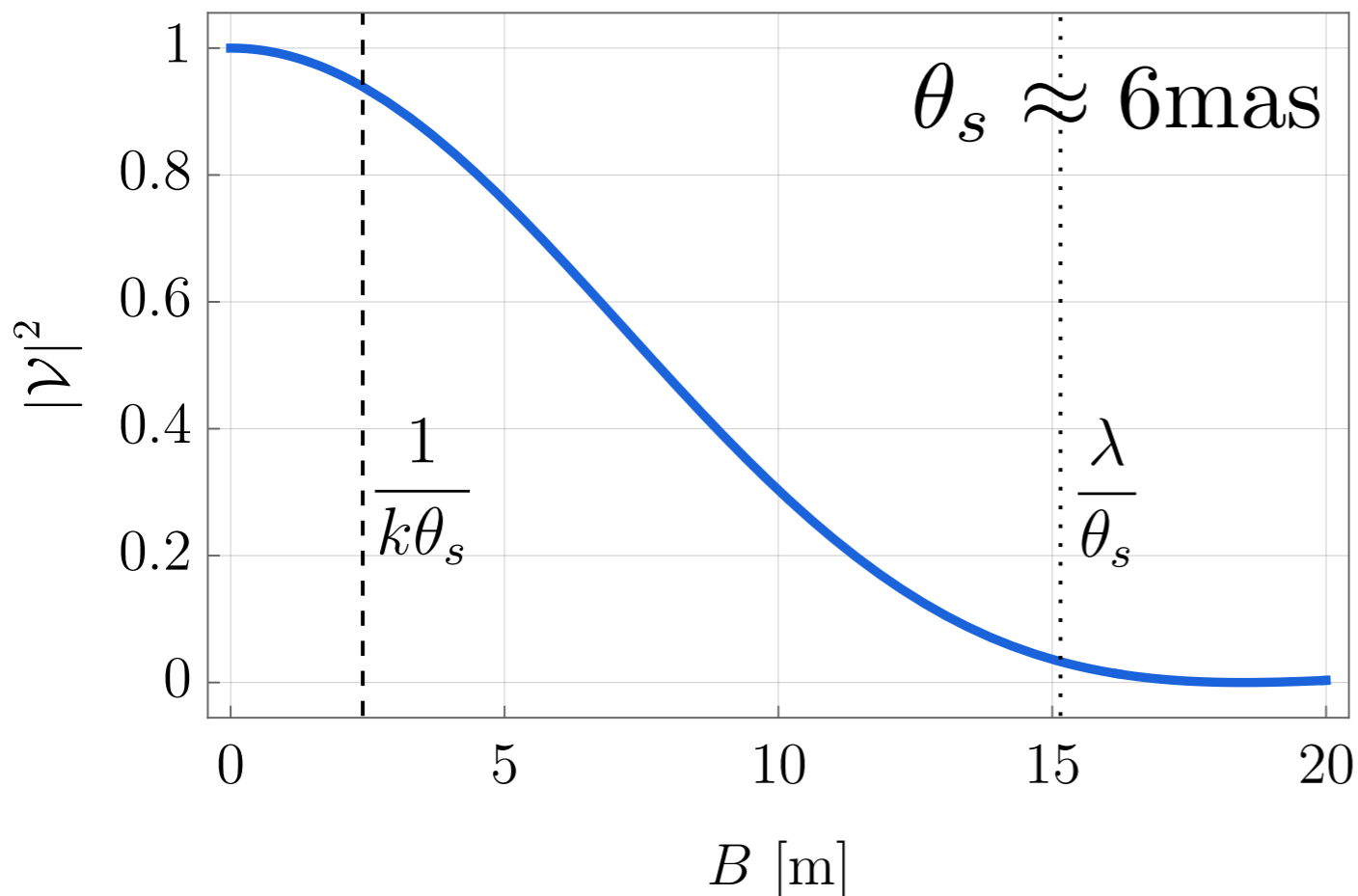
Stars are bright and have real visibilities:

Observable

$$\langle I_1 I_2 \rangle \sim \langle E_1 E_1^* E_2 E_2^* \rangle \sim |\text{Visibility}|^2 \sim \left| \text{FT} \left[\text{Image} \right] \right|^2$$

$$\text{Signal} \sim N_{\text{photon}}^2 |\mathcal{V}(B, \text{sky})|^2 \frac{\tau_c}{\sigma_t} \quad \text{Noise} \sim N_{\text{photon}}$$

Stars are bright and have real visibilities:



$$I = I_0 \Theta(\theta_s/2 - \theta)$$

$$\mathcal{V} = \frac{2J_1(kd\theta_s/2)}{kd\theta_s/2}$$

Traditional Approach

$$\text{Signal} \sim N_{\text{photon}}^2 |\mathcal{V}(\mathbf{B}, \text{sky})|^2 \frac{\tau_c}{\sigma_t}$$

$$\text{Noise} \sim N_{\text{photon}}$$

Traditional Approach

$$\text{Signal} \sim N_{\text{photon}}^2 |\mathcal{V}(\text{B, sky})|^2 \frac{\tau_c}{\sigma_t}$$

$$\text{Noise} \sim N_{\text{photon}}$$

Limitations

Traditional Solution

Traditional Approach

$$\text{Signal} \sim N_{\text{photon}}^2 |\mathcal{V}(\text{B, sky})|^2 \frac{\tau_c}{\sigma_t}$$

$$\text{Noise} \sim N_{\text{photon}}$$

Limitations

Traditional Solution

Coherence time of light $\tau_c \ll \sigma_t$

Traditional Approach

$$\text{Signal} \sim N_{\text{photon}}^2 |\mathcal{V}(\text{B, sky})|^2 \frac{\tau_c}{\sigma_t}$$

$$\text{Noise} \sim N_{\text{photon}}$$

Limitations

Traditional Solution

Coherence time of light $\tau_c \ll \sigma_t$

$$\tau_c \sim \frac{1}{\nu_0} \sim \text{fs}$$

Traditional Approach

$$\text{Signal} \sim N_{\text{photon}}^2 |\mathcal{V}(\text{B, sky})|^2 \frac{\tau_c}{\sigma_t}$$

$$\text{Noise} \sim N_{\text{photon}}$$

Limitations

Coherence time of light $\tau_c \ll \sigma_t$

$$\tau_c \sim \frac{1}{\nu_0} \sim \text{fs}$$

Traditional Solution

Filter:

Traditional Approach

$$\text{Signal} \sim N_{\text{photon}}^2 |\mathcal{V}(\text{B, sky})|^2 \frac{\tau_c}{\sigma_t}$$

$$\text{Noise} \sim N_{\text{photon}}$$

Limitations

Coherence time of light $\tau_c \ll \sigma_t$

$$\tau_c \sim \frac{1}{\nu_0} \sim \text{fs}$$

Traditional Solution

Filter: $\tau_c \rightarrow \frac{1}{\Delta\nu} \sim \text{ps}$

Traditional Approach

$$\text{Signal} \sim N_{\text{photon}}^2 |\mathcal{V}(\text{B, sky})|^2 \frac{\tau_c}{\sigma_t}$$

$$\text{Noise} \sim N_{\text{photon}}$$

Limitations

Coherence time of light $\tau_c \ll \sigma_t$

$$\tau_c \sim \frac{1}{\nu_0} \sim \text{fs}$$

Traditional Solution

Filter: $\tau_c \rightarrow \frac{1}{\Delta\nu} \sim \text{ps}$

PMTs:

Traditional Approach

$$\text{Signal} \sim N_{\text{photon}}^2 |\mathcal{V}(\text{B, sky})|^2 \frac{\tau_c}{\sigma_t}$$

$$\text{Noise} \sim N_{\text{photon}}$$

Limitations

Coherence time of light $\tau_c \ll \sigma_t$

$$\tau_c \sim \frac{1}{\nu_0} \sim \text{fs}$$

Traditional Solution

Filter: $\tau_c \rightarrow \frac{1}{\Delta\nu} \sim \text{ps}$

PMTs: $\sigma_t \sim 10\text{ns}$

Traditional Approach

$$\text{Signal} \sim N_{\text{photon}}^2 |\mathcal{V}(\text{B, sky})|^2 \frac{\tau_c}{\sigma_t}$$

$$\text{Noise} \sim N_{\text{photon}}$$

Limitations

Coherence time of light $\tau_c \ll \sigma_t$

$$\tau_c \sim \frac{1}{\nu_0} \sim \text{fs}$$

Shot noise limited

Traditional Solution

Filter: $\tau_c \rightarrow \frac{1}{\Delta\nu} \sim \text{ps}$

PMTs: $\sigma_t \sim 10\text{ns}$

Traditional Approach

$$\text{Signal} \sim N_{\text{photon}}^2 |\mathcal{V}(\text{B, sky})|^2 \frac{\tau_c}{\sigma_t}$$

$$\text{Noise} \sim N_{\text{photon}}$$

Limitations

Coherence time of light $\tau_c \ll \sigma_t$

$$\tau_c \sim \frac{1}{\nu_0} \sim \text{fs}$$

Shot noise limited

Traditional Solution

Filter: $\tau_c \rightarrow \frac{1}{\Delta\nu} \sim \text{ps}$

PMTs: $\sigma_t \sim 10\text{ns}$

Large mirrors

Traditional Approach

$$\text{Signal} \sim N_{\text{photon}}^2 |\mathcal{V}(\text{B, sky})|^2 \frac{\tau_c}{\sigma_t}$$

$$\text{Noise} \sim N_{\text{photon}}$$

Limitations

Coherence time of light $\tau_c \ll \sigma_t$

$$\tau_c \sim \frac{1}{\nu_0} \sim \text{fs}$$

Shot noise limited

Traditional Solution

Filter: $\tau_c \rightarrow \frac{1}{\Delta\nu} \sim \text{ps}$

PMTs: $\sigma_t \sim 10\text{ns}$

Large mirrors

Nearby sources

Traditional Approach

$$\text{Signal} \sim N_{\text{photon}}^2 |\mathcal{V}(\text{B, sky})|^2 \frac{\tau_c}{\sigma_t}$$

$$\text{Noise} \sim N_{\text{photon}}$$

Limitations

Coherence time of light $\tau_c \ll \sigma_t$

$$\tau_c \sim \frac{1}{\nu_0} \sim \text{fs}$$

Shot noise limited

Traditional Solution

Filter: $\tau_c \rightarrow \frac{1}{\Delta\nu} \sim \text{ps}$

PMTs: $\sigma_t \sim 10\text{ns}$

Large mirrors

Nearby sources $m \lesssim 2$

Why today?

$$\text{Signal} \sim N_{\text{photon}}^2 |\mathcal{V}(\text{B, sky})|^2 \frac{\tau_c}{\sigma_t}$$

$$\text{Noise} \sim N_{\text{photon}}$$

Limitations

Coherence time of light $\tau_c \ll \sigma_t$

$$\tau_c \sim \frac{1}{\nu_0} \sim \text{fs}$$

Shot noise limited

New Technologies

Why today?

New Technologies

$$\text{Signal} \sim N_{\text{photon}}^2 |\mathcal{V}(\mathbf{B}, \text{sky})|^2 \frac{\tau_c}{\sigma_t}$$

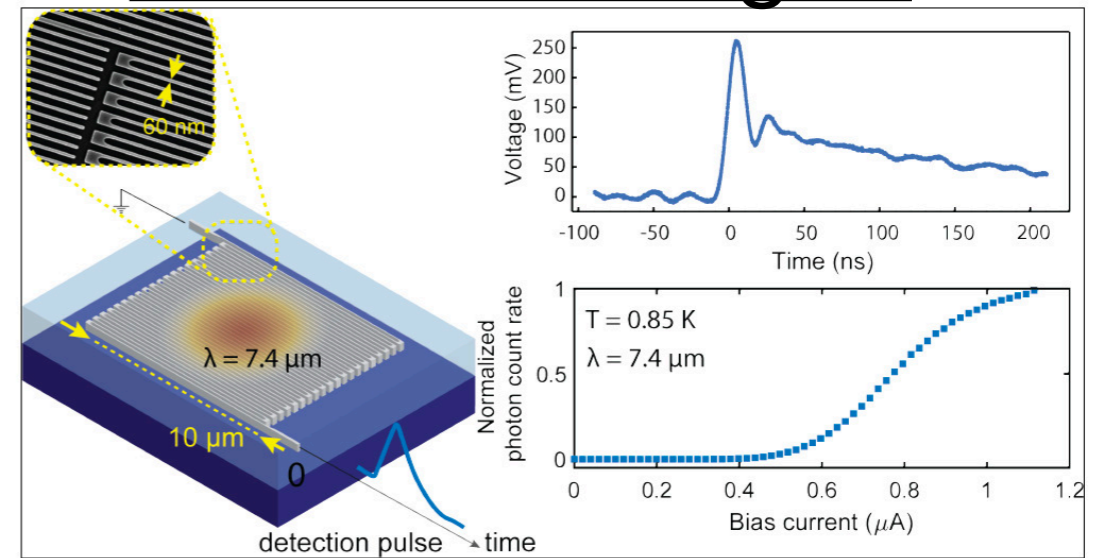
$$\text{Noise} \sim N_{\text{photon}}$$

Limitations

Coherence time of light $\tau_c \ll \sigma_t$

$$\tau_c \sim \frac{1}{\nu_0} \sim \text{fs}$$

Shot noise limited



Fast Single-Photon Detection

$$\sigma_t^{\text{SNSPD, SPAD}} \sim 10\text{ps}$$

Why today?

New Technologies

$$\text{Signal} \sim N_{\text{photon}}^2 |\mathcal{V}(\mathbf{B}, \text{sky})|^2 \frac{\tau_c}{\sigma_t}$$

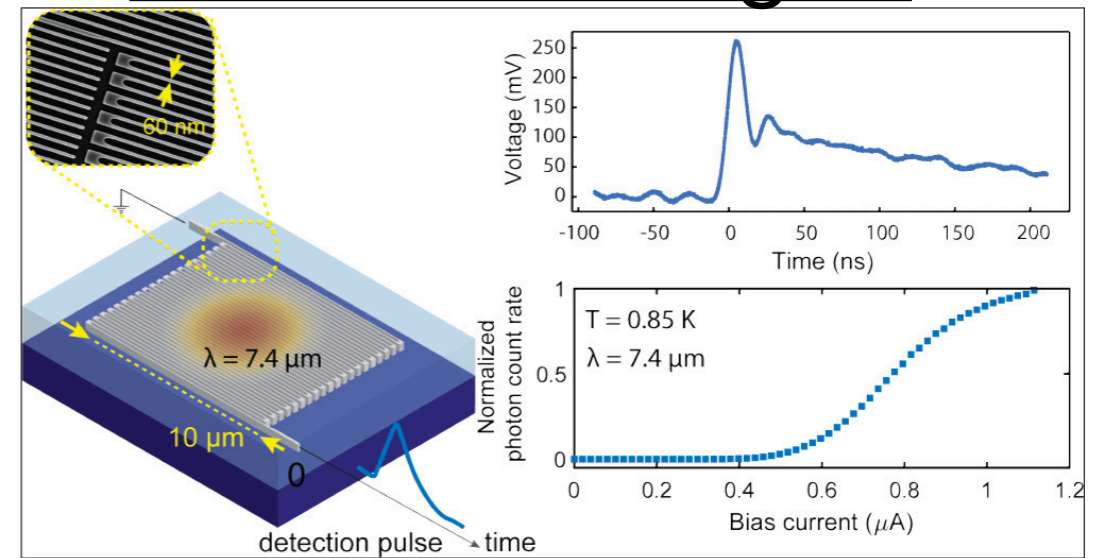
$$\text{Noise} \sim N_{\text{photon}}$$

Limitations

Coherence time of light $\tau_c \ll \sigma_t$

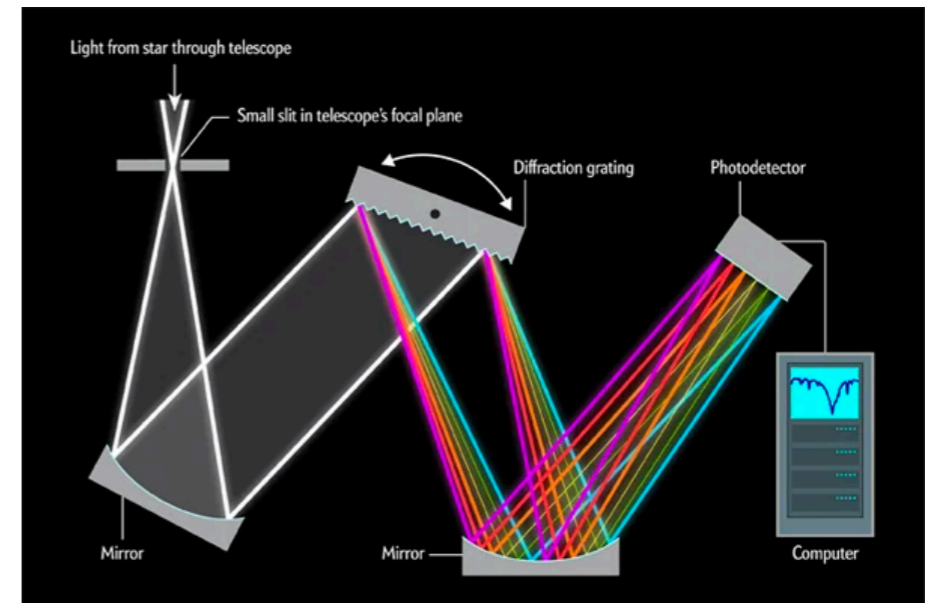
$$\tau_c \sim \frac{1}{\nu_0} \sim \text{fs}$$

Shot noise limited



Fast Single-Photon Detection

$$\sigma_t^{\text{SNSPD, SPAD}} \sim 10\text{ps}$$



Multi-Channel Spectroscopy

$$\Delta k \sim \frac{k}{\mathcal{R}}, \quad \mathcal{R} \sim \text{thousands}$$

Why today?

New Technologies

$$\text{Signal} \sim N_{\text{photon}}^2 |\mathcal{V}(\mathbf{B}, \text{sky})|^2 \frac{\tau_c}{\sigma_t} \sqrt{\mathcal{R}}$$

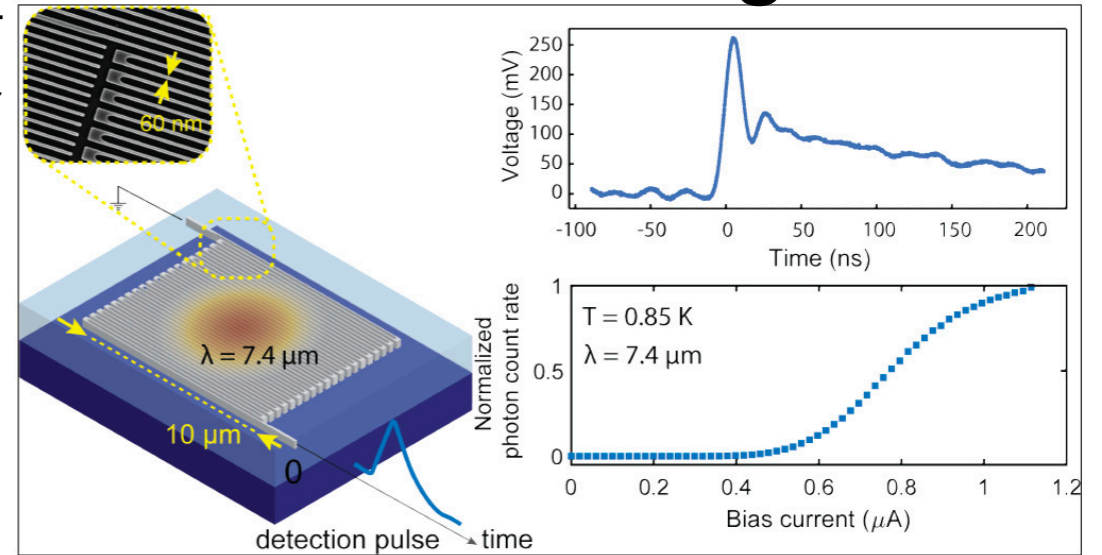
$$\text{Noise} \sim N_{\text{photon}}$$

Limitations

Coherence time of light $\tau_c \ll \sigma_t$

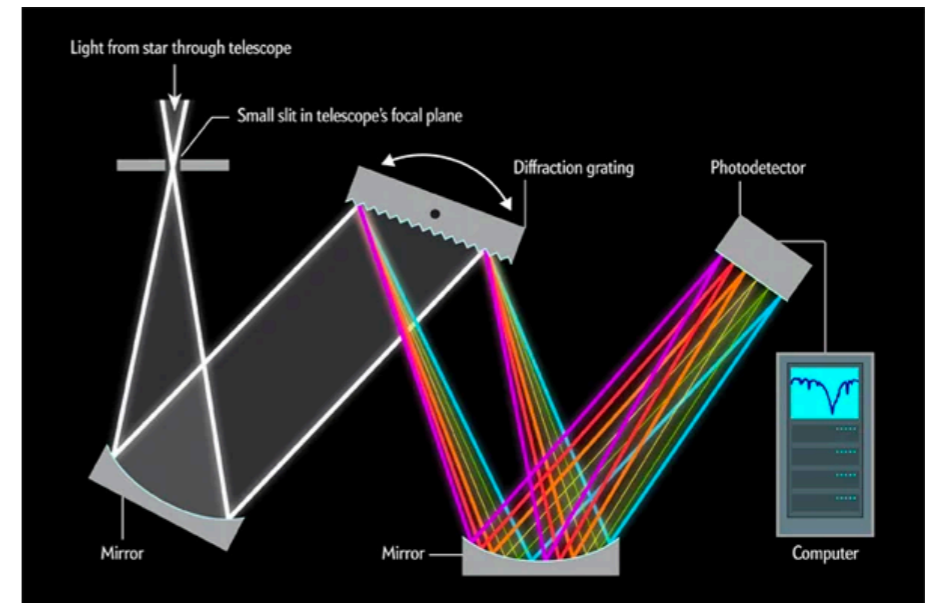
$$\tau_c \sim \frac{1}{\nu_0} \sim \text{fs}$$

Shot noise limited



Fast Single-Photon Detection

$$\sigma_t^{\text{SNSPD, SPAD}} \sim 10\text{ps}$$



Multi-Channel Spectroscopy

$$\Delta k \sim \frac{k}{\mathcal{R}}, \quad \mathcal{R} \sim \text{thousands}$$

Why today?

New Technologies

$$\text{Signal} \sim N_{\text{photon}}^2 |\mathcal{V}(\mathbf{B}, \text{sky})|^2 \frac{\tau_c}{\sigma_t} \sqrt{\mathcal{R}}$$

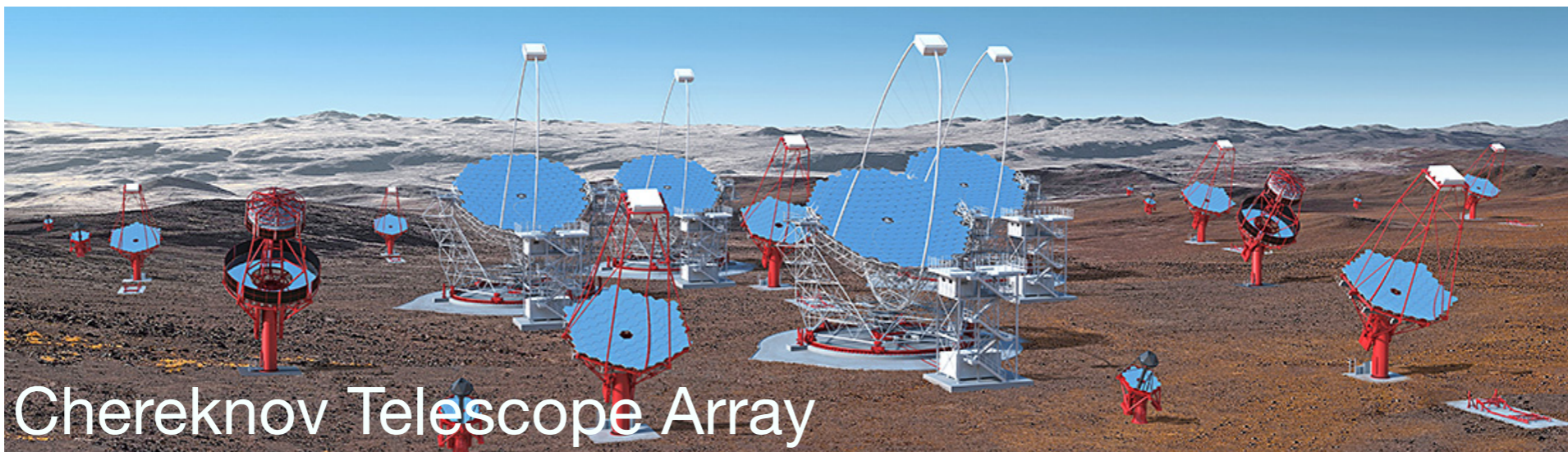
$$\text{Noise} \sim N_{\text{photon}}$$

Limitations

Coherence time of light $\tau_c \ll \sigma_t$

$$\tau_c \sim \frac{1}{\nu_0} \sim \text{fs}$$

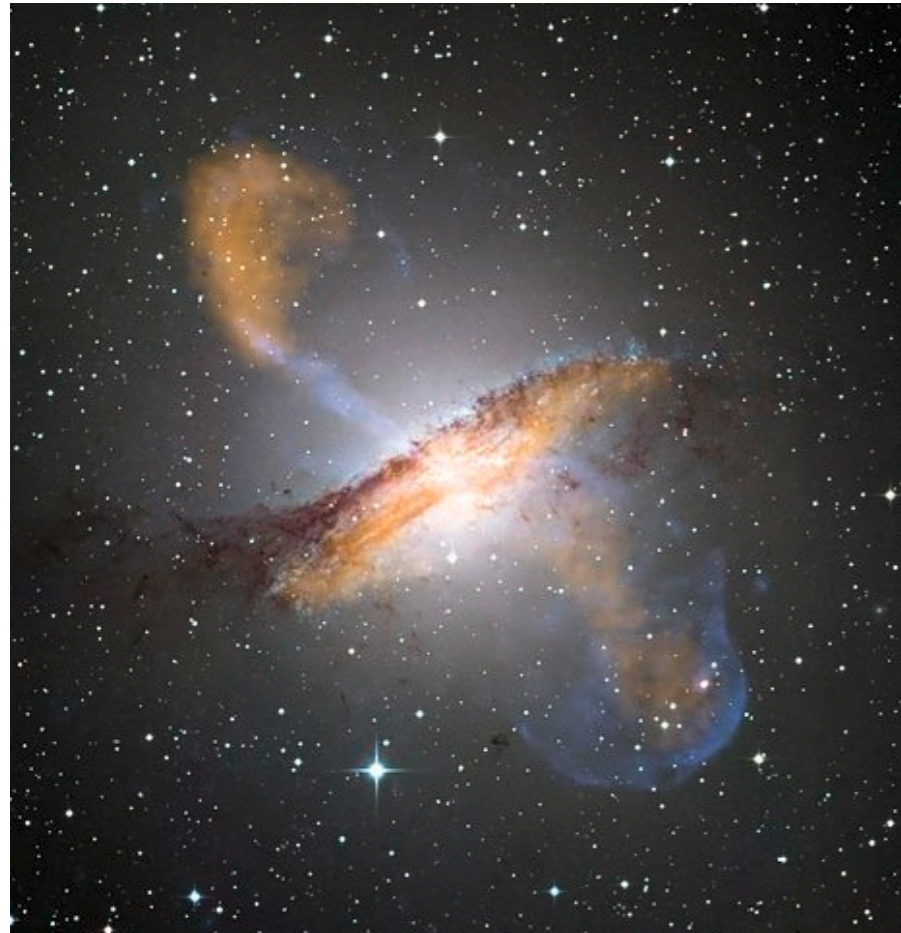
Shot noise limited



Chereknov Telescope Array

Active Galactic Nuclei

Supermassive Black Holes accreting gas

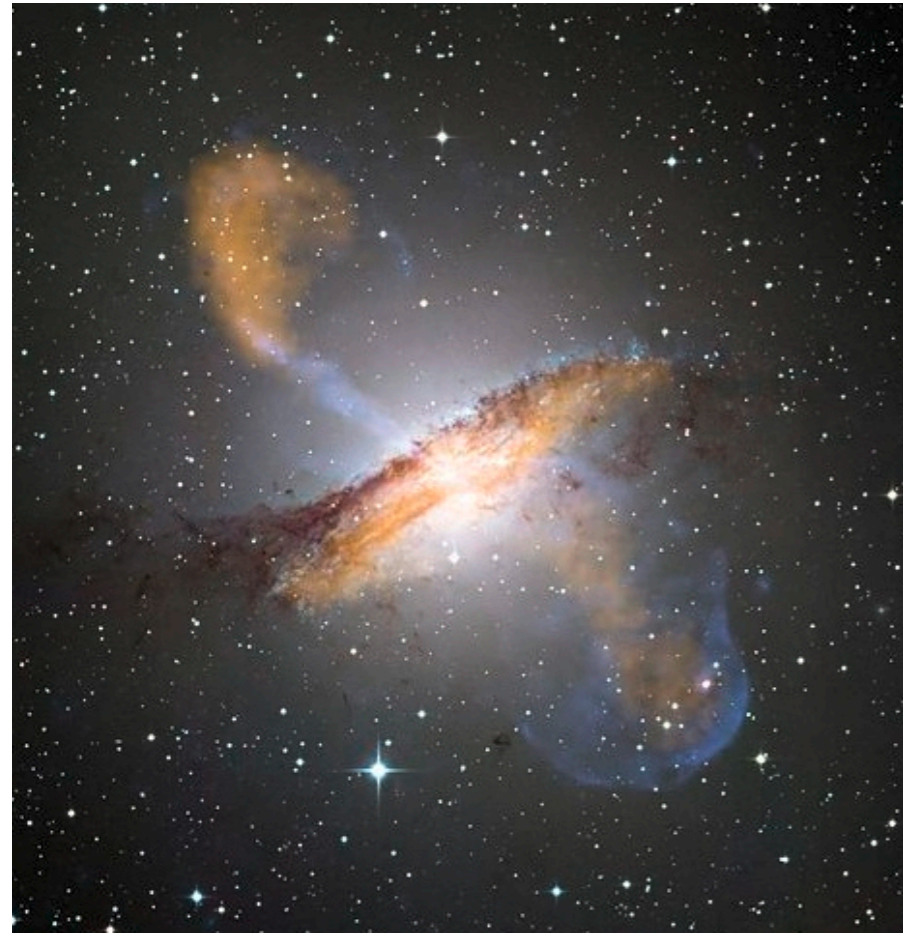


Centaurus A

Active Galactic Nuclei

Supermassive Black Holes accreting gas

$$\theta_{\text{ISCO}} \sim 0.02 - 0.2 \mu\text{as}$$



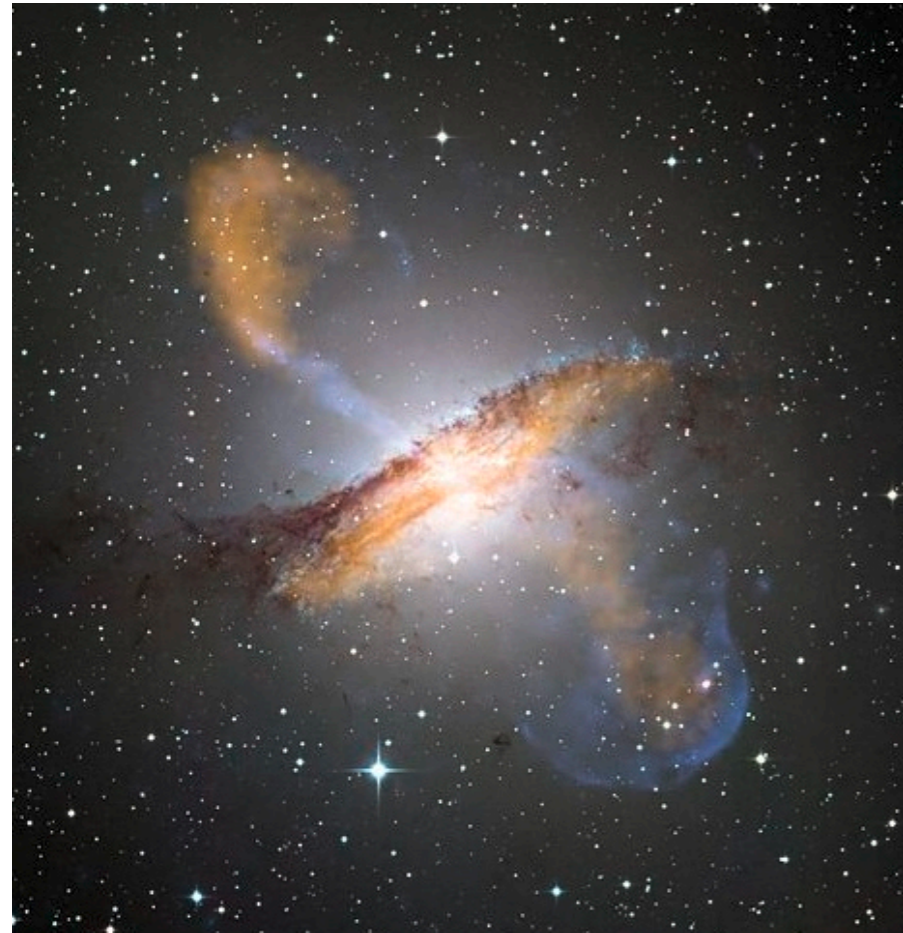
Centaurus A

Active Galactic Nuclei

Supermassive Black Holes accreting gas

$$\theta_{\text{ISCO}} \sim 0.02 - 0.2 \mu\text{as}$$

$$\theta_{\text{mean}} \sim 5 \mu\text{as}$$



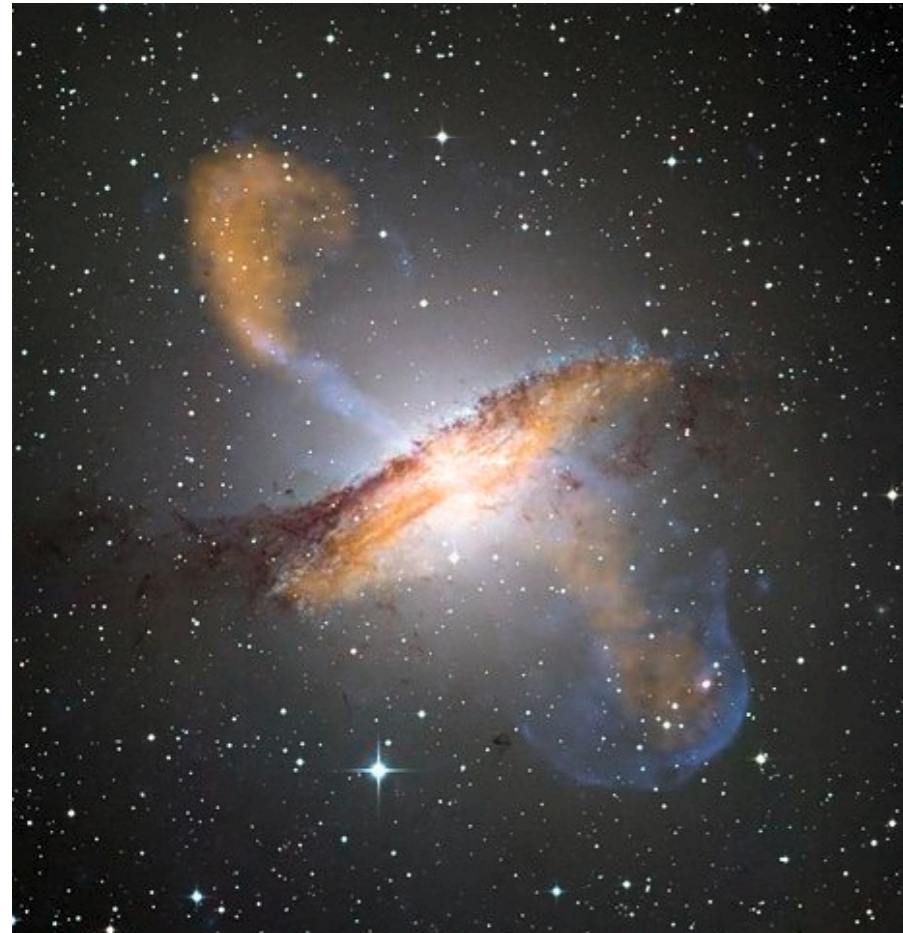
Centaurus A

Active Galactic Nuclei

Supermassive Black Holes accreting gas

$\theta_{\text{ISCO}} \sim 0.02 - 0.2 \mu\text{as}$ Baseline $\sim 460 - 4000\text{km}$

$\theta_{\text{mean}} \sim 5 \mu\text{as}$



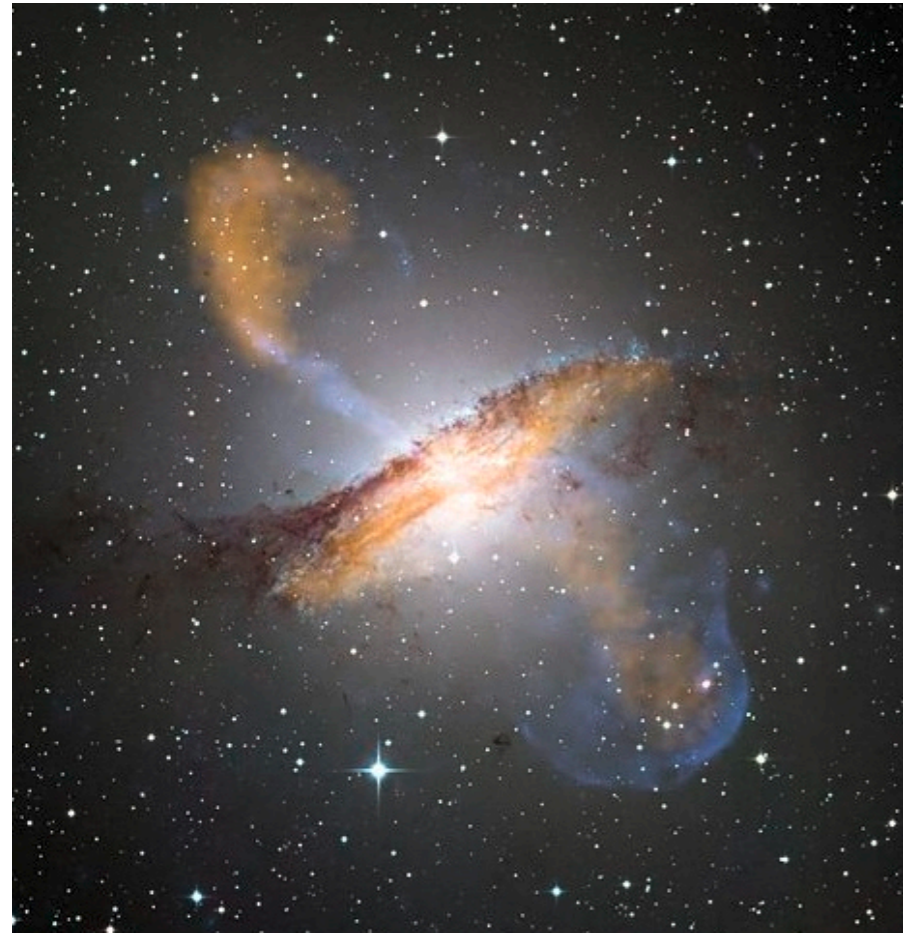
Centaurus A

Active Galactic Nuclei

Supermassive Black Holes accreting gas

$\theta_{\text{ISCO}} \sim 0.02 - 0.2 \mu\text{as}$ Baseline $\sim 460 - 4000\text{km}$

$\theta_{\text{mean}} \sim 5 \mu\text{as}$ Baseline $\sim 20\text{km}$



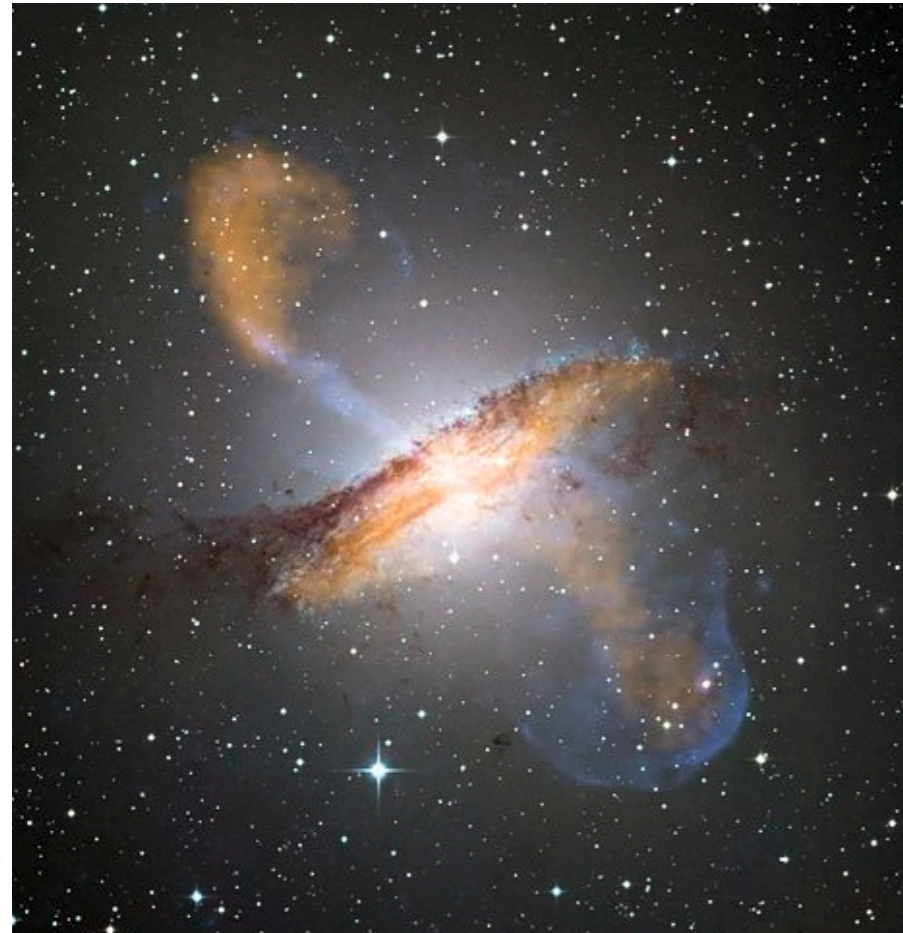
Centaurus A

Active Galactic Nuclei

Supermassive Black Holes accreting gas

$\theta_{\text{ISCO}} \sim 0.02 - 0.2 \mu\text{as}$ Baseline $\sim 460 - 4000\text{km}$

$\theta_{\text{mean}} \sim 5 \mu\text{as}$ Baseline $\sim 20\text{km}$



Centaurus A

Two applications:

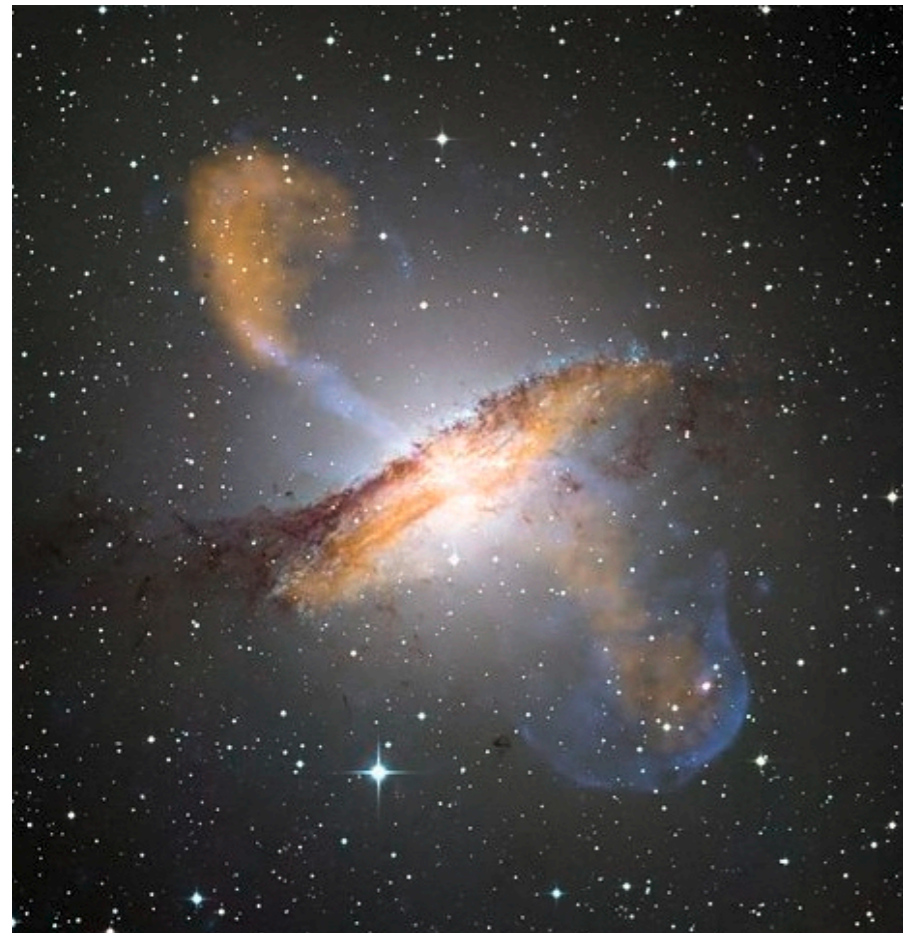
[N. Dalal, **MG**, C. Gammie, S. Gralla, N. Murray, 2024]

Active Galactic Nuclei

Supermassive Black Holes accreting gas

$\theta_{\text{ISCO}} \sim 0.02 - 0.2 \mu\text{as}$ Baseline $\sim 460 - 4000\text{km}$

$\theta_{\text{mean}} \sim 5 \mu\text{as}$ Baseline $\sim 20\text{km}$



Centaurus A

Two applications:

1. Resolve accretion disks of **nearby** AGNs and study their physics

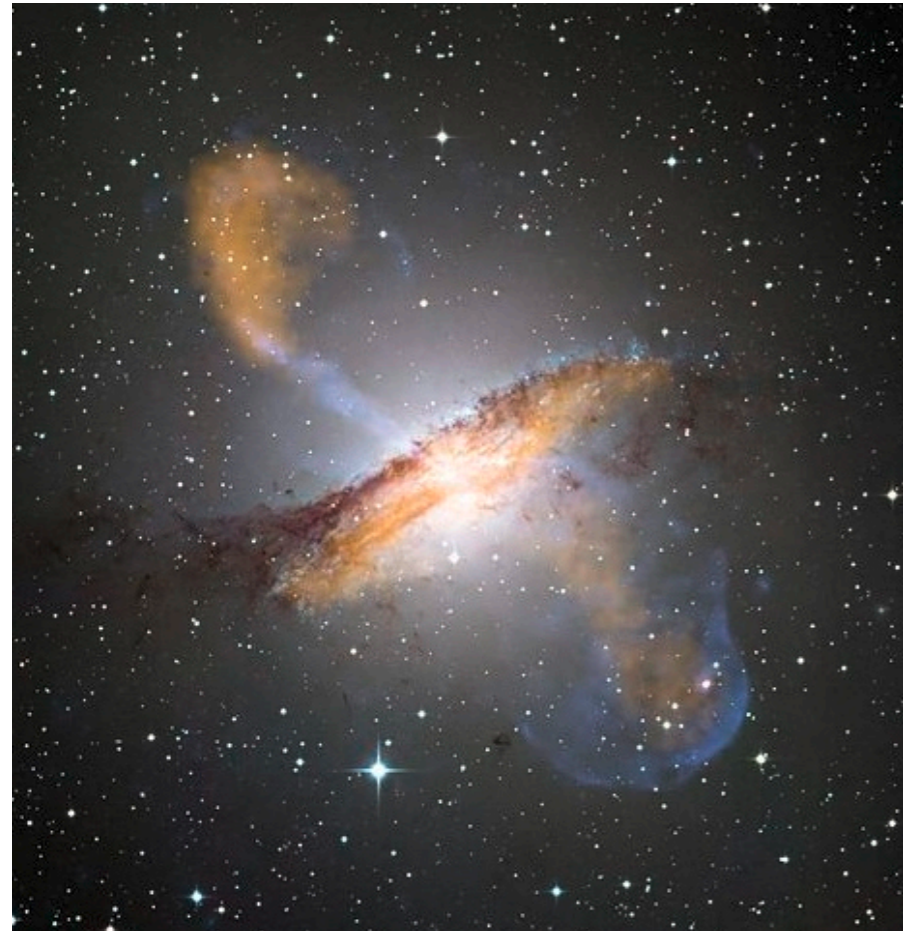
[N. Dalal, **MG**, C. Gammie, S. Gralla, N. Murray, 2024]

Active Galactic Nuclei

Supermassive Black Holes accreting gas

$\theta_{\text{ISCO}} \sim 0.02 - 0.2 \mu\text{as}$ Baseline $\sim 460 - 4000\text{km}$

$\theta_{\text{mean}} \sim 5 \mu\text{as}$ Baseline $\sim 20\text{km}$



Centaurus A

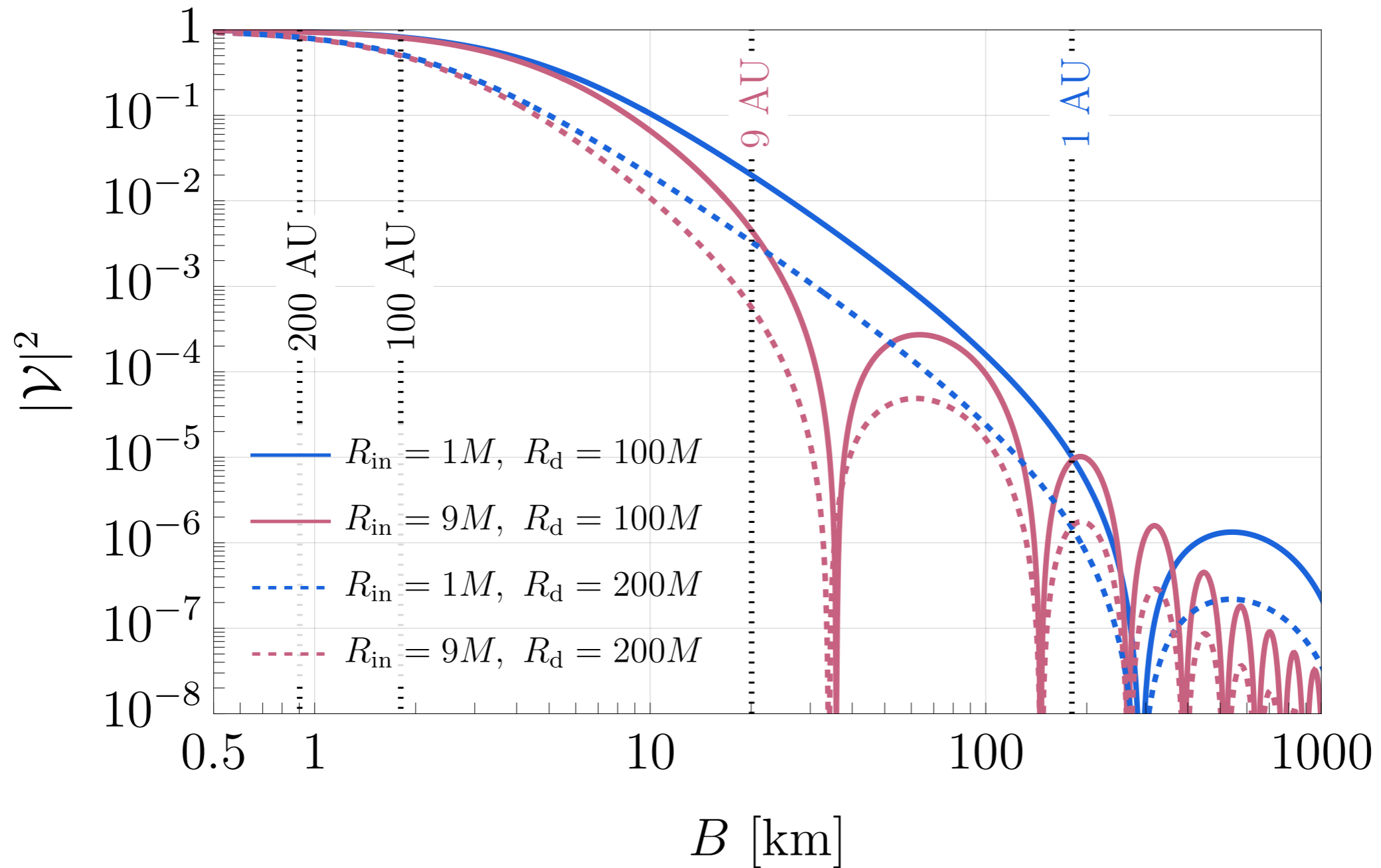
Two applications:

1. Resolve accretion disks of **nearby** AGNs and study their physics
2. Resolve the Broad Line Region of **distant** AGN and probe H_0

[N. Dalal, **MG**, C. Gammie, S. Gralla, N. Murray, 2024]

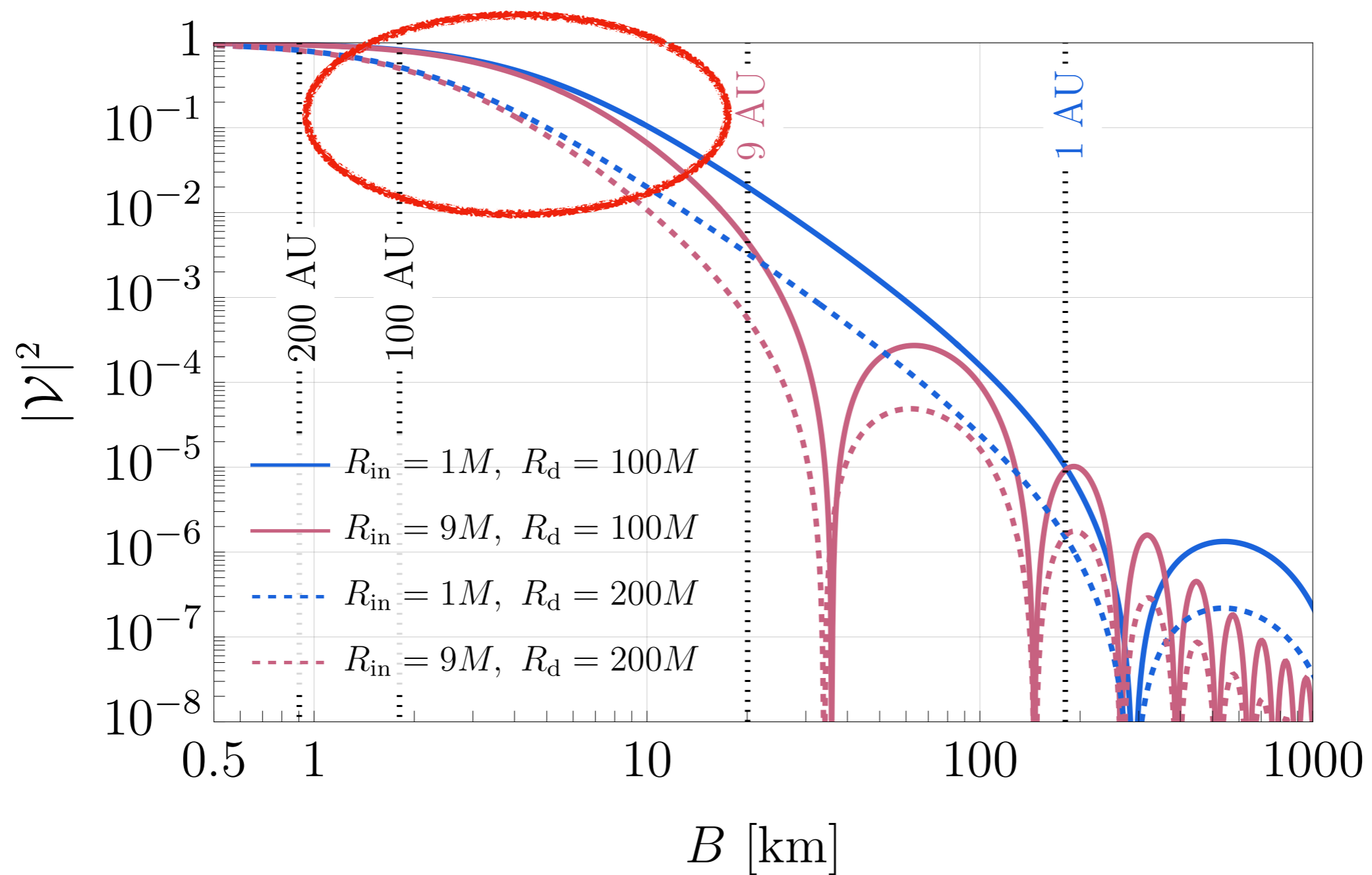
Application 1: AGN disks

Toy example: Shakura-Sunyaev



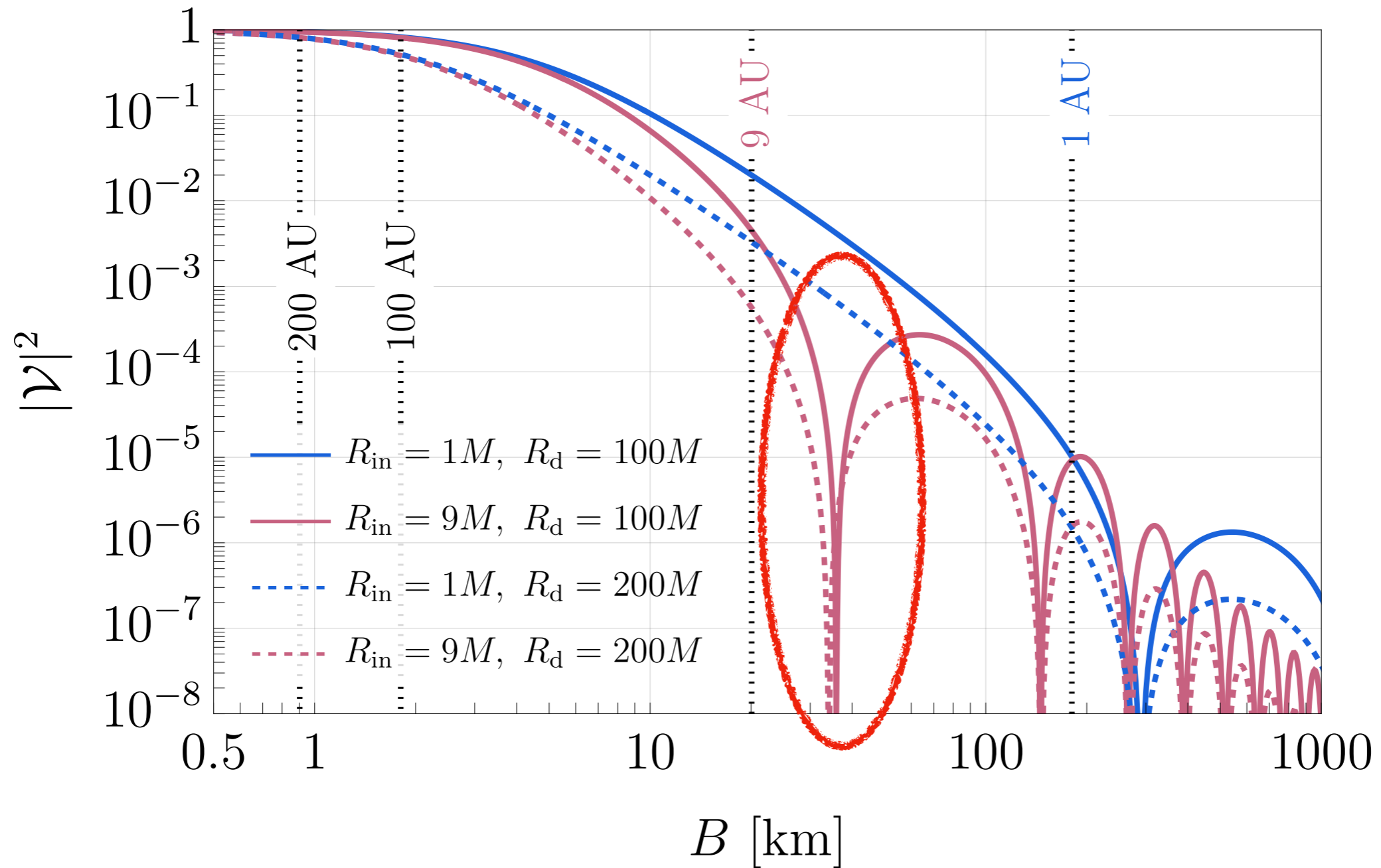
$$T \sim T_0 \left(\frac{R_0}{R} \right)^n \left[1 - \left(\frac{R_{\text{ISCO}}}{R} \right)^{\frac{1}{2}} \right]^{\frac{1}{4}}$$

Toy example: Shakura-Sunyaev



$$T \sim T_0 \left(\frac{R_0}{R} \right)^n \left[1 - \left(\frac{R_{\text{ISCO}}}{R} \right)^{\frac{1}{2}} \right]^{\frac{1}{4}}$$

Toy example: Shakura-Sunyaev



$$T \sim T_0 \left(\frac{R_0}{R} \right)^n \left[1 - \left(\frac{R_{\text{ISCO}}}{R} \right)^{\frac{1}{2}} \right]^{\frac{1}{4}}$$

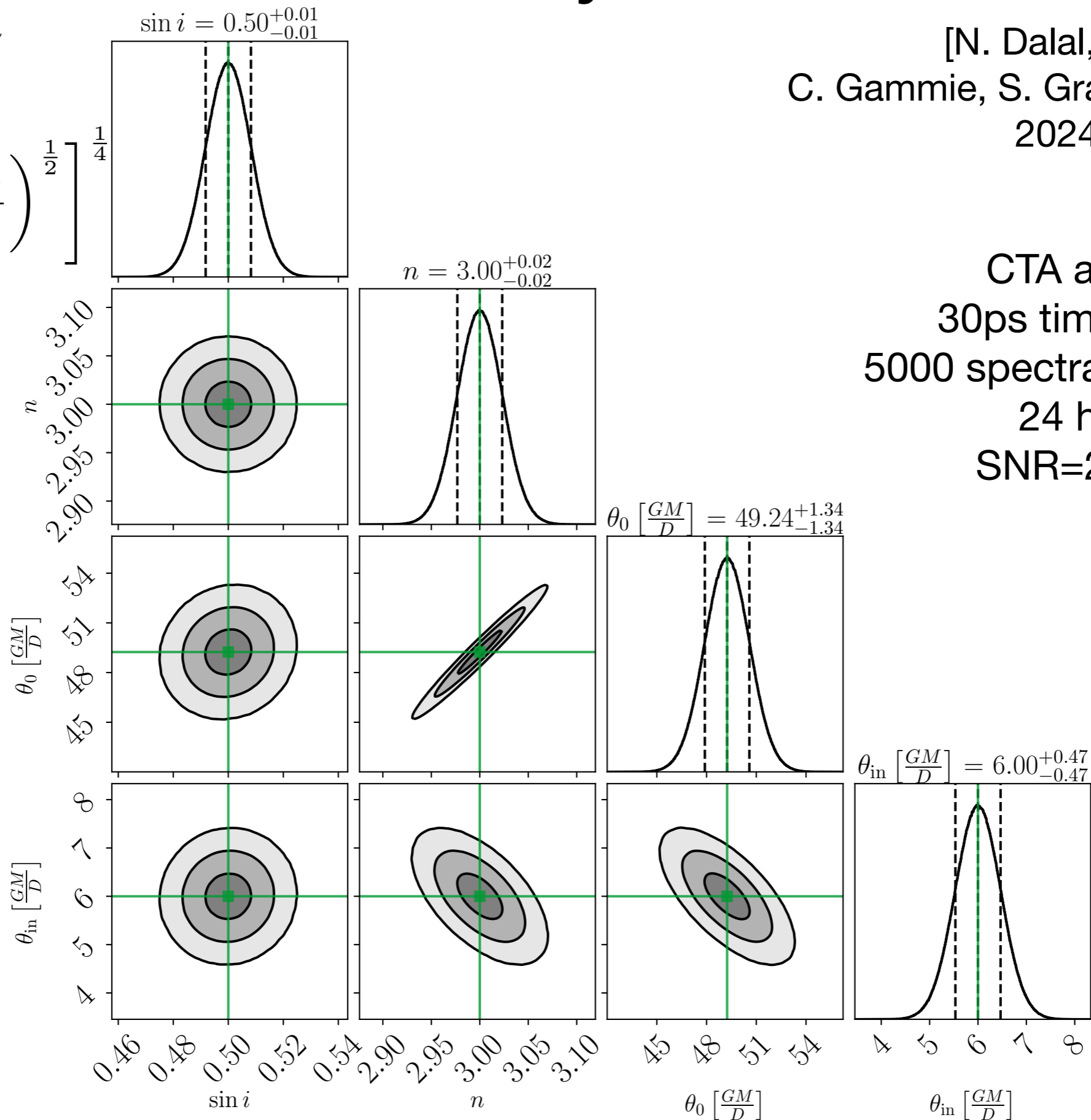
Shakura-Sunyaev Fisher

$$T \sim T_0 \left(\frac{R_0}{R} \right)^n$$

$$\times \left[1 - \left(\frac{R_{\text{ISCO}}}{R} \right)^{\frac{1}{2}} \right]^{\frac{1}{4}}$$

[N. Dalal, **MG**,
C. Gammie, S. Gralla, N. Murray,
2024]

CTA array
30ps time-jitter
5000 spectral channels
24 hrs
SNR=2750



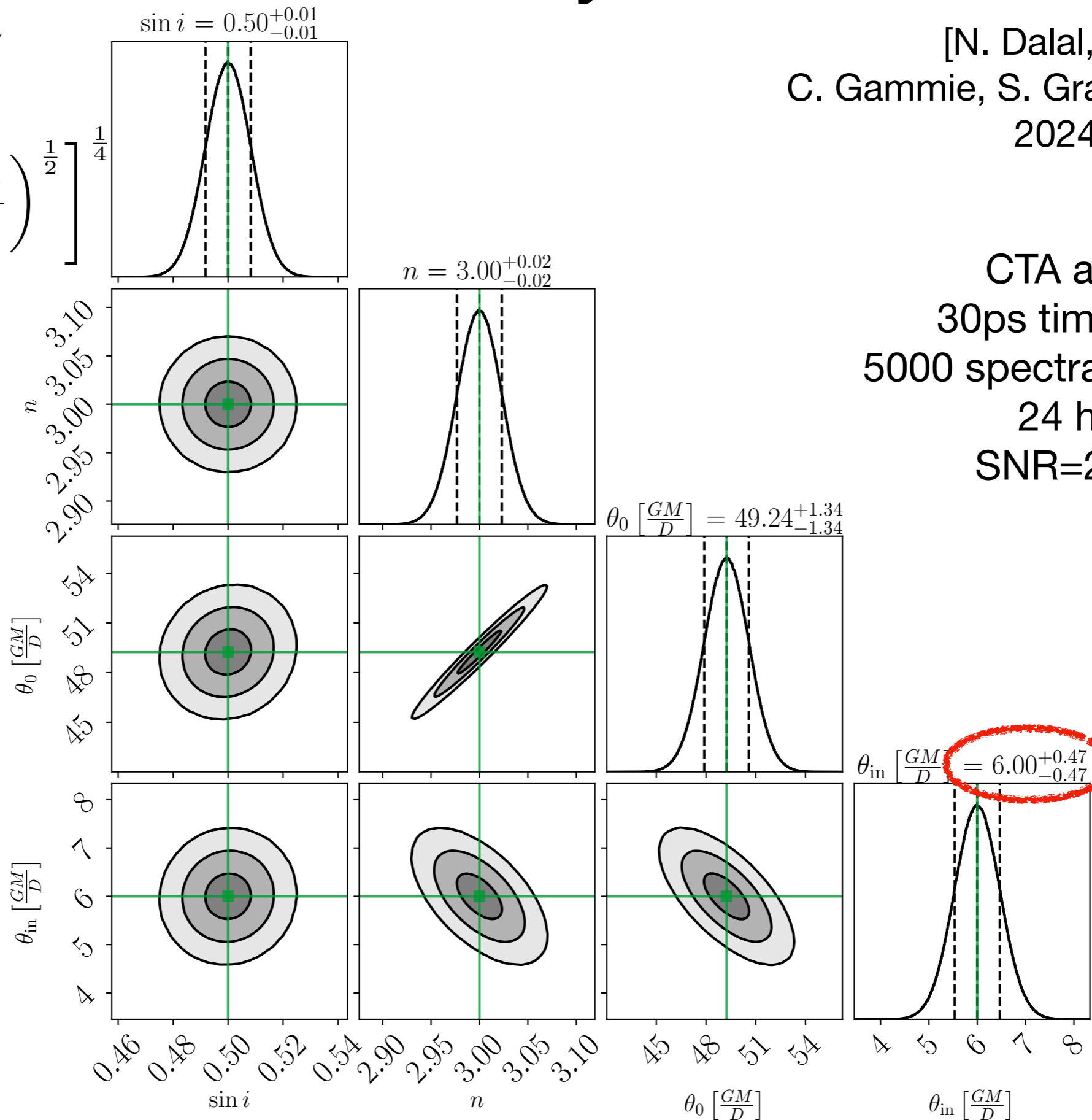
Shakura-Sunyaev Fisher

$$T \sim T_0 \left(\frac{R_0}{R} \right)^n$$

$$\times \left[1 - \left(\frac{R_{\text{ISCO}}}{R} \right)^{\frac{1}{2}} \right]^{\frac{1}{4}}$$

[N. Dalal, **MG**,
C. Gammie, S. Gralla, N. Murray,
2024]

CTA array
30ps time-jitter
5000 spectral channels
24 hrs
SNR=2750

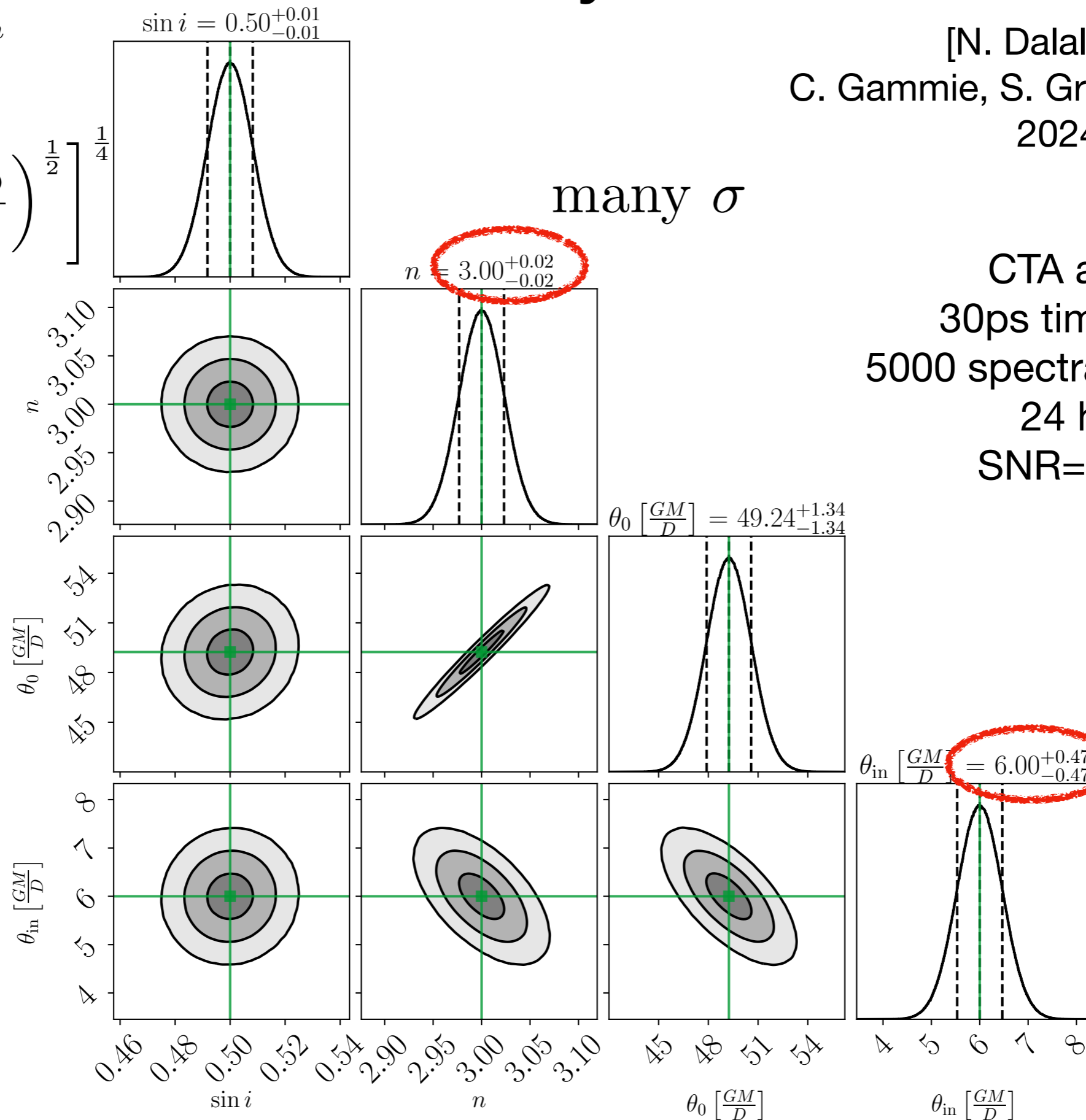


Shakura-Sunyaev Fisher

$$T \sim T_0 \left(\frac{R_0}{R} \right)^n$$

$$\times \left[1 - \left(\frac{R_{\text{ISCO}}}{R} \right)^{\frac{1}{2}} \right]^{\frac{1}{4}}$$

[N. Dalal, **MG**,
C. Gammie, S. Gralla, N. Murray,
2024]



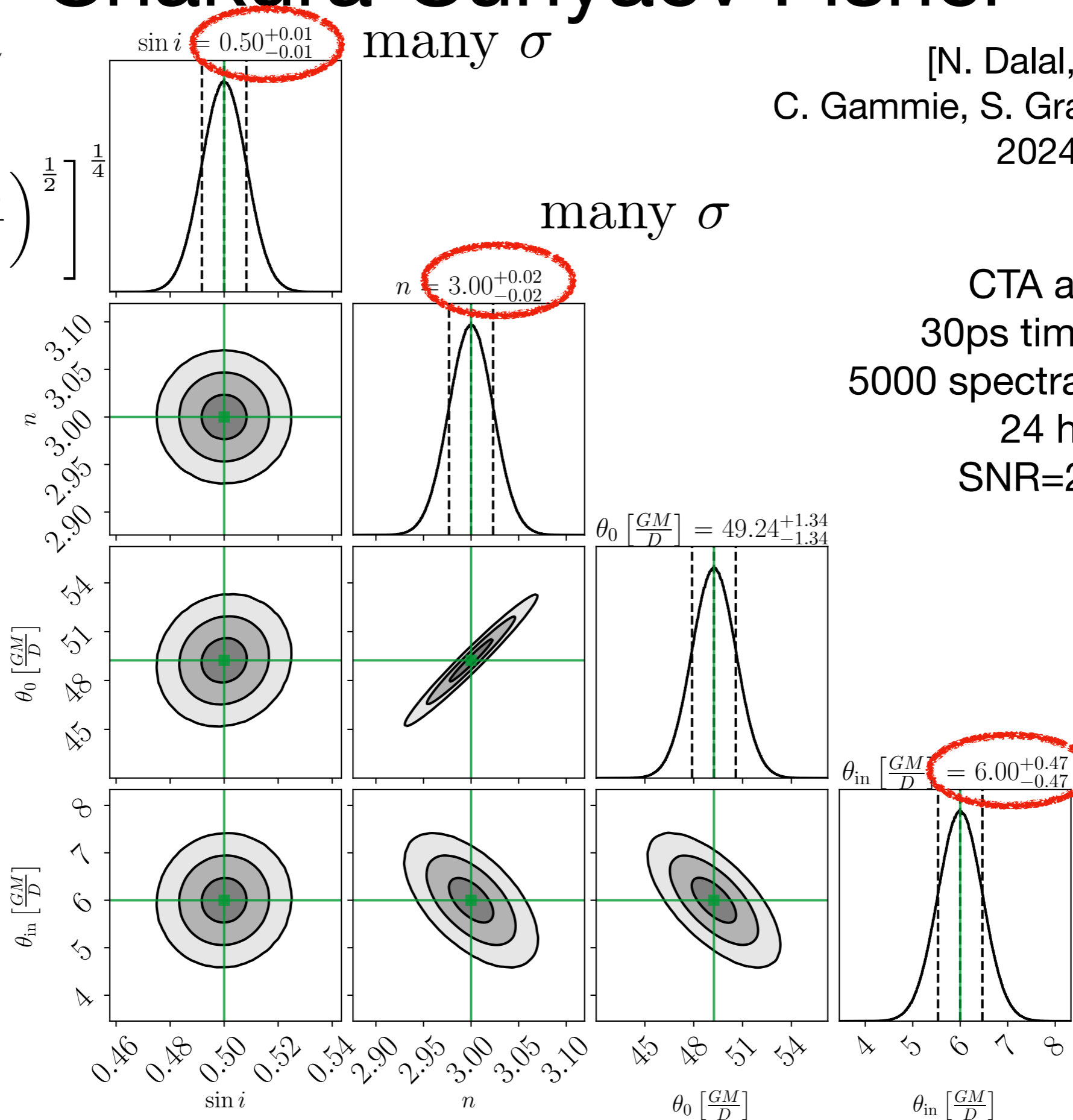
CTA array
30ps time-jitter
5000 spectral channels
24 hrs
SNR=2750

Shakura-Sunyaev Fisher

$$T \sim T_0 \left(\frac{R_0}{R} \right)^n$$

$$\times \left[1 - \left(\frac{R_{\text{ISCO}}}{R} \right)^{\frac{1}{2}} \right]^{\frac{1}{4}}$$

[N. Dalal, **MG**,
C. Gammie, S. Gralla, N. Murray,
2024]



CTA array
30ps time-jitter
5000 spectral channels
24 hrs
SNR=2750

Why is this useful?

Why is this useful?

Inclination: Probes unification model of AGNs

Why is this useful?

Inclination: Probes unification model of AGNs

Slope: Probes departure from classical thin disk theory

Why is this useful?

Inclination: Probes unification model of AGNs

Slope: Probes departure from classical thin disk theory

Inner structure: Can measure environment at the BH,
spin?

Why is this useful?

Inclination: Probes unification model of AGNs

Slope: Probes departure from classical thin disk theory

Inner structure: Can measure environment at the BH,
spin?

No other way to do this!

Application 2: H_0

Application 2: H_0

We need:

Application 2: H_0

We need: 1. One angular size $\theta \sim \frac{L}{D}$

Application 2: H_0

We need: 1. One angular size $\theta \sim \frac{L}{D}$
→ Intensity Interferometry

Application 2: H_0

- We need:
1. One angular size $\theta \sim \frac{L}{D}$
→ Intensity Interferometry
 2. The dimensionful size $\sim L$

Application 2: H_0

- We need:
1. One angular size $\theta \sim \frac{L}{D}$
→ Intensity Interferometry
 2. The dimensionful size $\sim L$
→ Reverberation Mapping

Application 2: H_0

- We need:
1. One angular size $\theta \sim \frac{L}{D}$
→ Intensity Interferometry
 2. The dimensionful size $\sim L$
→ Reverberation Mapping
 3. A redshift $H_0 \sim \frac{z}{D}$

Application 2: H_0

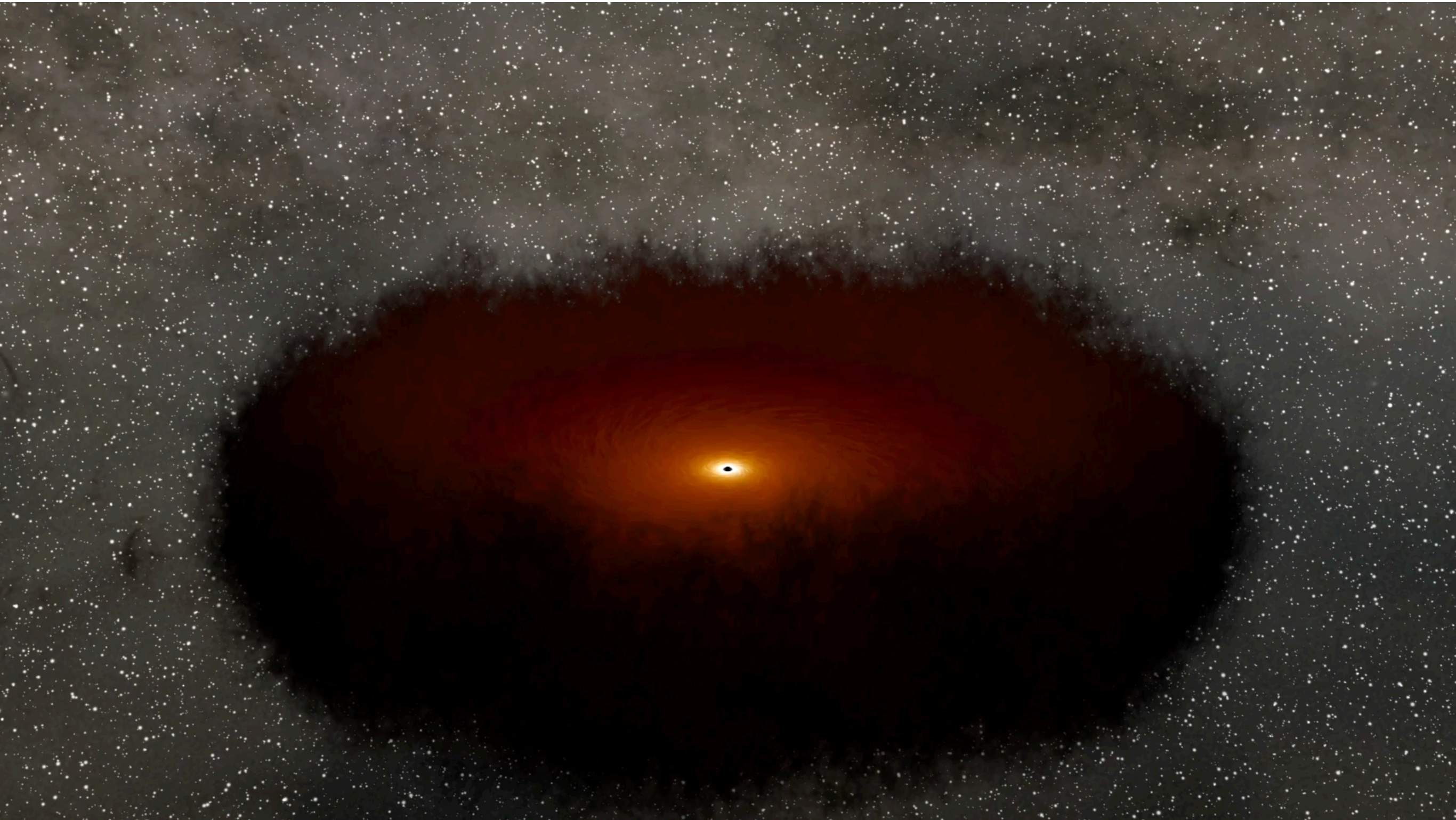
- We need:
1. One angular size $\theta \sim \frac{L}{D}$
→ Intensity Interferometry
 2. The dimensionful size $\sim L$
→ Reverberation Mapping
 3. A redshift $H_0 \sim \frac{z}{D}$
→ Line emission

Application 2: H_0

- We need:
1. One angular size $\theta \sim \frac{L}{D}$
→ Intensity Interferometry
 2. The dimensionful size $\sim L$
→ Reverberation Mapping
 3. A redshift $H_0 \sim \frac{z}{D}$
→ Line emission



Reverberation Mapping



Reverberation Mapping



Reverberation Mapping



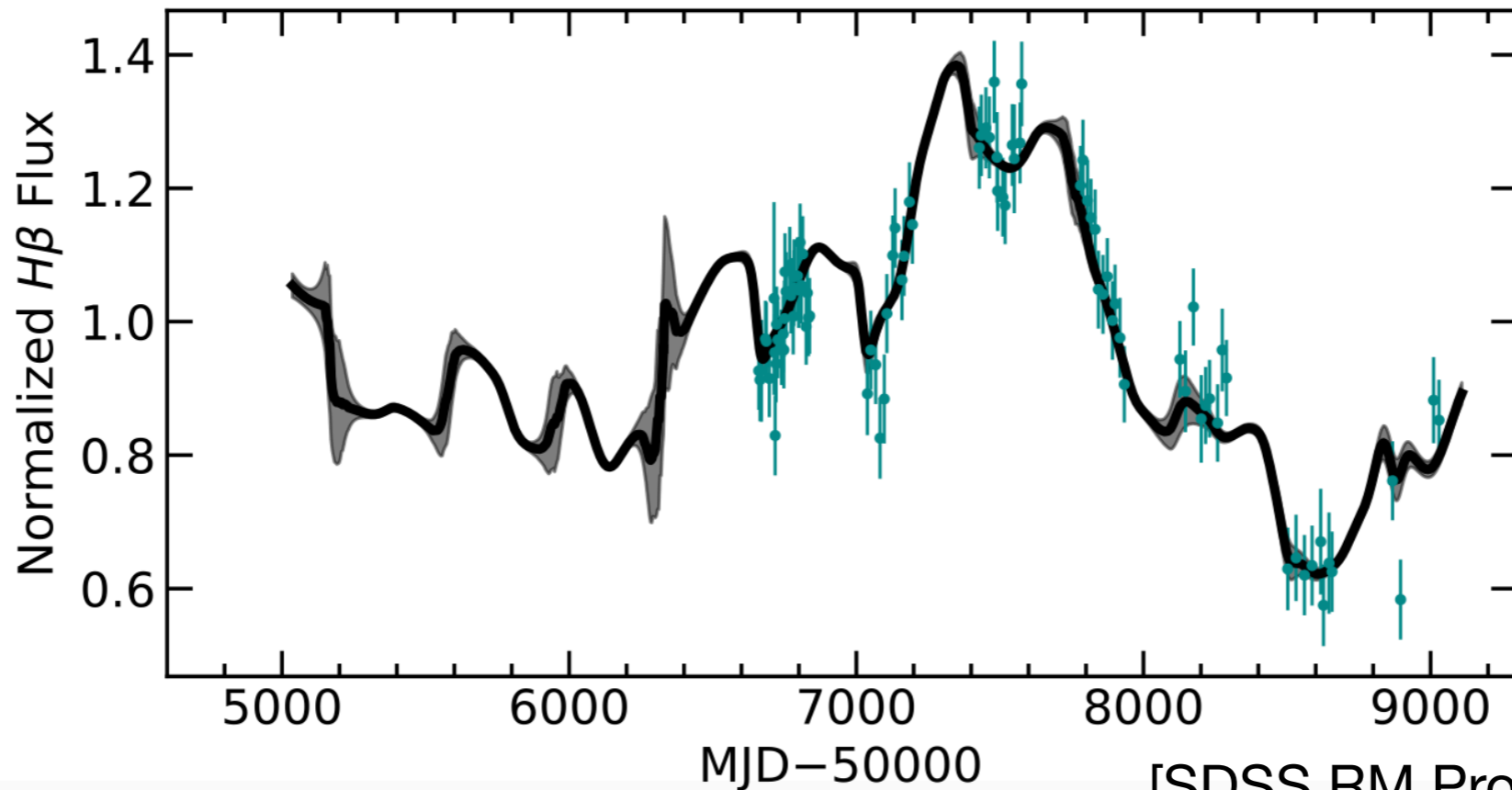
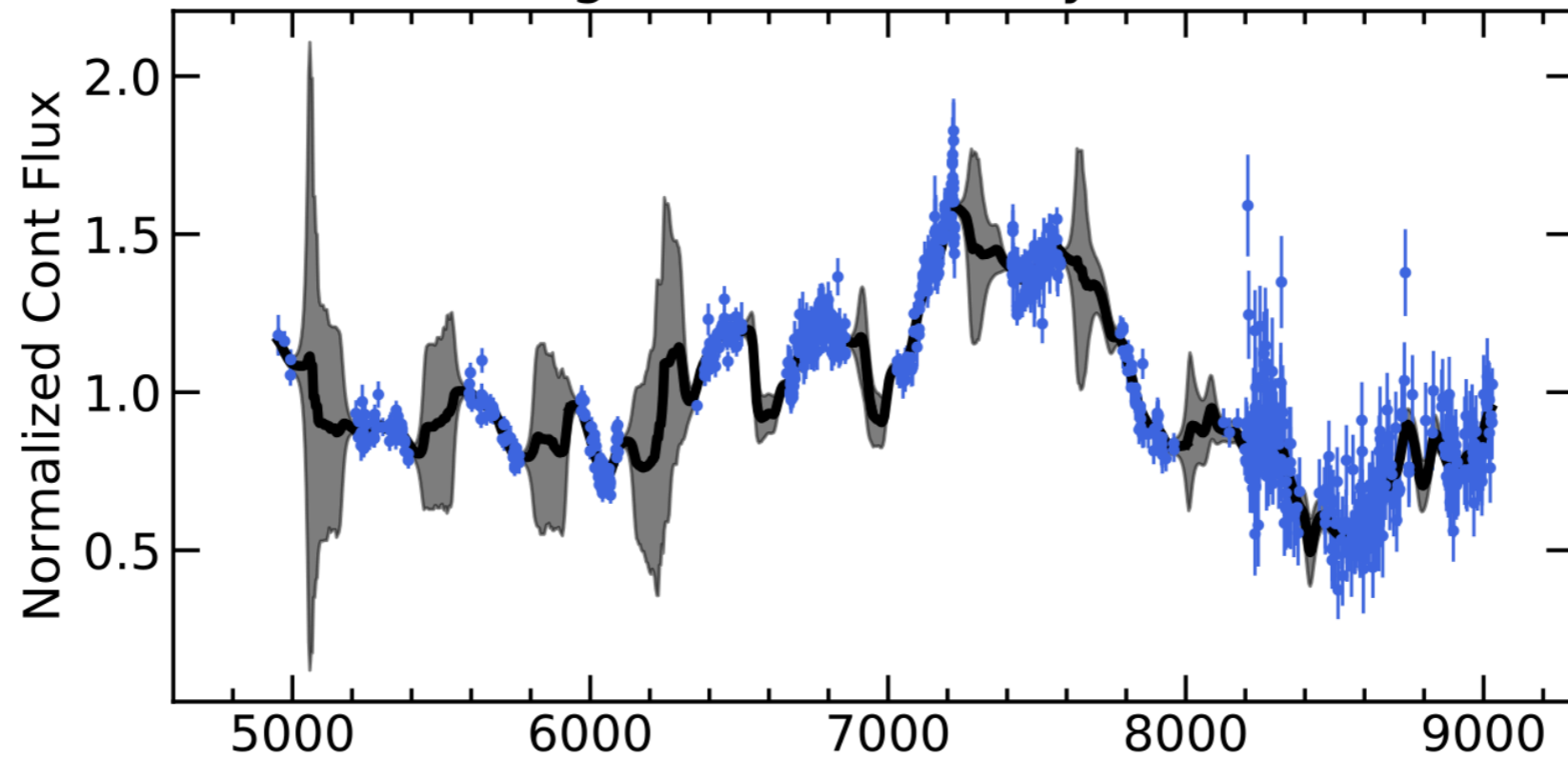
Reverberation Mapping



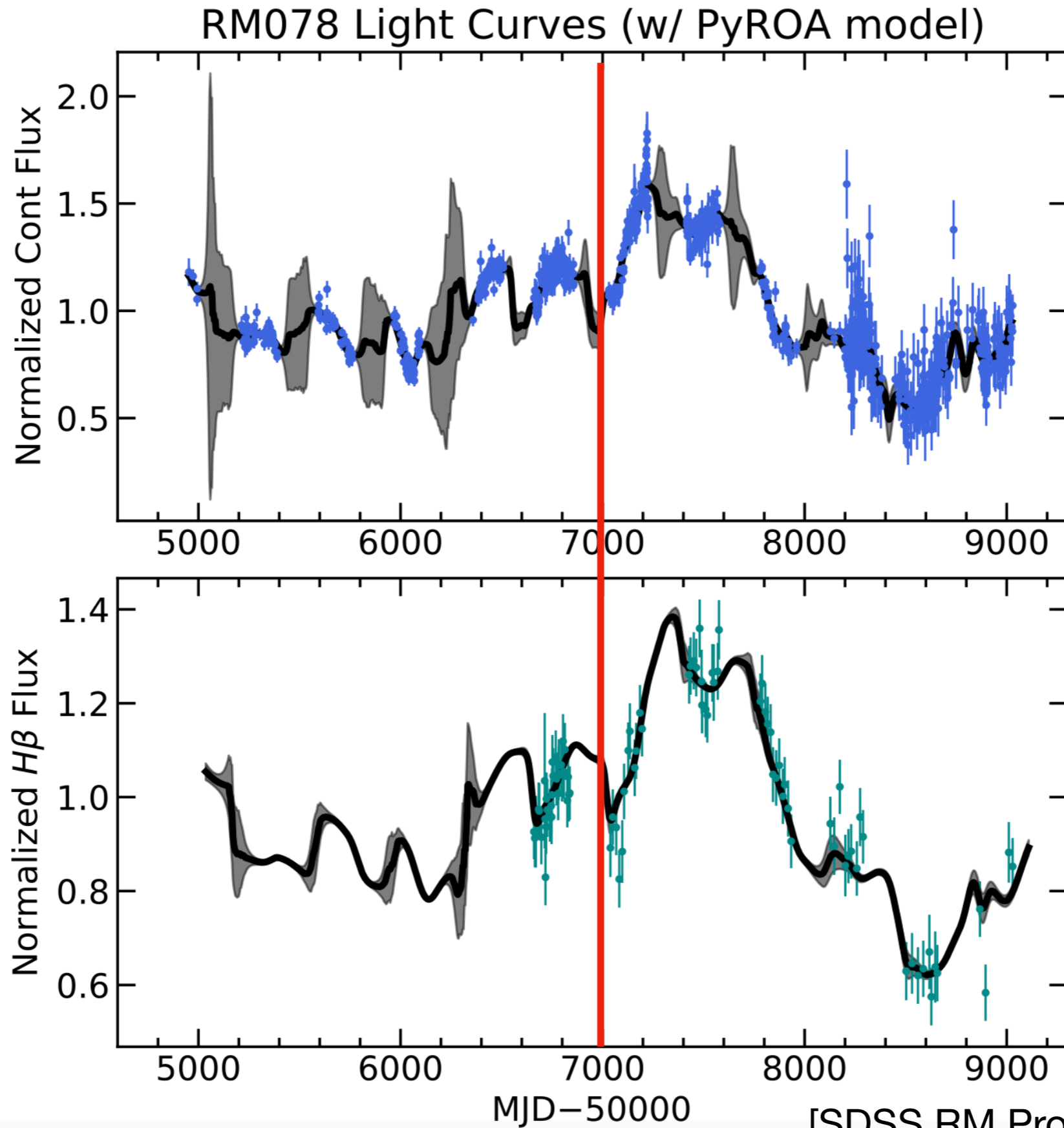
Time-delay gives physical size

Reverberation Mapping

RM078 Light Curves (w/ PyROA model)

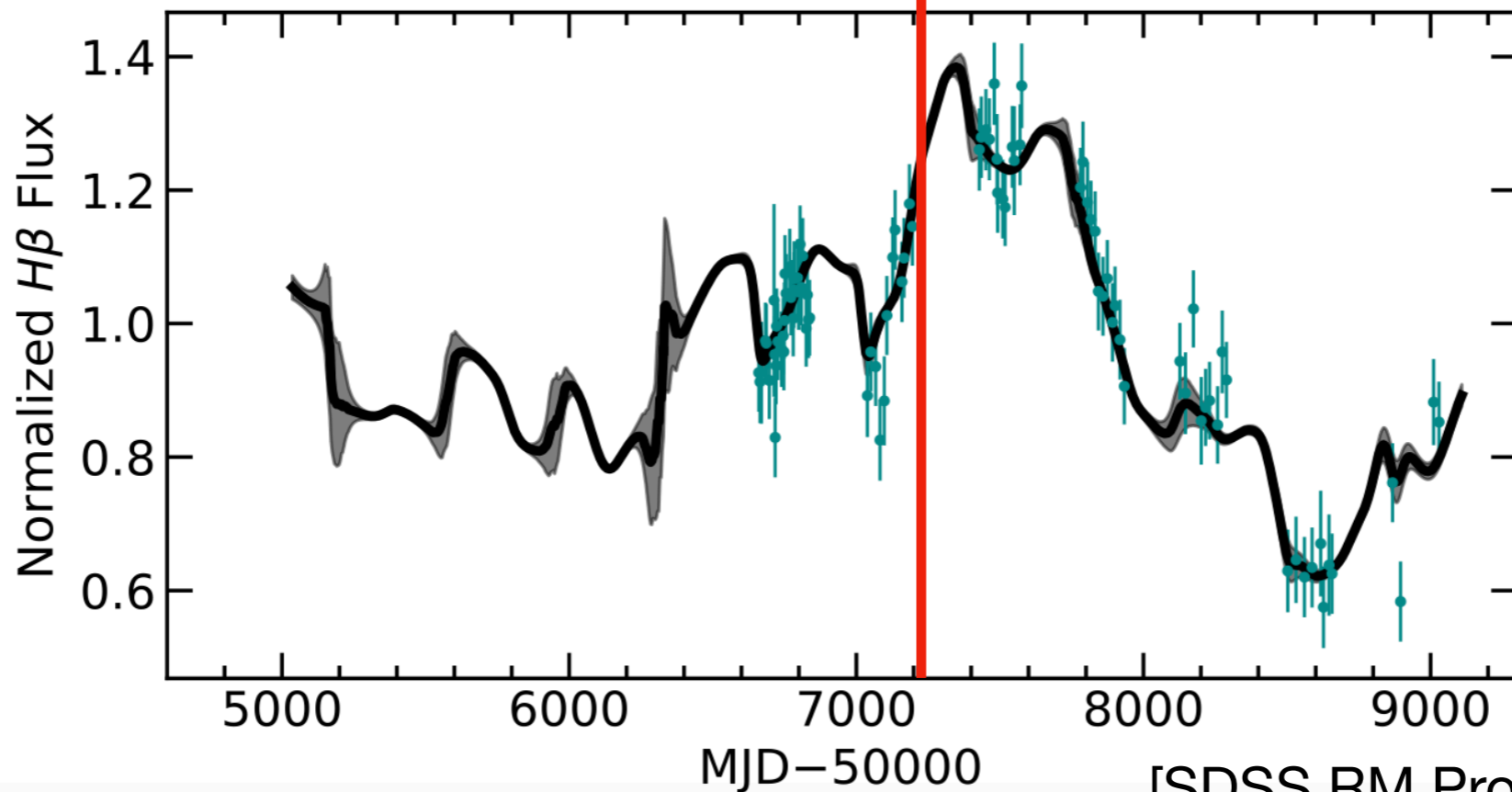
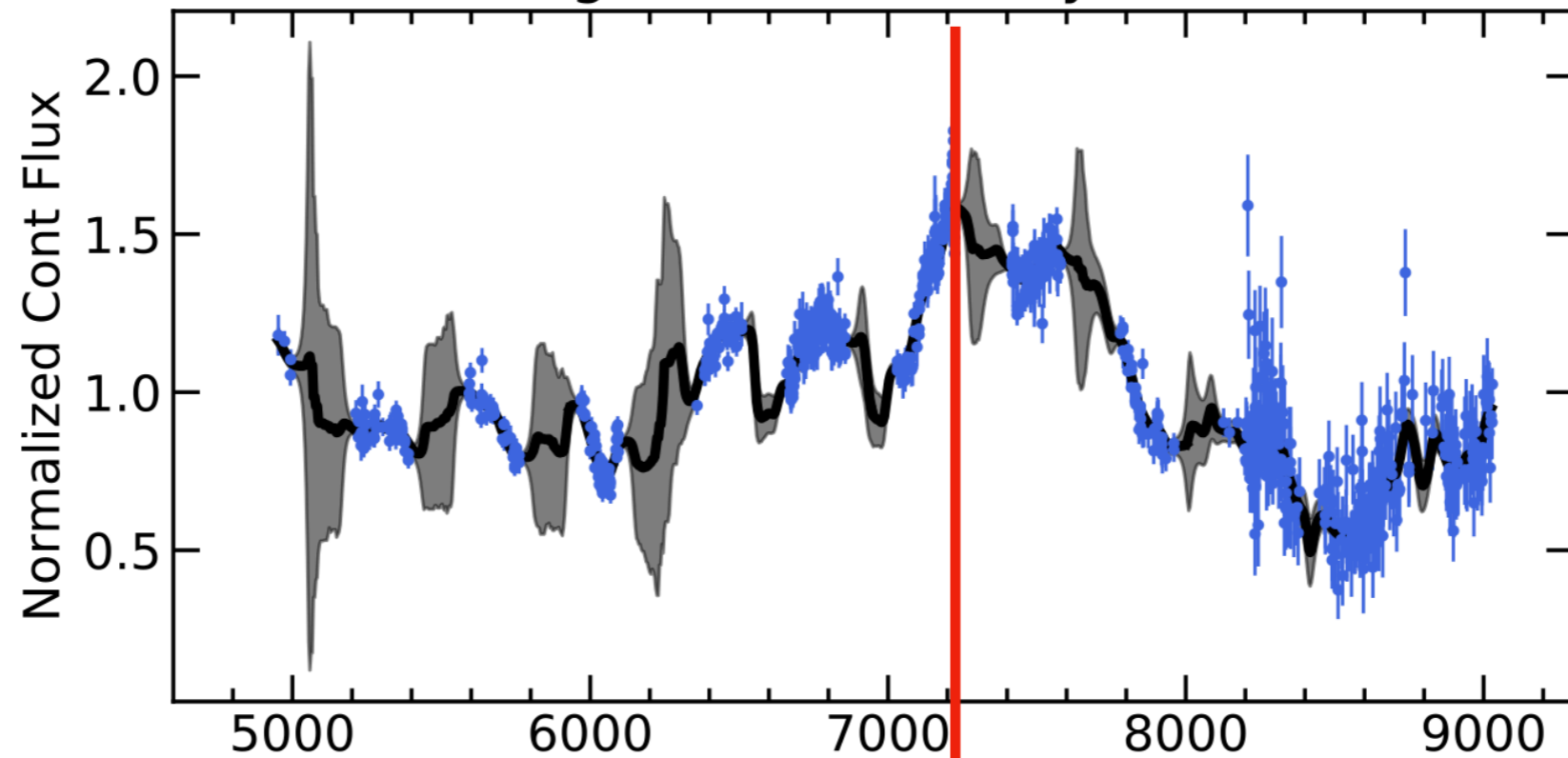


Reverberation Mapping



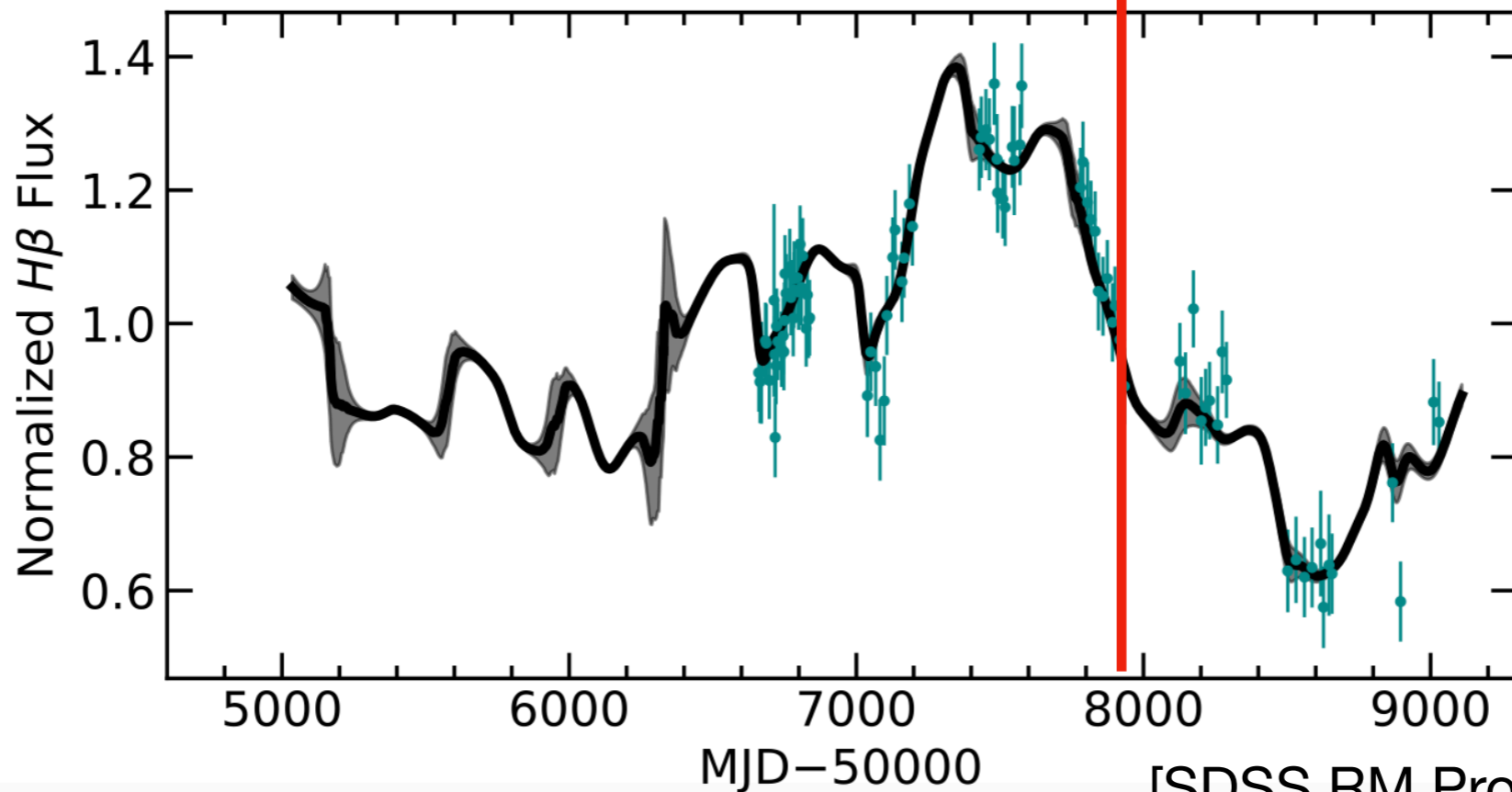
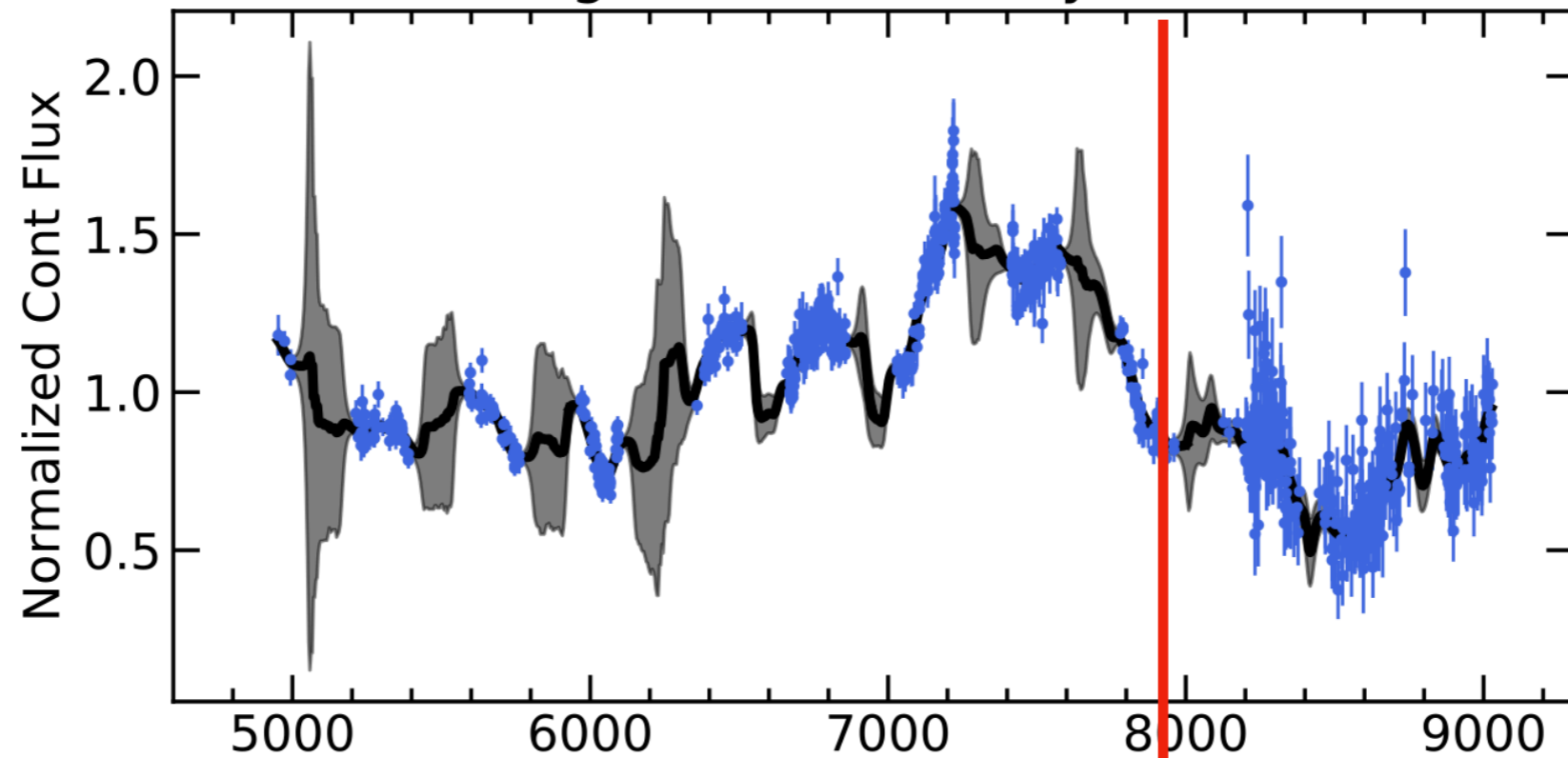
Reverberation Mapping

RM078 Light Curves (w/ PyROA model)



Reverberation Mapping

RM078 Light Curves (w/ PyROA model)



Application 2: H_0

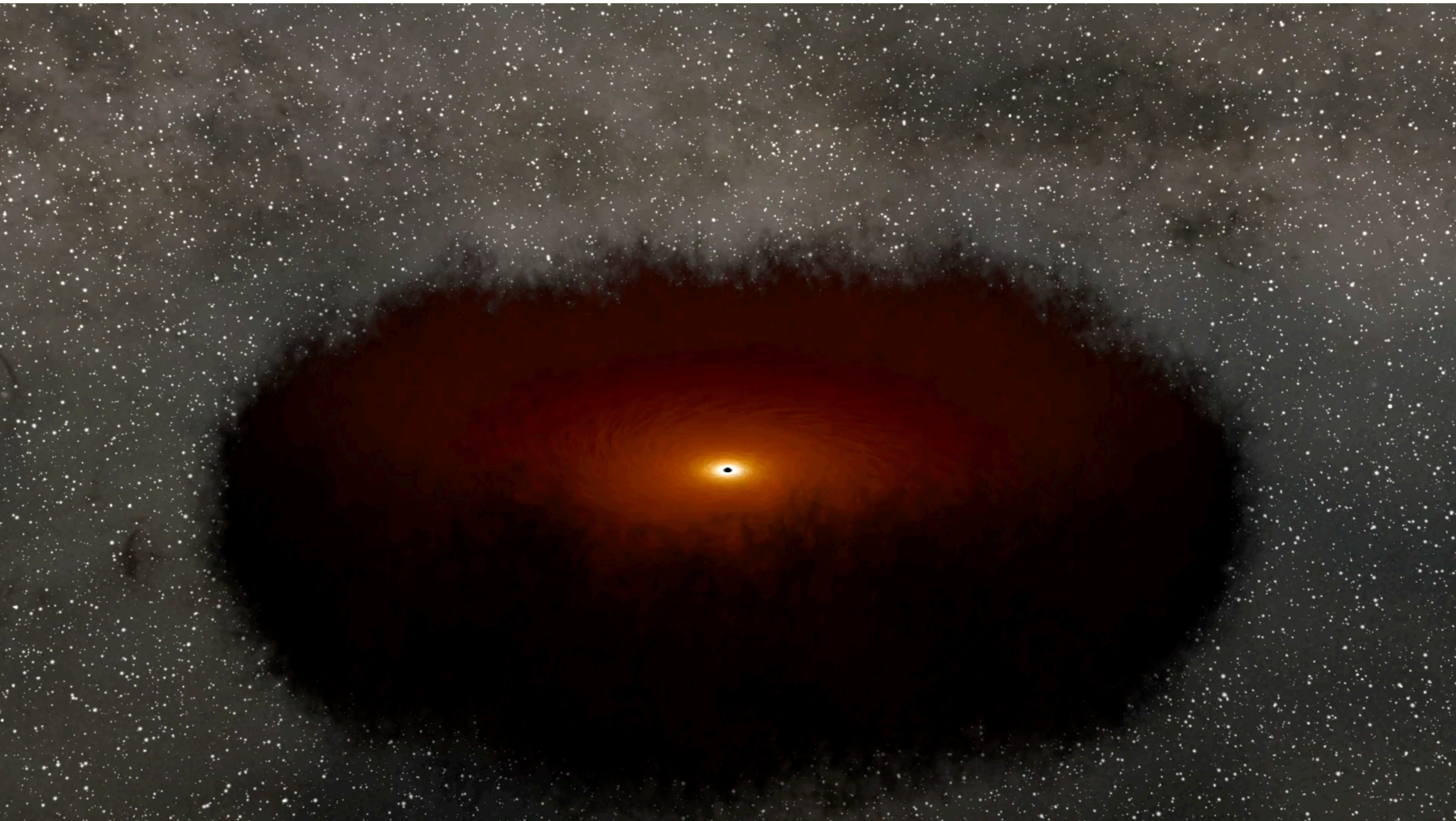
- We need:
1. One angular size $\theta \sim \frac{L}{D}$
→ Intensity Interferometry
 2. The dimensionful size $\sim L$
→ Reverberation Mapping
 3. A redshift $H_0 \sim \frac{z}{D}$
→ Line emission



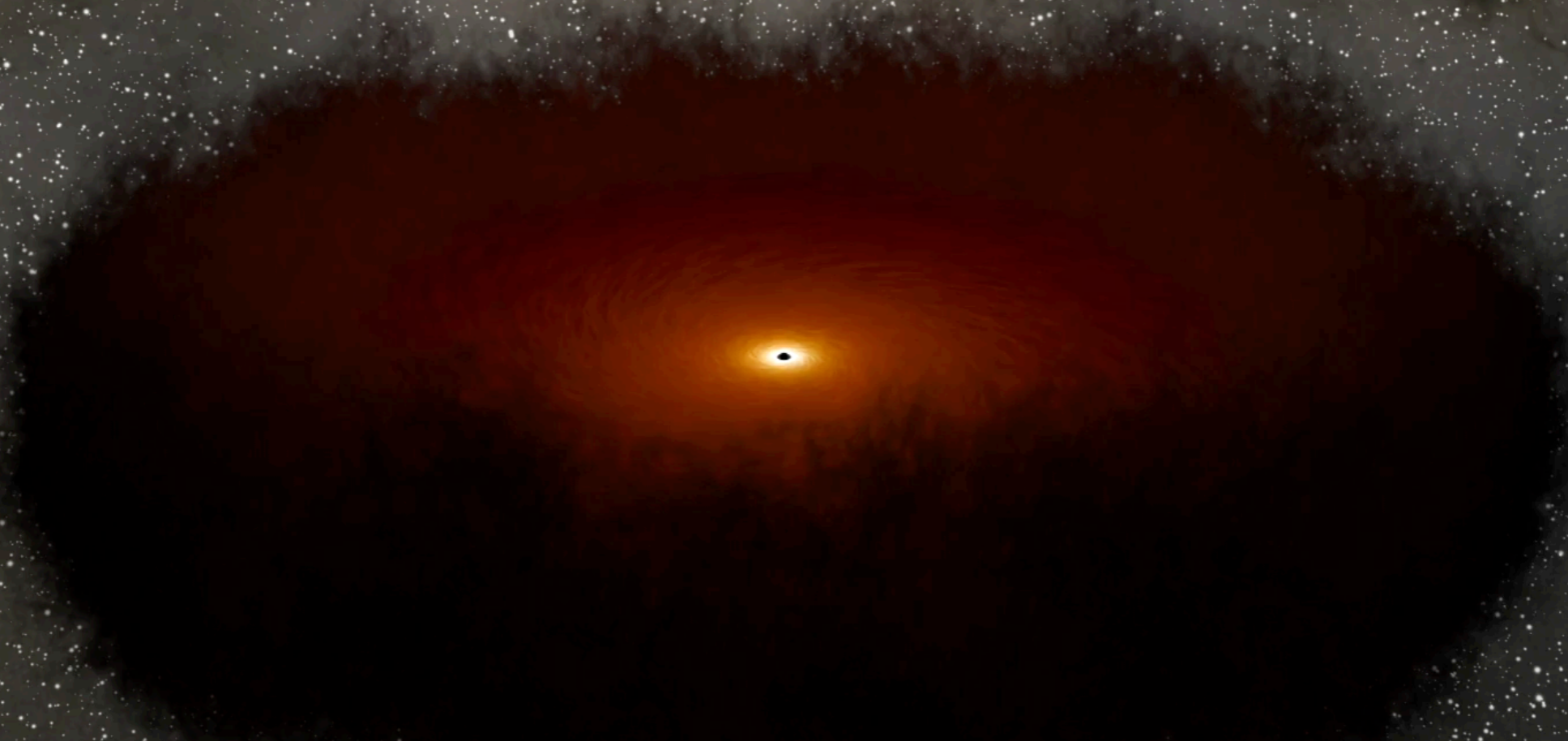
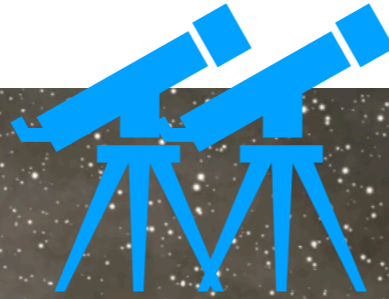
Application 2: H_0

- We need:
1. One angular size $\theta \sim \frac{L}{D}$
→ Intensity Interferometry
 2. The dimensionful size $\sim L$ ✓
→ Reverberation Mapping
 3. A redshift $H_0 \sim \frac{z}{D}$ ✓
→ Line emission

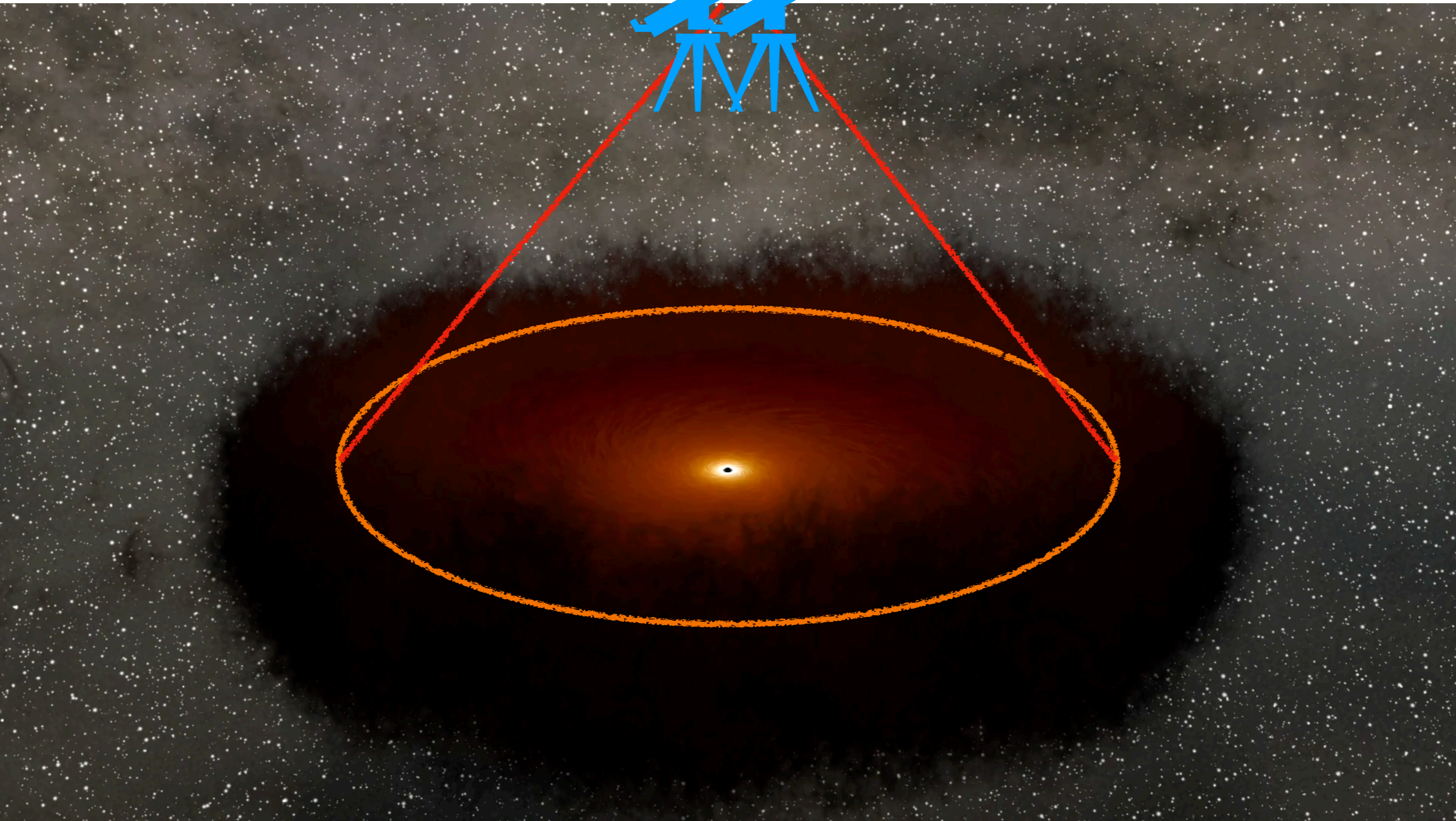
Intensity Interferometry



Intensity Interferometry





Intensity Interferometry



Intensity Interferometry gives angular size

[N. Dalal, **MG**, C. Gammie, S. Gralla, N. Murray, 2024]

Application 2: H_0

- We need:
1. One angular size $\theta \sim \frac{L}{D}$
→ Intensity Interferometry
 2. The dimensionful size $\sim L$
→ Reverberation Mapping 
 3. A redshift $H_0 \sim \frac{z}{D}$
→ Line emission 

Application 2: H_0

We need:

1. One angular size $\theta \sim \frac{L}{D}$
→ Intensity Interferometry



2. The dimensionful size $\sim L$
→ Reverberation Mapping



3. A redshift $H_0 \sim \frac{z}{D}$
→ Line emission



Distance error *per* AGN - spectroscopy

CTA-like array

$$v/c \sim 0.01$$

30ps time-jitter

$$T_{\text{obs}} = 24\text{hrs}$$

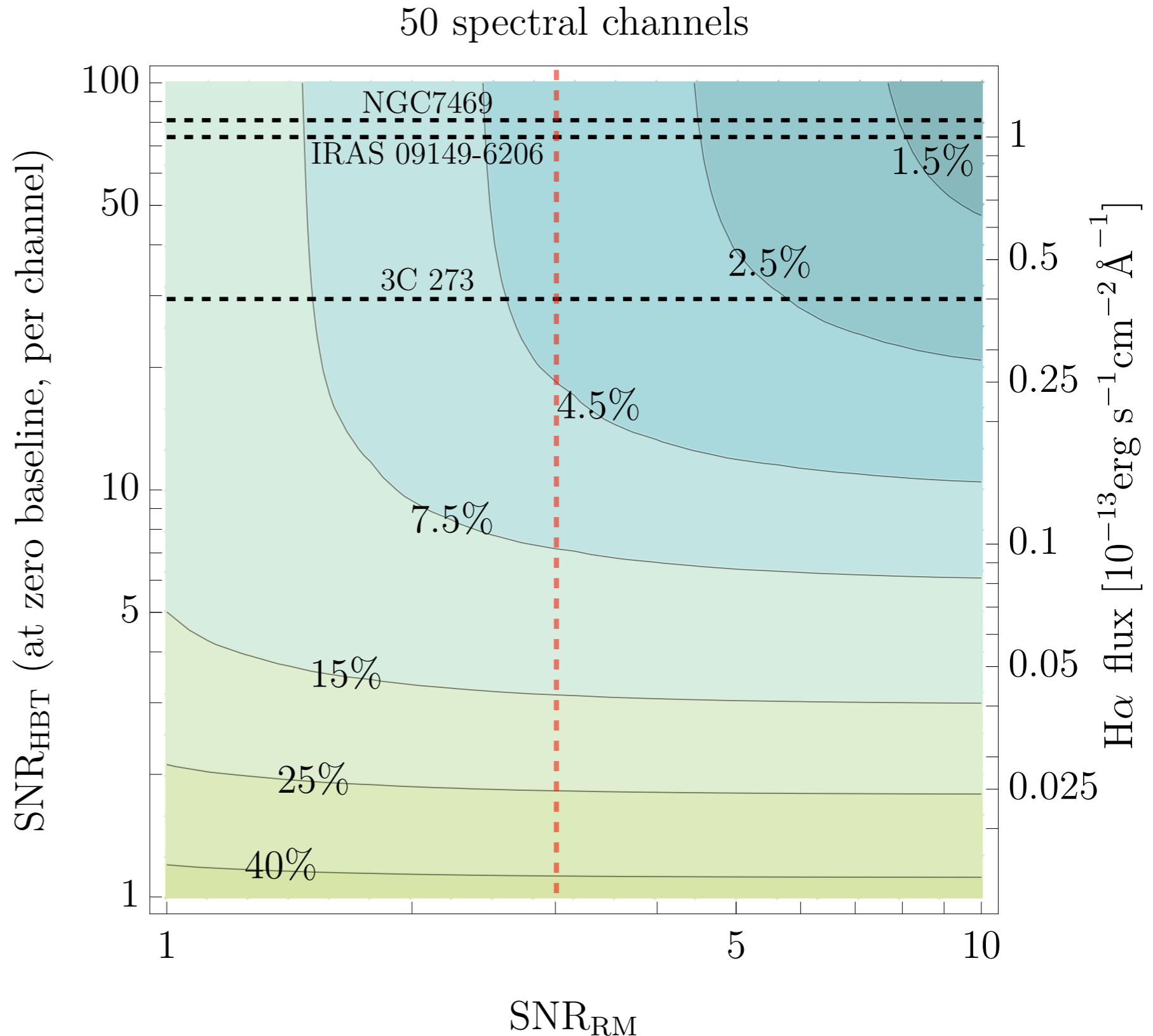
$$\mathcal{R} = 5000, \quad 50 \text{ channels}$$

$$\text{SNR} \approx 73 \text{ per channel}$$

IRAS 09149-6206, $z=0.057$

NGC 7469, $z=0.016$

3C 273, $z=0.158$



Conclusions

Conclusions

Long Baseline Intensity Interferometry: optical interferometry over **arbitrary baselines**

Conclusions

Long Baseline Intensity Interferometry: optical interferometry over **arbitrary baselines**

New technologies allow us to resolve bright AGNs

Conclusions

Long Baseline Intensity Interferometry: optical interferometry over **arbitrary baselines**

New technologies allow us to resolve bright AGNs

- Large and cheap photon buckets +

Conclusions

Long Baseline Intensity Interferometry: optical interferometry over **arbitrary baselines**

New technologies allow us to resolve bright AGNs

- Large and cheap photon buckets +
- Modern ultrafast photodetection +

Conclusions

Long Baseline Intensity Interferometry: optical interferometry over **arbitrary baselines**

New technologies allow us to resolve bright AGNs

- Large and cheap photon buckets +
- Modern ultrafast photodetection +
- Spectroscopy

Conclusions

Long Baseline Intensity Interferometry: optical interferometry over **arbitrary baselines**

New technologies allow us to resolve bright AGNs

- Large and cheap photon buckets +
- Modern ultrafast photodetection +
- Spectroscopy

Applications:

Conclusions

Long Baseline Intensity Interferometry: optical interferometry over **arbitrary** baselines

New technologies allow us to resolve bright AGNs

- Large and cheap photon buckets +
- Modern ultrafast photodetection +
- Spectroscopy

Applications:

- ▶ Geometric measurement of the **Hubble constant**
 - enough to **resolve tension**

Conclusions

Long Baseline Intensity Interferometry: optical interferometry over **arbitrary** baselines

New technologies allow us to resolve bright AGNs

- Large and cheap photon buckets +
- Modern ultrafast photodetection +
- Spectroscopy

Applications:

- ▶ Geometric measurement of the **Hubble constant**
 - enough to **resolve tension**
- ▶ Detailed properties of **AGN accretion disks**

Conclusions

Long Baseline Intensity Interferometry: optical interferometry over **arbitrary** baselines

New technologies allow us to resolve bright AGNs

- Large and cheap photon buckets +
- Modern ultrafast photodetection +
- Spectroscopy

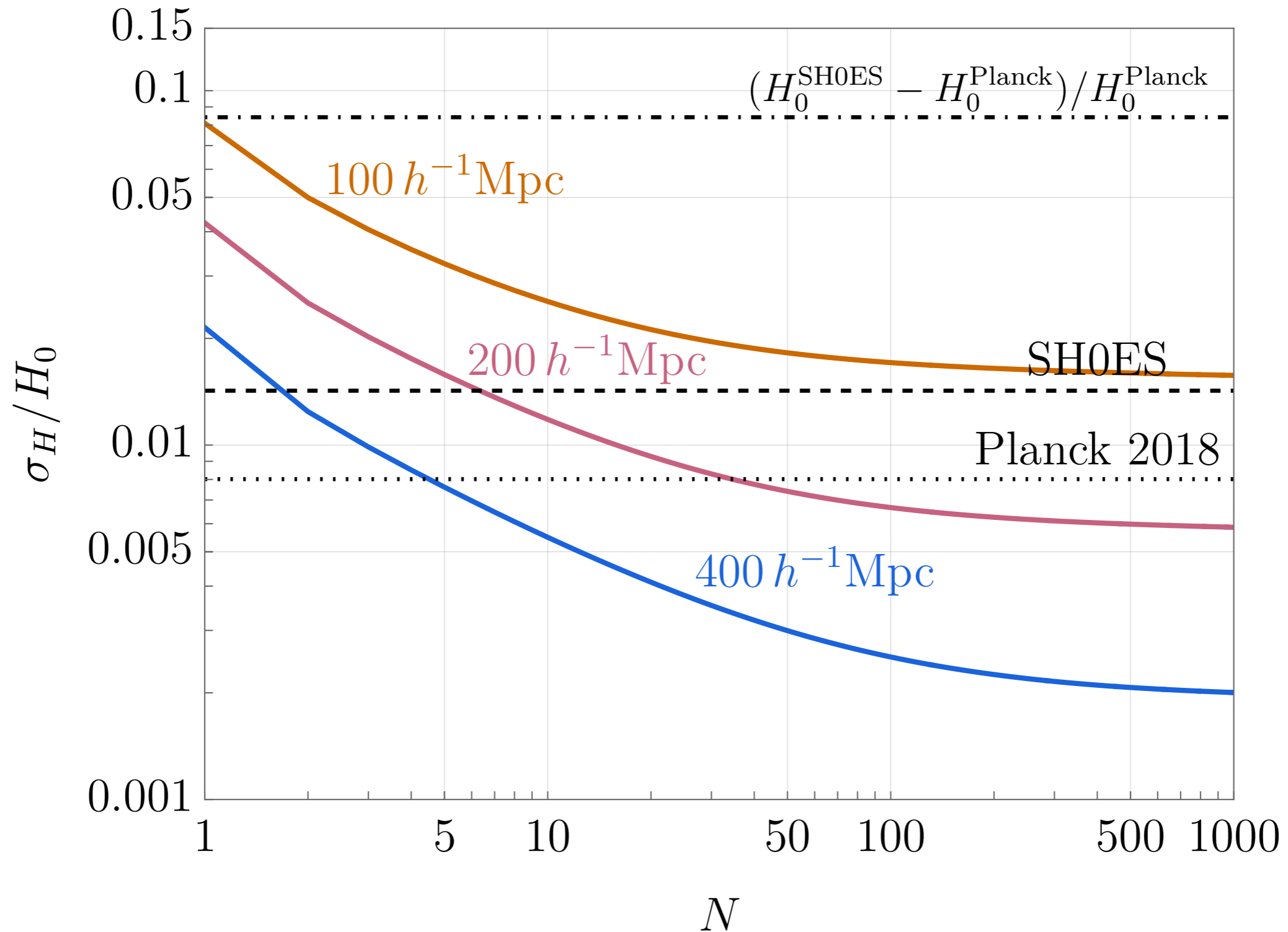
Applications:

- ▶ Geometric measurement of the **Hubble constant**
 - enough to **resolve tension**
- ▶ Detailed properties of **AGN accretion disks**
- ▶ Sensitivity to the innermost part of the disk and the hole

Thank you!

AGN Extras

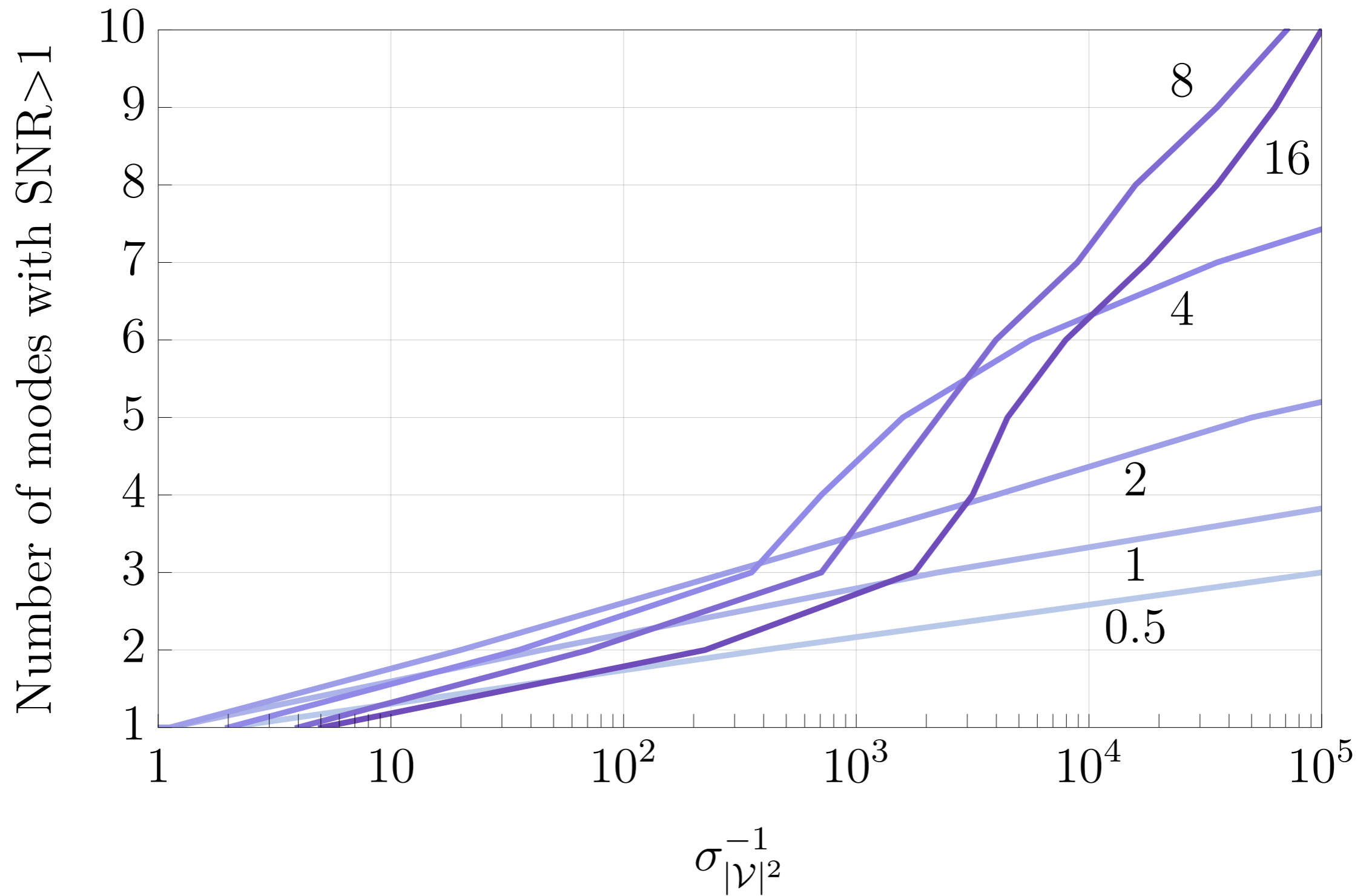
Sample variance on H0



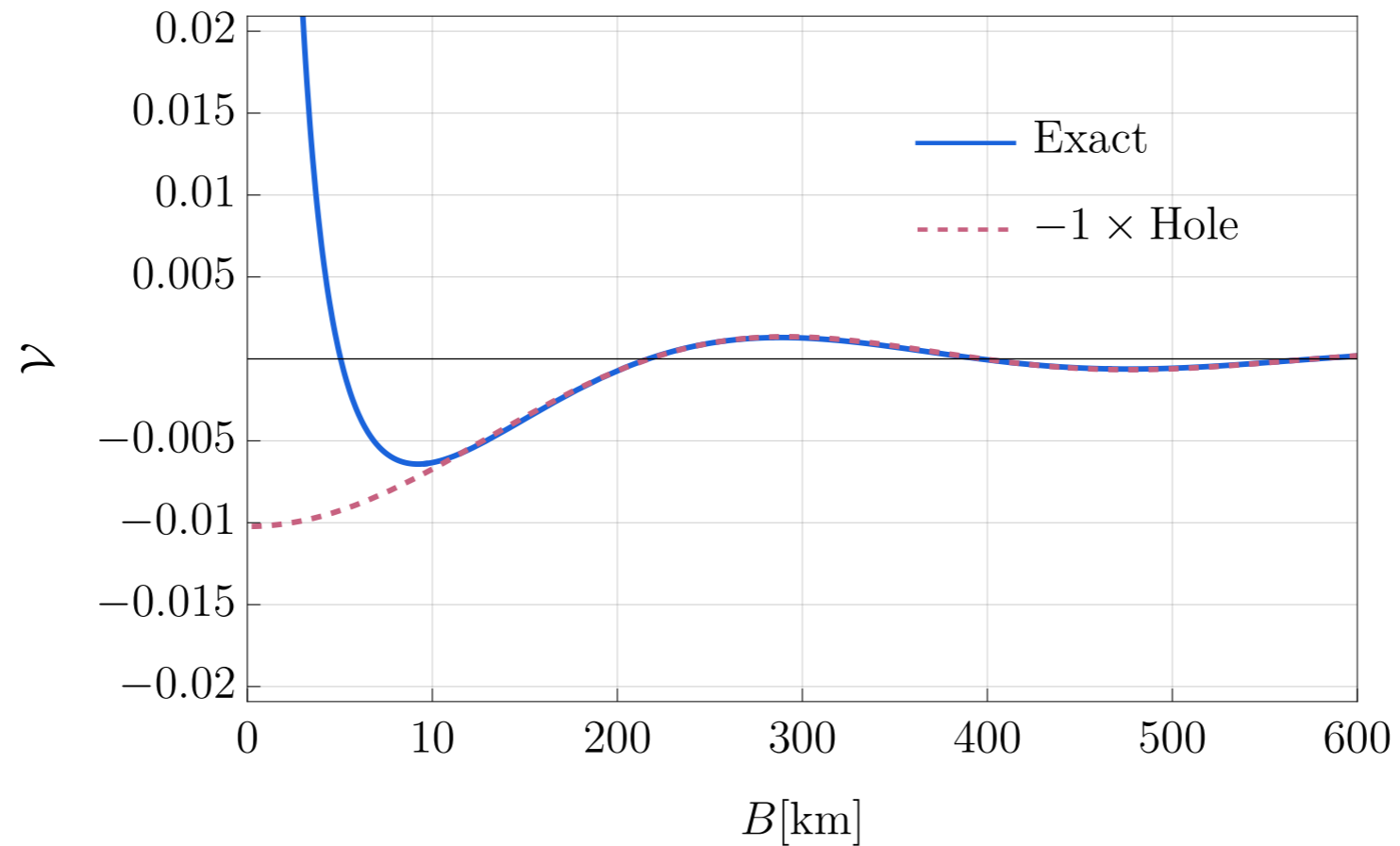
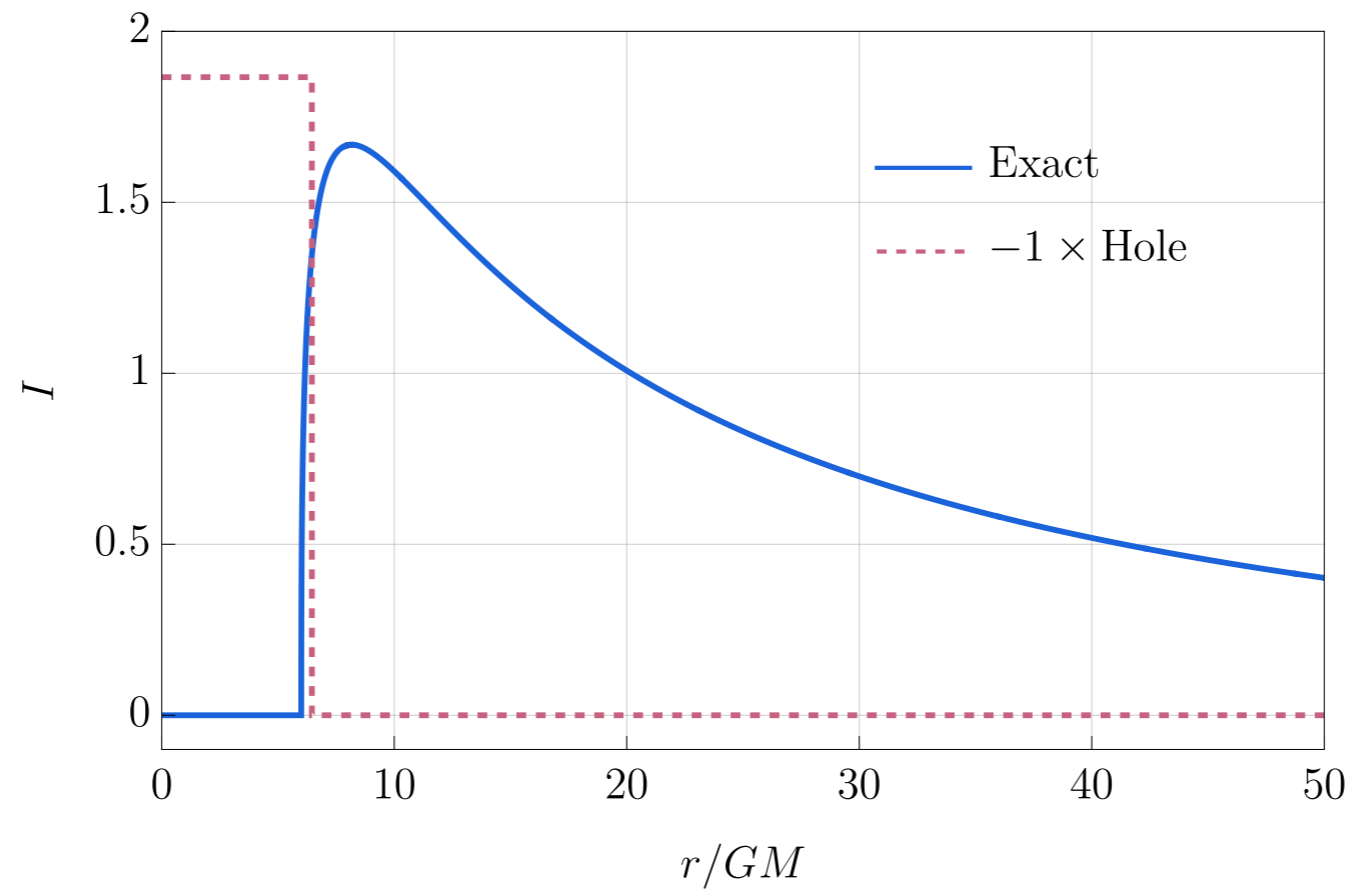
$$\sigma_H^2 = \sigma_{\text{CV}}^2 + \frac{v^2}{R_{\text{max}}^2} \frac{1}{N_{\text{obj}}}, \quad v \approx 630 \text{ km/s}$$

[Riess et al. 2022]
[Planck 2018]

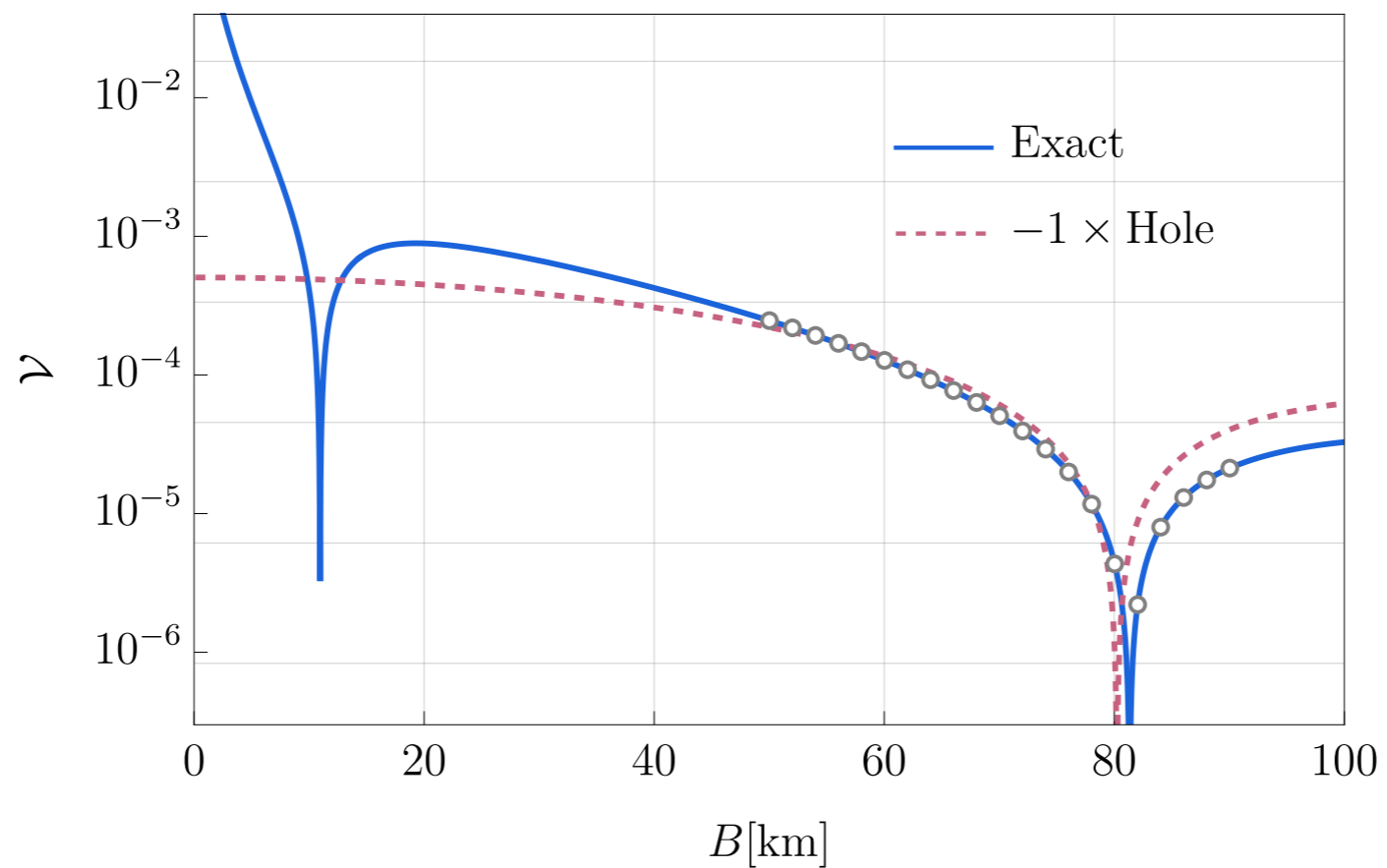
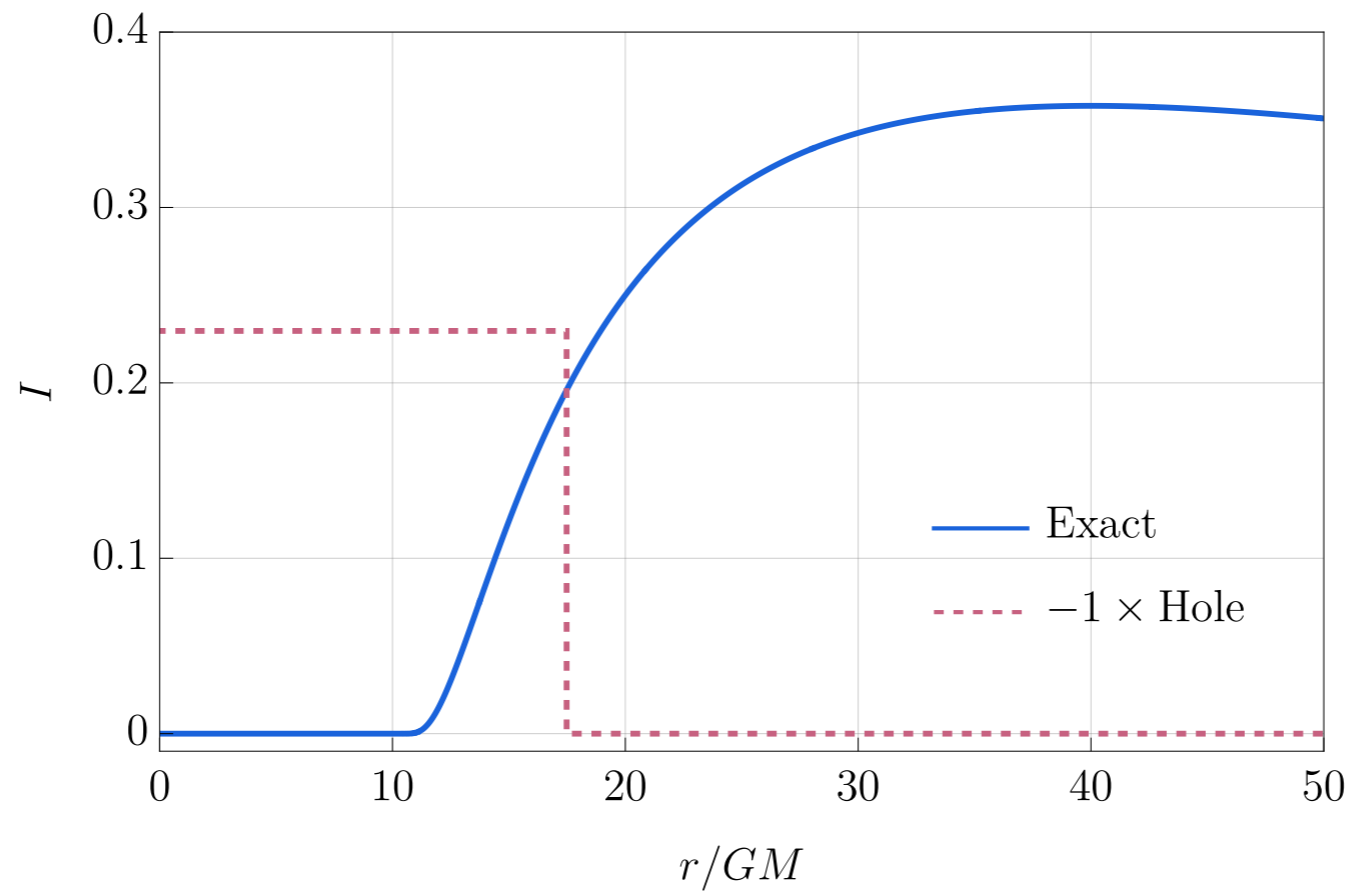
Principal component analysis



Sharp hole profile



Wide hole profile



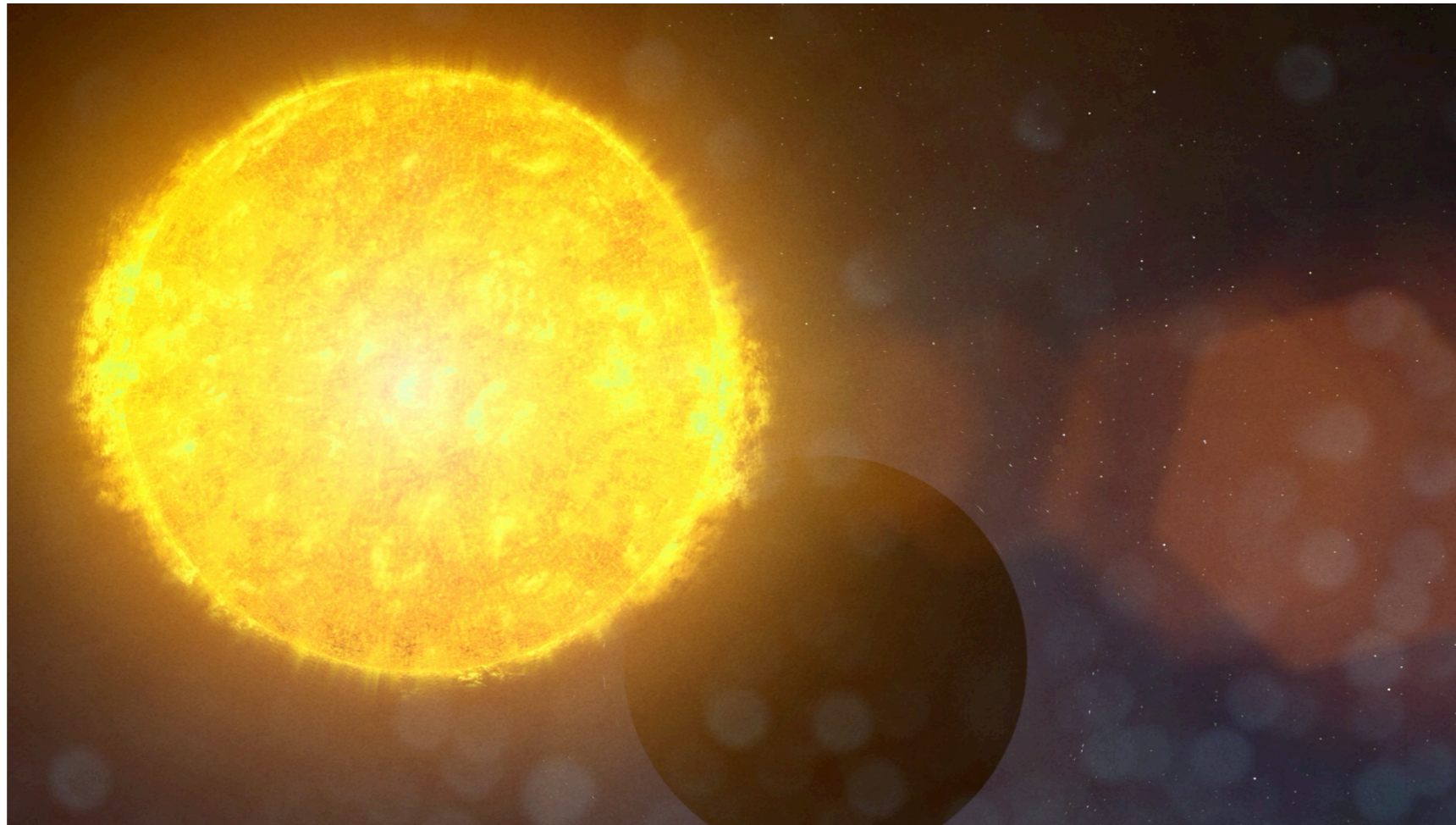
H0 redshifts

SNe Ia Riess: $0.023 < z < 0.15$

Just Cepheids, $z < 0.011$

H0LiCOW: $z=0.41$, HE 0435-1223

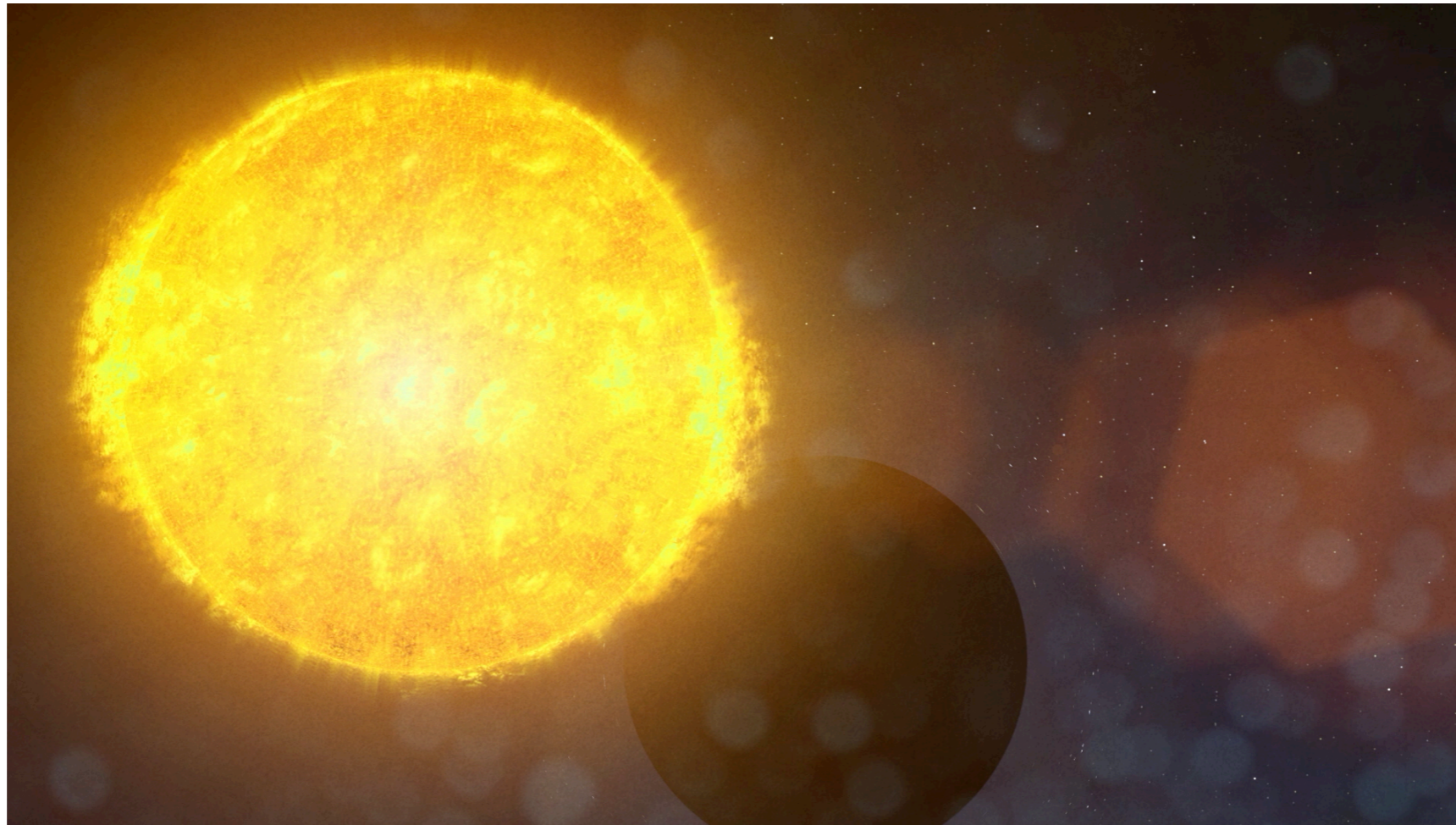
Future



[N. Dalal, **MG**, C. Gammie, S. Gralla,
N. Murray, March 2024, to appear]

Future

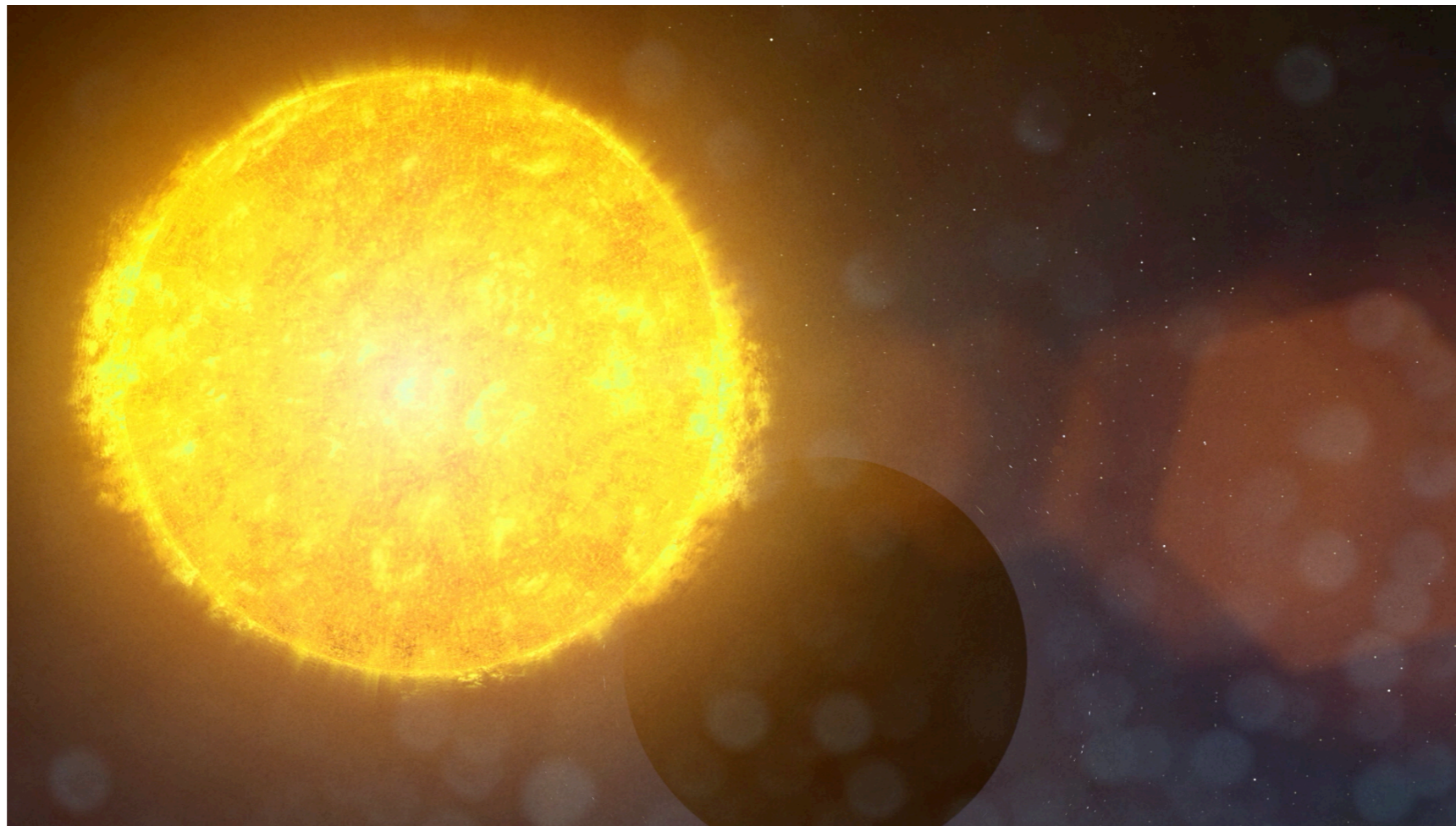
Tidal Disruption Events



[N. Dalal, **MG**, C. Gammie, S. Gralla,
N. Murray, March 2024, to appear]

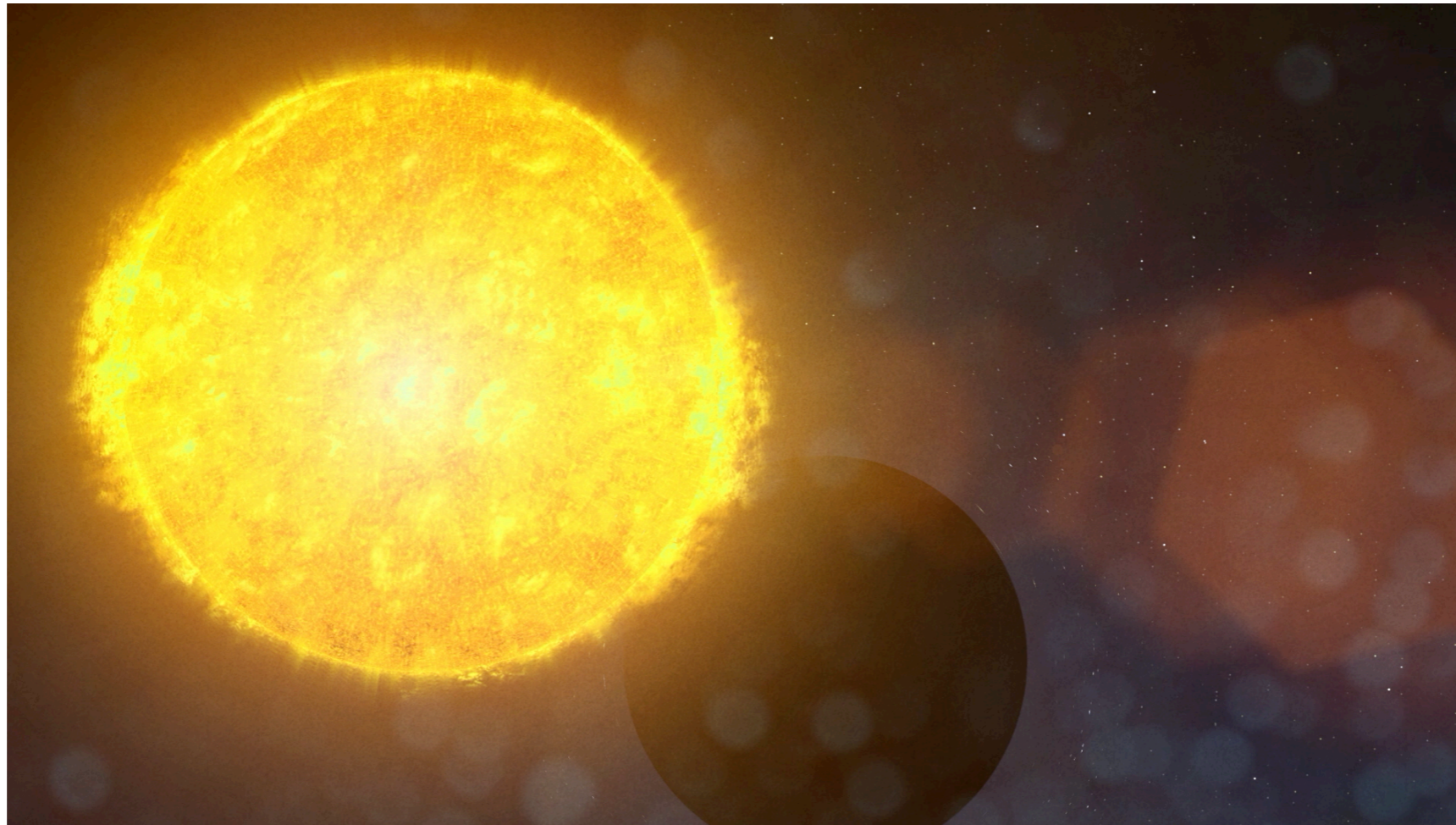
Future

Tidal Disruption Events



Future

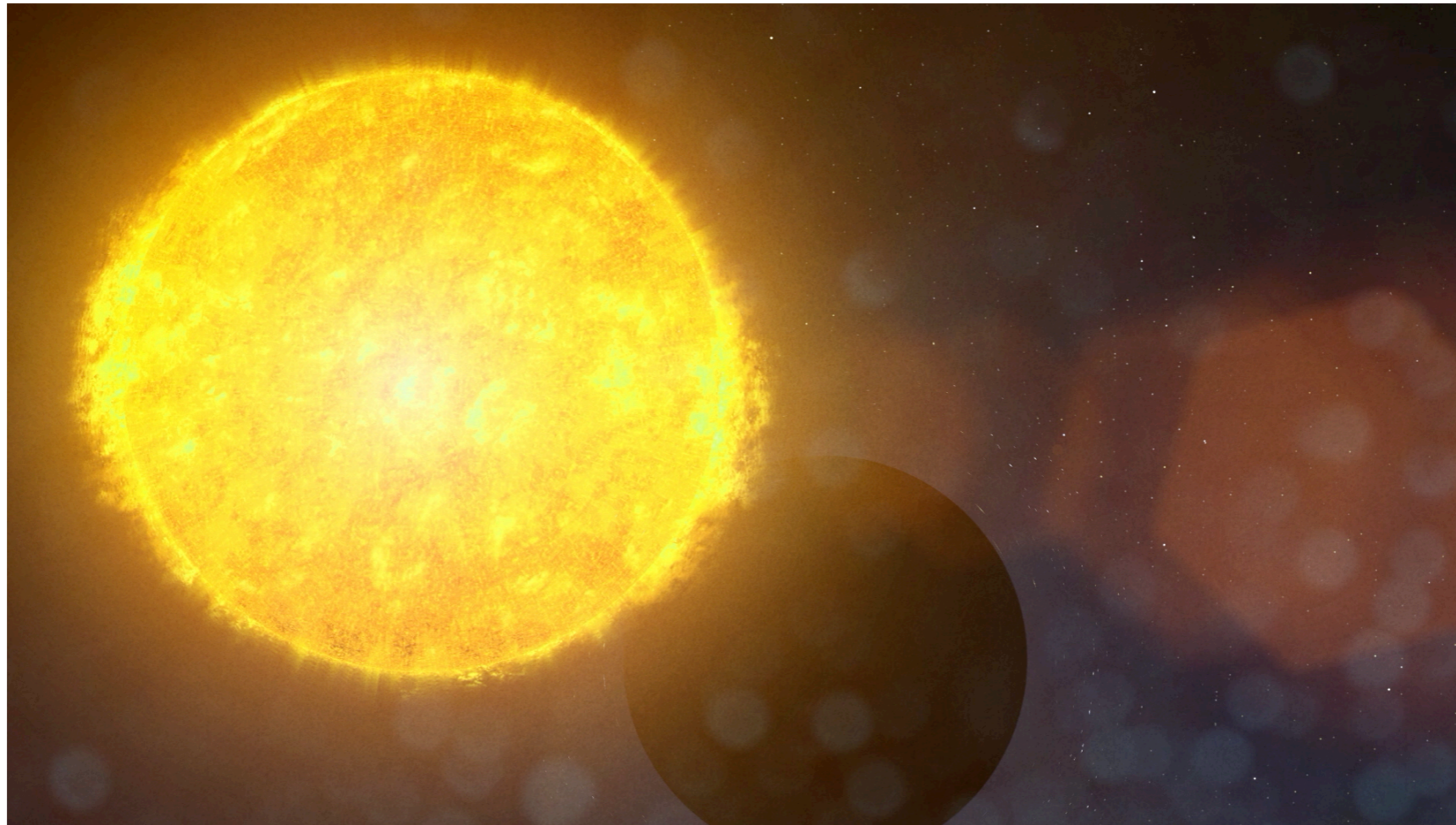
Tidal Disruption Events



Fainter, magnitude 16

Future

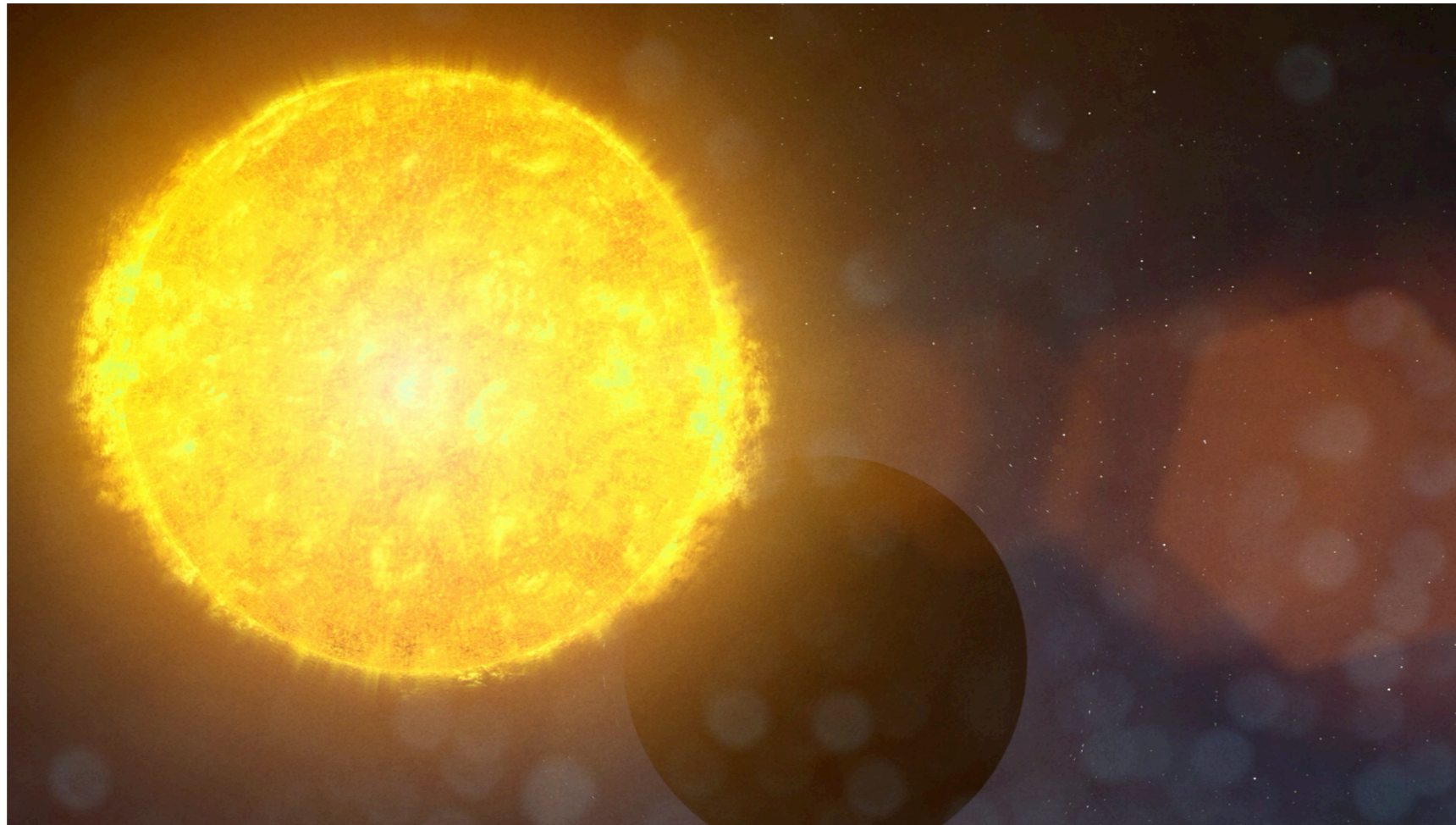
Tidal Disruption Events



Fainter, magnitude 16, SNR \sim 30 in 24hrs

Future

Tidal Disruption Events

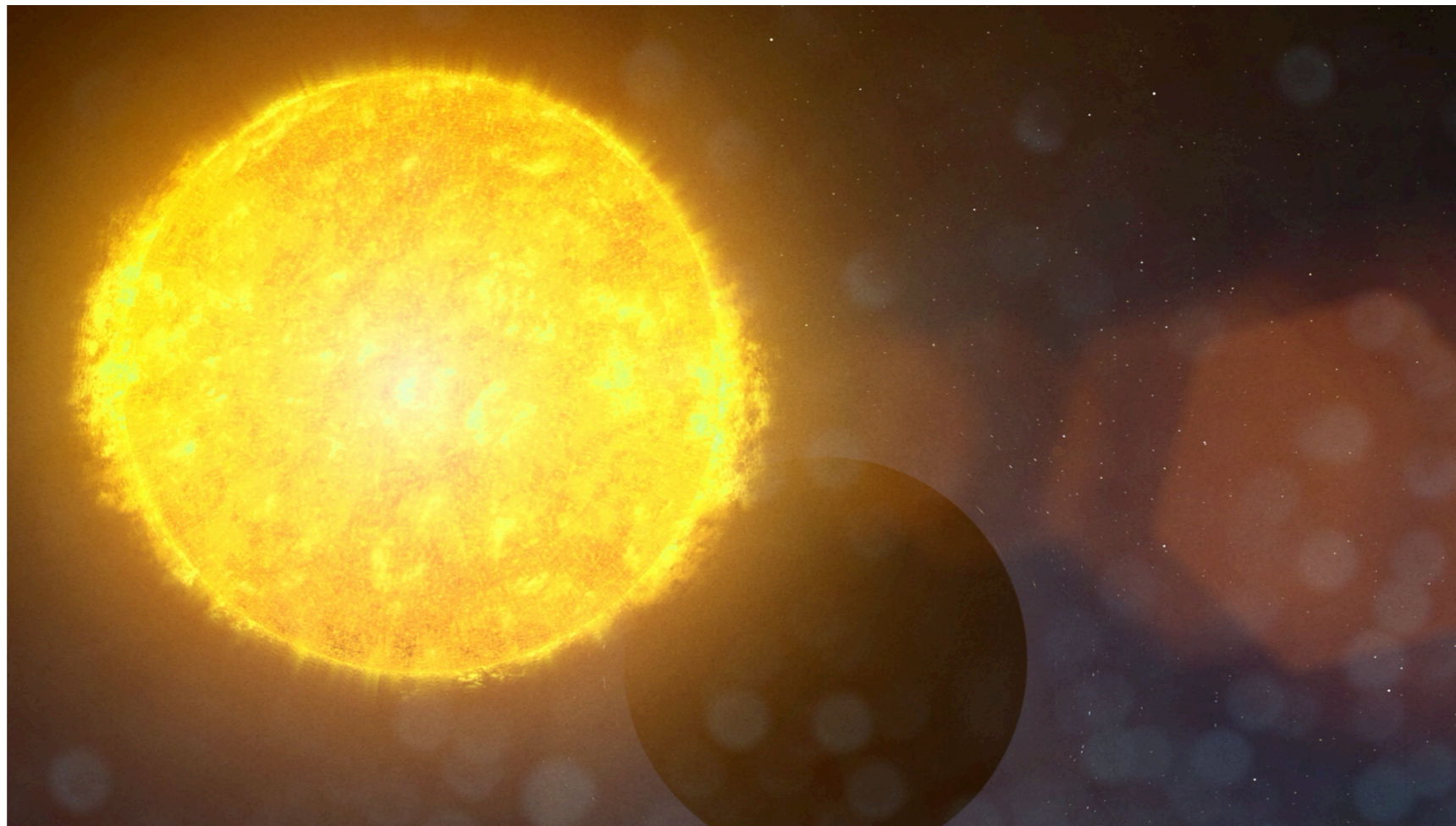


Fainter, magnitude 16, SNR \sim 30 in 24hrs

Last weeks to months

Future

Tidal Disruption Events



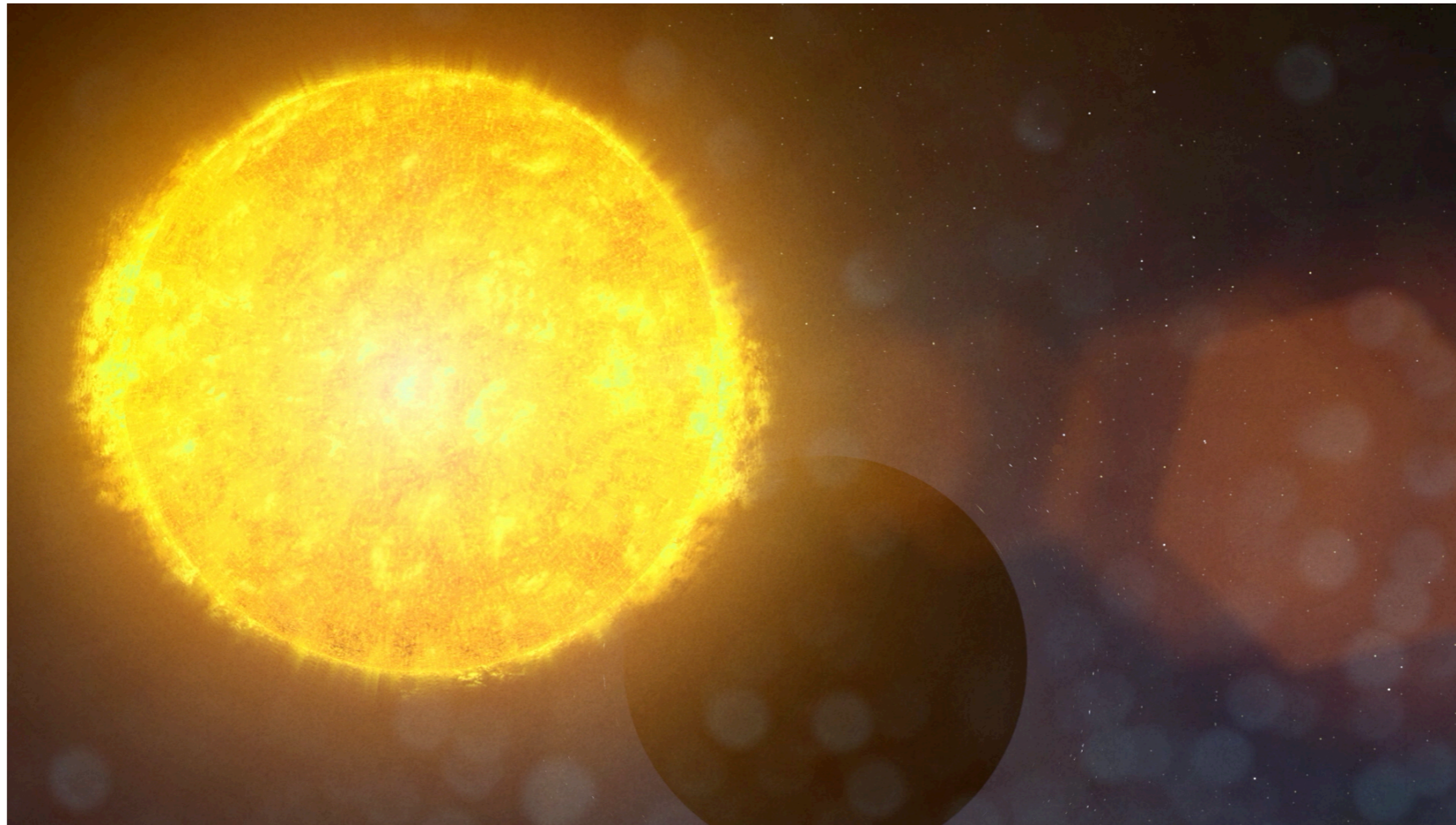
Fainter, magnitude 16, SNR \sim 30 in 24hrs

Last weeks to months

Physics poorly understood

Future

Tidal Disruption Events



Fainter, magnitude 16, SNR \sim 30 in 24hrs

Last weeks to months

Physics poorly understood

Measures BH spin

[N. Dalal, **MG**, C. Gammie, S. Gralla,
N. Murray, March 2024, to appear]

Future

[N. Dalal, **MG**, C. Gammie, S. Gralla,
N. Murray, March 2024, to appear]

Future*

[N. Dalal, **MG**, C. Gammie, S. Gralla,
N. Murray, March 2024, to appear]

Future*

*Crazy

Future*

Photon Rings



*Crazy

Future*

Photon Rings



Strong gravitational lensing

*Crazy

Future*

Photon Rings



Strong gravitational lensing

Width 1% of size, resolvable with $B=1000$ s of km

*Crazy

Future*

Photon Rings



Strong gravitational lensing

Width 1% of size, resolvable with $B=1000$ s of km

5 month total exposure time

*Crazy

[N. Dalal, **MG**, C. Gammie, S. Gralla,
N. Murray, March 2024, to appear]

Future*

Photon Rings



Strong gravitational lensing

Width 1% of size, resolvable with $B=1000$ s of km

5 month total exposure time

Square-km of glass!

*Crazy

[N. Dalal, **MG**, C. Gammie, S. Gralla,
N. Murray, March 2024, to appear]

Future*

Photon Rings



Strong gravitational lensing

Width 1% of size, resolvable with $B=1000$ s of km

5 month total exposure time

Square-km of glass!

But:

*Crazy

[N. Dalal, **MG**, C. Gammie, S. Gralla,
N. Murray, March 2024, to appear]

Future*

Photon Rings



Strong gravitational lensing

Width 1% of size, resolvable with $B=1000$ s of km

5 month total exposure time

Square-km of glass!

But: Only way to do this

*Crazy

Future*

Photon Rings



Strong gravitational lensing

Width 1% of size, resolvable with $B=1000$ s of km

5 month total exposure time

Square-km of glass!

But: Only way to do this

Probes strong-field GR

*Crazy

[N. Dalal, **MG**, C. Gammie, S. Gralla,
N. Murray, March 2024, to appear]

Future*

Photon Rings



Strong gravitational lensing

Width 1% of size, resolvable with B=1000s of km

5 month total exposure time

Square-km of glass!

But: Only way to do this

Probes strong-field GR

Also Imaging with $\langle I_1 I_2 I_3 \rangle$

*Crazy

[N. Dalal, **MG**, C. Gammie, S. Gralla,
N. Murray, March 2024, to appear]

Future*

Photon Rings



Strong gravitational lensing

Width 1% of size, resolvable with $B=1000$ s of km

5 month total exposure time

Square-km of glass!

But: Only way to do this

Probes strong-field GR

Also Imaging with $\langle I_1 I_2 I_3 \rangle$

People have been as crazy: LFAST, $20,000m^2$, \$60M, \$8000 per telescope

[Roger Angel et al.]

*Crazy

[N. Dalal, **MG**, C. Gammie, S. Gralla,
N. Murray, March 2024, to appear]

Future*

Photon Rings



Strong gravitational lensing

Width 1% of size, resolvable with $B=1000$ s of km

5 month total exposure time

Square-km of glass!

But: Only way to do this

Probes strong-field GR

Also Imaging with $\langle I_1 I_2 I_3 \rangle$

People have been as crazy: LFAST, $20.000m^2$, \$60M, \$8000 per telescope

[Roger Angel et al.]

*Crazy

[N. Dalal, **MG**, C. Gammie, S. Gralla,
N. Murray, March 2024, to appear]

Future*

Photon Rings



Strong gravitational lensing

Width 1% of size, resolvable with B=1000s of km

5 month total exposure time

Square-km of glass!

But: Only way to do this

Probes strong-field GR

Also Imaging with $\langle I_1 I_2 I_3 \rangle$

People have been as crazy: LFAST, $20.000m^2$, \$60M, \$8000 per telescope

[Roger Angel et al.]

*Crazy?

[N. Dalal, **MG**, C. Gammie, S. Gralla,
N. Murray, March 2024, to appear]

Distance error *per* AGN - one pixel

CTA-like array

$$v/c \sim 0.01$$

30ps time-jitter

$$T_{\text{obs}} = 24\text{hrs}$$

$\mathcal{R} = 5000$, 50 channels

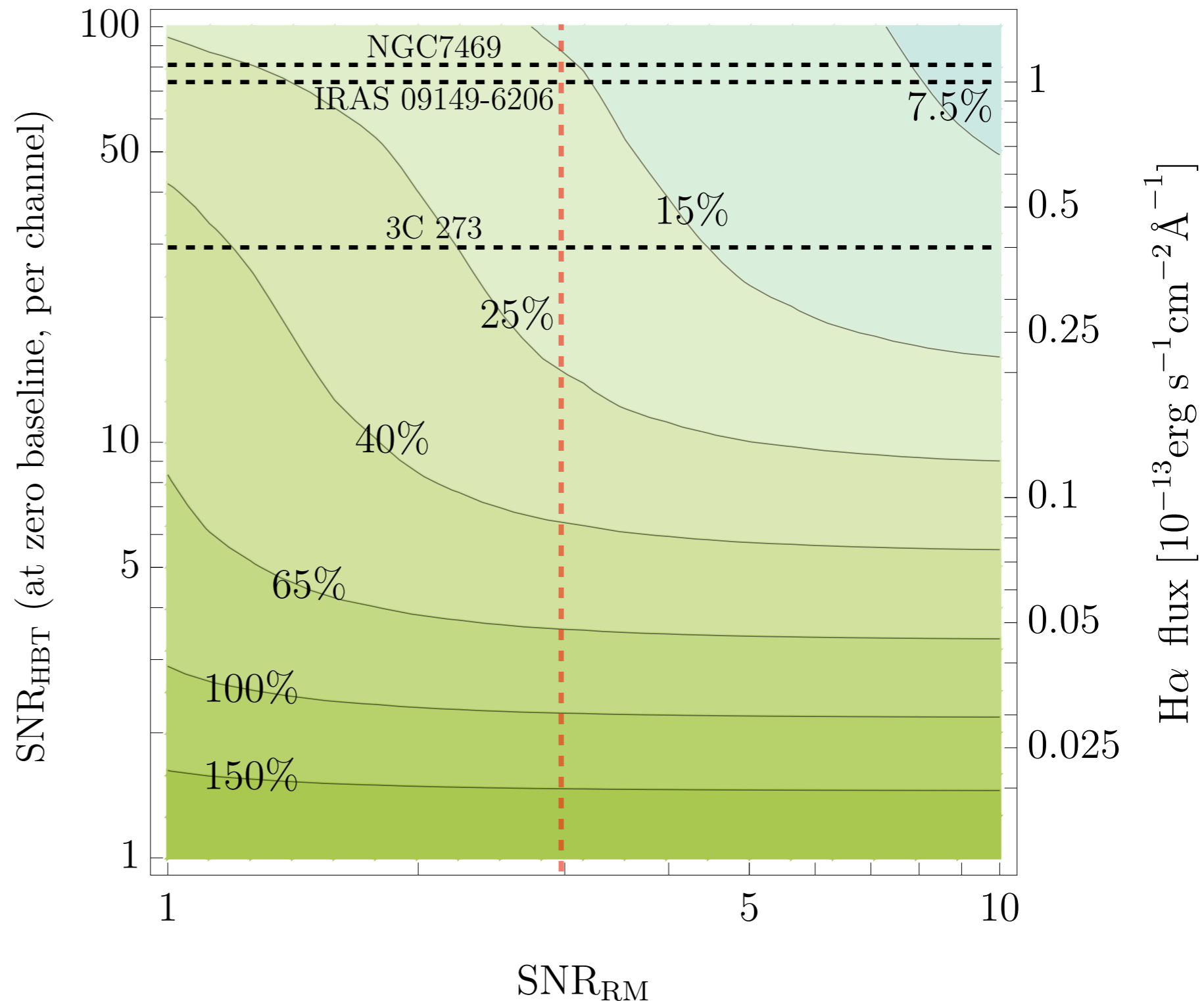
SNR ≈ 73 per channel

IRAS 09149-6206, $z=0.057$

NGC 7469, $z=0.016$

3C 273, $z=0.158$

Single narrow-band filter



Distance error *per* AGN - one pixel

Single narrow-band filter

CTA-like array

$$v/c \sim 0.01$$

30ps time-jitter

$$T_{\text{obs}} = 24\text{hrs}$$

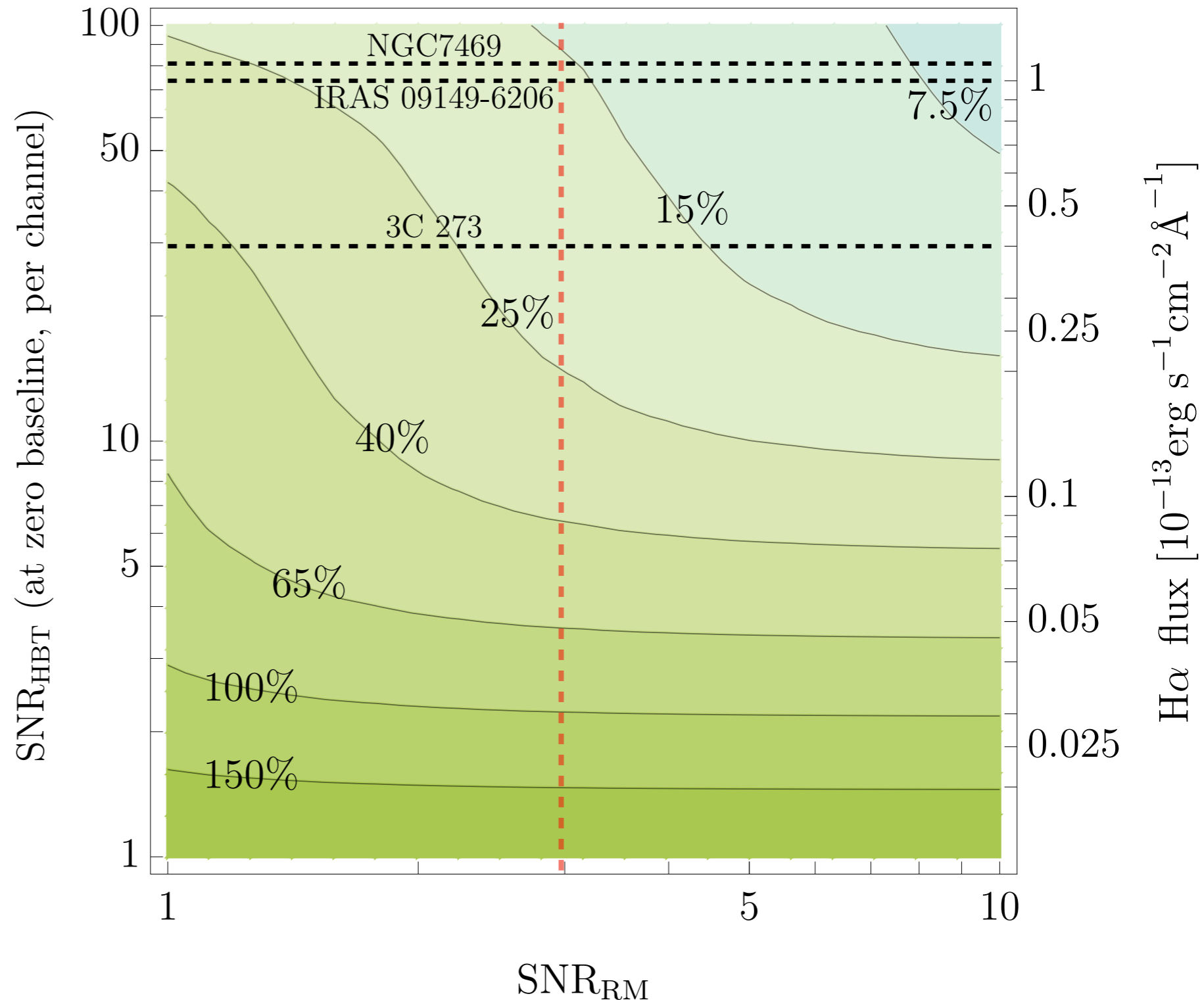
$\mathcal{R} = 5000$, 50 channels

SNR ≈ 73 per channel

IRAS 09149-6206, $z=0.057$

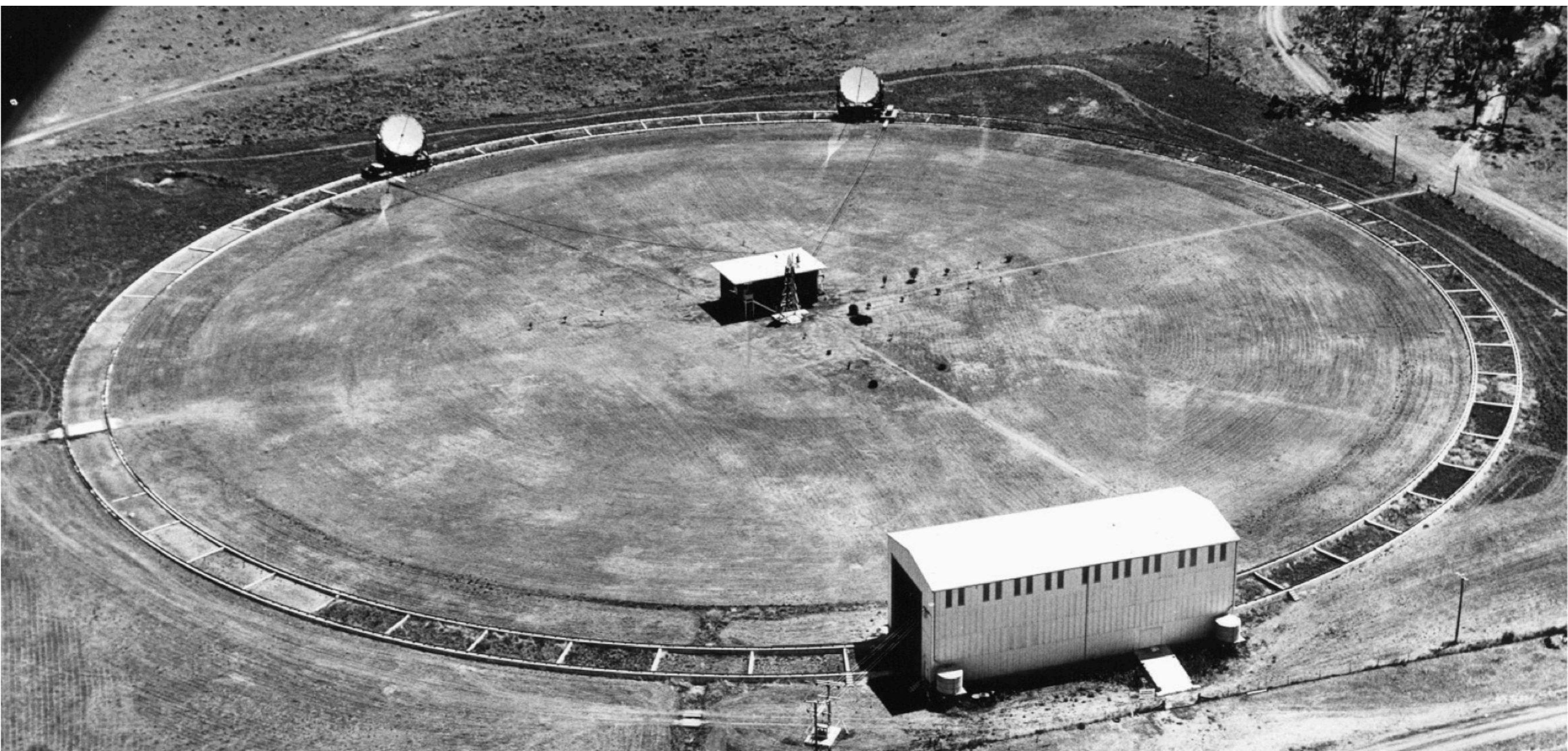
NGC 7469, $z=0.016$

3C 273, $z=0.158$

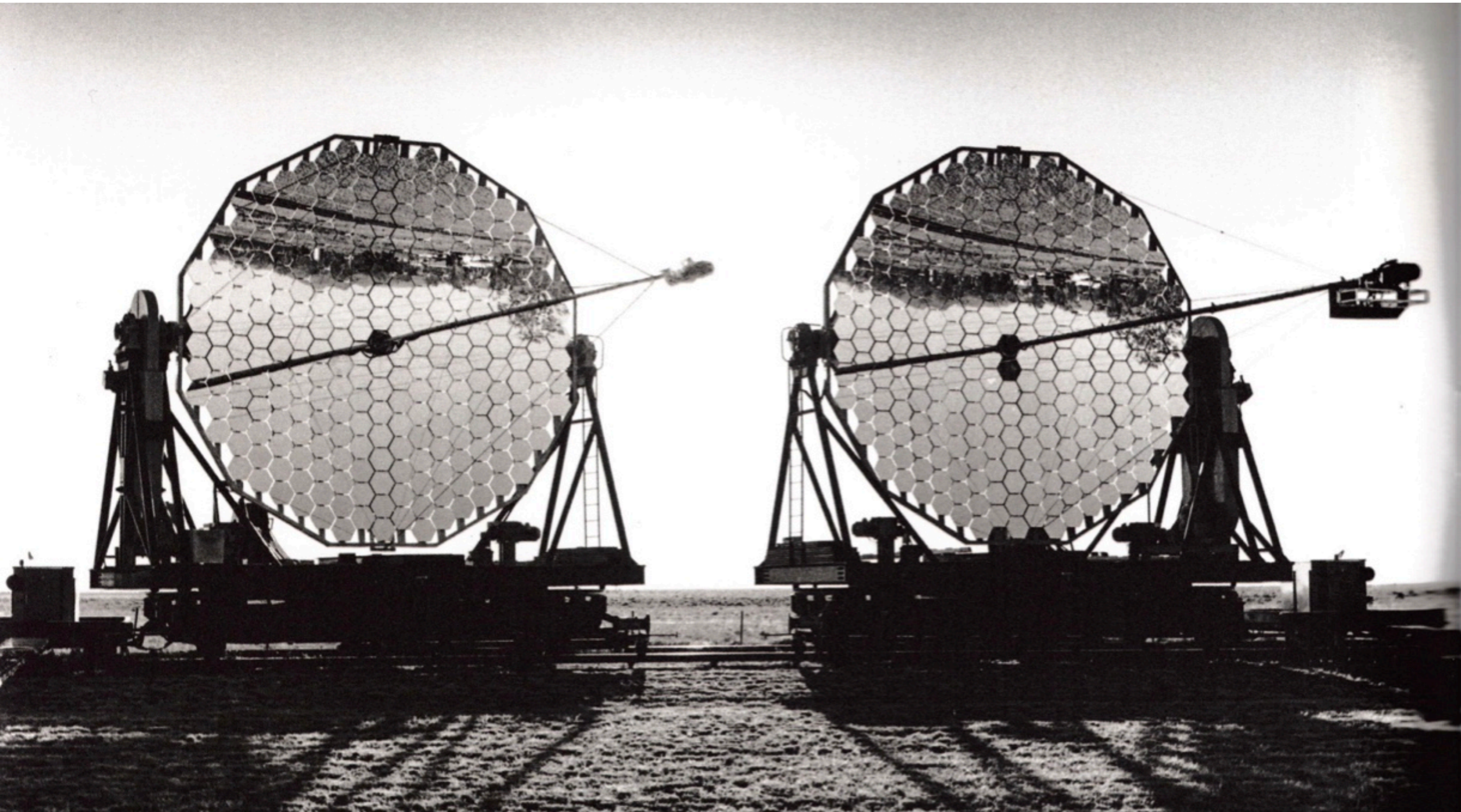


But is it feasible?

Narrabri Stellar Intensity Interferometer



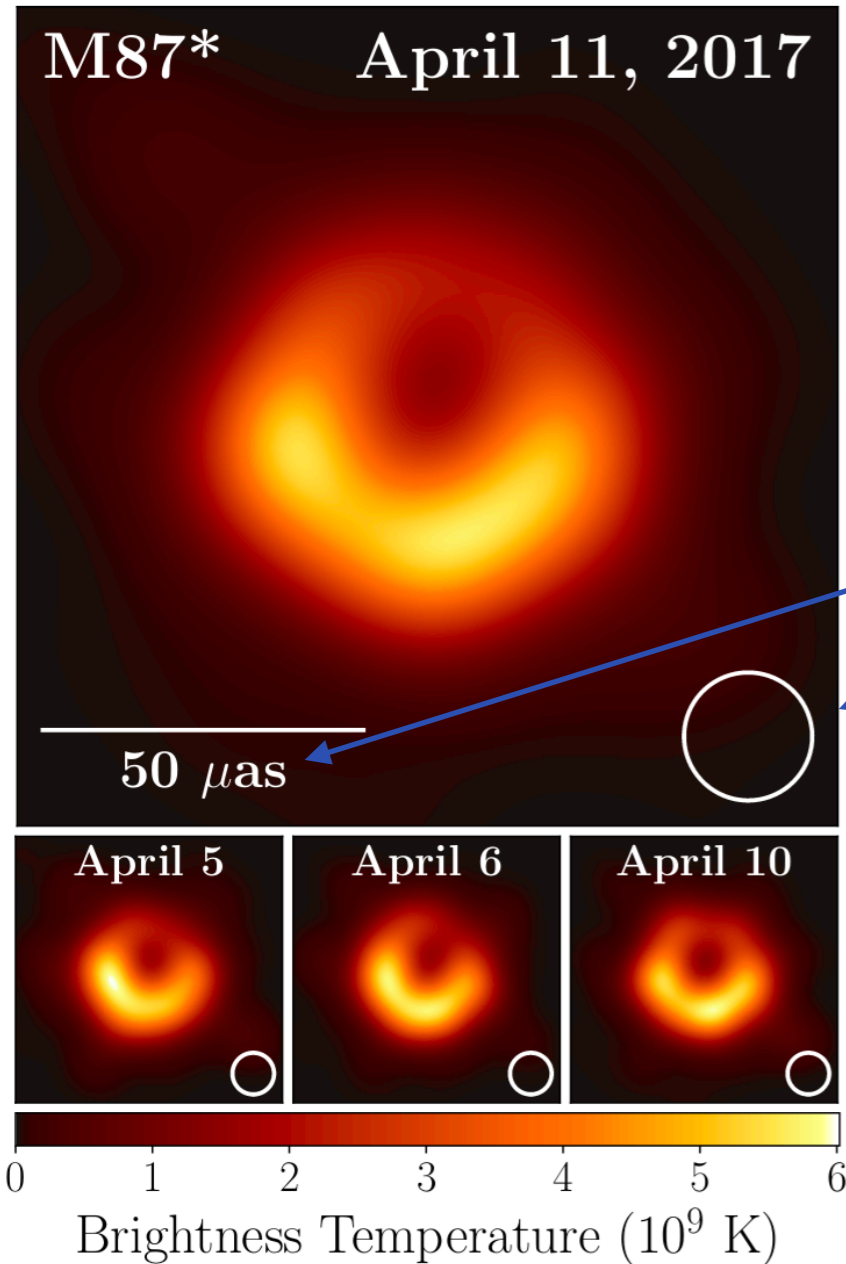
Narrabri Stellar Intensity Interferometer



Narrabri Stellar Intensity Interferometer

Star number	Star name	Type	Zero-baseline correlation $c_N \pm \sigma$	Angular diameter $\times 10^{-3}$ sec of arc		Temperature [$T_e(F) \pm \sigma$]/K
				$\theta_{UD} \pm \sigma$	$\theta_{LD} \pm \sigma$	
472	α Eri	B 3 (Vp)	0.98 ± 0.05	1.85 ± 0.07	1.92 ± 0.07	$13\,700 \pm 600$
1713	β Ori	B 8 (Ia)	0.98 ± 0.08	2.43 ± 0.05	2.55 ± 0.05	$11\,500 \pm 700$
1790	γ Ori	B 2 (III)	1.03 ± 0.07	0.70 ± 0.04	0.72 ± 0.04	$20\,800 \pm 1300$
1903	ϵ Ori	B 0 (Ia)	0.86 ± 0.07	0.67 ± 0.04	0.69 ± 0.04	$24\,500 \pm 2000$
1948	ζ Ori	O 9.5 (Ib)	0.60 ± 0.06	0.47 ± 0.04	0.48 ± 0.04	$26\,100 \pm 2200$
2004	κ Ori	B 0.5 (Ia)	1.18 ± 0.09	0.44 ± 0.03	0.45 ± 0.03	$30\,400 \pm 2000$
2294	β CMa	B 1 (II-III)	1.07 ± 0.08	0.50 ± 0.03	0.52 ± 0.03	$25\,300 \pm 1500$
2326	α Car	F 0 (Ib-II)	0.75 ± 0.22	6.1 ± 0.7	6.6 ± 0.8	7500 ± 250
2421	γ Gem	A 0 (IV)	1.17 ± 0.09	1.32 ± 0.09	1.39 ± 0.09	9600 ± 500
2491	α CMa	A 1 (V)	0.91 ± 0.06	5.60 ± 0.15	5.89 ± 0.16	$10\,250 \pm 150$
2618	ϵ CMa	B 2 (II)	0.89 ± 0.06	0.77 ± 0.05	0.80 ± 0.05	$20\,800 \pm 1300$
2693	δ CMa	F 8 (Ia)	0.93 ± 0.18	3.29 ± 0.46	3.60 ± 0.50	—
2827	η CMa	B 5 (Ia)	0.99 ± 0.09	0.72 ± 0.06	0.75 ± 0.06	$14\,200 \pm 1300$
2943	α CMi	F 5 (IV-V)	0.98 ± 0.10	5.10 ± 0.16	5.50 ± 0.17	6500 ± 200
3165	ζ Pup	O 5 (f)	1.04 ± 0.08	0.41 ± 0.03	0.42 ± 0.03	$30\,700 \pm 2500$
3207	γ^2 Vel	WC 8+O 9 (I)	—	0.43 ± 0.05	0.44 ± 0.05	$29\,000 \pm 3000$
3685	β Car	A 1 (IV)	1.01 ± 0.06	1.51 ± 0.07	1.59 ± 0.07	9500 ± 350
3982	α Leo	B 7 (V)	1.12 ± 0.07	1.32 ± 0.06	1.37 ± 0.06	$12\,700 \pm 800$
4534	β Leo	A 3 (V)	1.17 ± 0.10	1.25 ± 0.09	1.33 ± 0.10	9050 ± 450

Narrabri Stellar Intensity Interferometer



Star number	Star name	Type	Zero-baseline correlation $c_N \pm \sigma$	Angular diameter $\times 10^{-3}$ sec of arc		Temperature [$T_e(F) \pm \sigma$]/K
				$\theta_{UD} \pm \sigma$	$\theta_{LD} \pm \sigma$	
472	α Eri	B 3 (Vp)	0.98 ± 0.05	1.85 ± 0.07	1.92 ± 0.07	$13\,700 \pm 600$
1713	β Ori	B 8 (Ia)	0.98 ± 0.08	2.43 ± 0.05	2.55 ± 0.05	$11\,500 \pm 700$
1790	γ Ori	B 2 (III)	1.03 ± 0.07	0.70 ± 0.04	0.72 ± 0.04	$20\,800 \pm 1300$
1903	ϵ Ori	B 0 (Ia)	0.86 ± 0.07	0.67 ± 0.04	0.69 ± 0.04	$24\,500 \pm 2000$
1948	ζ Ori	O 9.5 (Ib)	0.60 ± 0.06	0.47 ± 0.04	0.48 ± 0.04	$26\,100 \pm 2200$
2004	κ Ori	B 0.5 (Ia)	1.18 ± 0.09	0.44 ± 0.03	0.45 ± 0.03	$30\,400 \pm 2000$
2294	β CMa	B 1 (II–III)	1.07 ± 0.08	0.50 ± 0.03	0.52 ± 0.03	$25\,300 \pm 1500$
2326	α Car	F 0 (Ib–II)	0.75 ± 0.22	6.1 ± 0.7	6.6 ± 0.8	7500 ± 250
2421	γ Gem	A 0 (IV)	1.17 ± 0.09	1.32 ± 0.09	1.39 ± 0.09	9600 ± 500
2491	α CMa	A 1 (V)	0.91 ± 0.06	5.60 ± 0.15	5.89 ± 0.16	$10\,250 \pm 150$
2618	ϵ CMa	B 2 (II)	0.89 ± 0.06	0.77 ± 0.05	0.80 ± 0.05	$20\,800 \pm 1300$
2693	δ CMa	F 8 (Ia)	0.93 ± 0.18	3.29 ± 0.46	3.60 ± 0.50	—
2827	η CMa	B 5 (Ia)	0.99 ± 0.09	0.72 ± 0.06	0.75 ± 0.06	$14\,200 \pm 1300$
2943	α CMi	F 5 (IV–V)	0.98 ± 0.10	5.10 ± 0.16	5.50 ± 0.17	6500 ± 200
3165	ζ Pup	O 5 (f)	1.04 ± 0.08	0.41 ± 0.03	0.42 ± 0.03	$30\,700 \pm 2500$
3207	γ^2 Vel	WC 8+O 9 (I)	—	0.43 ± 0.05	0.44 ± 0.05	$29\,000 \pm 3000$
3685	β Car	A 1 (IV)	1.01 ± 0.06	1.51 ± 0.07	1.59 ± 0.07	9500 ± 350
3982	α Leo	B 7 (V)	1.12 ± 0.07	1.32 ± 0.06	1.37 ± 0.06	$12\,700 \pm 800$
4534	β Leo	A 3 (V)	1.17 ± 0.10	1.25 ± 0.09	1.33 ± 0.10	9050 ± 450

Photon buckets work and are cheap

Photon buckets work and are cheap

29 August 2022

LFAST, the Large Fiber Array Spectroscopic Telescope

[Roger Angel](#), [Chad Bender](#), [Joel Berkson](#), [Nick Didato](#), [John Ford](#), [Peter Gray](#), [Buell Jannuzi](#), [Dean Ketelsen](#), [Daewook Kim](#), [Gilberto Chavez Lopez](#), [Andrew Monson](#), [Chang-Jin Oh](#), [Jason Patrou](#), [Matthew Rademacher](#), [Christian Schwab](#), [Melanie Sisco](#), [Rich Wortley](#), [Andrew Young](#)

[Author Affiliations +](#)

Proceedings Volume 12182, Ground-based and Airborne Telescopes IX; 121821U (2022)

<https://doi.org/10.1117/12.2629655>

Event: [SPIE Astronomical Telescopes + Instrumentation](#), 2022, Montréal, Québec, Canada

Photon buckets work and are cheap

29 August 2022

LFAST, the Large Fiber Array Spectroscopic Telescope

Roger Angel, Chad Bender, Joel Berkson, Nick Didato, John Ford, Peter Gray, Buell Jannuzi, Dean Ketelsen, Daewook Kim, Gilberto Chavez Lopez, Andrew Monson, Chang-Jin Oh, Jason Patrou, Matthew Rademacher, Christian Schwab, Melanie Sisco, Rich Wortley, Andrew Young

[Author Affiliations +](#)

Proceedings Volume 12182, Ground-based and Airborne Telescopes IX; 121821U (2022)

<https://doi.org/10.1117/12.2629655>

Event: [SPIE Astronomical Telescopes + Instrumentation](#), 2022, Montréal, Québec, Canada

Abstract

The LFAST concept is to use thousands of small telescopes combined by fibers for high resolution ($R=150,000$) spectroscopy, in a way that will realize large cost savings and lead to an affordable aperture as large as $20,000 \text{ m}^2$. Such large aperture is needed, for example, to make a comprehensive search for biosignatures in the atmospheres of transiting exoplanets. Each unit telescope of 0.76 m aperture (0.43 m^2) will focus the image of a single star onto a small ($17 \text{ }\mu\text{m}$ core) fiber, subtending 1.32 arcsec . Our telescope design calls for a spherical mirror, with a 4-lens assembly at prime focus that corrects not only for spherical aberration, but also for atmospheric dispersion down to 30° elevation, from $390 \text{ nm} - 1700 \text{ nm}$, and for rapid image motion caused by seeing or wind jitter. A method for rapid production of such mirrors has been tested, in which a disc of borosilicate float glass is slumped over a high-precision polished mandrel to an accuracy that greatly reduces subsequent optical finishing time. A method for active thermal control of mirror figure using Peltier devices will be incorporated. The projected cost of each unit telescope, when mass produced by the thousand, would then be approximately $\$8,000$. The telescopes will be mounted in the open in groups of 20 located 12 m apart. The mirrors will be arrayed on either side of a central, pedestal-mounted alt-az drive using commercial worm gear bearings. Protection against rain and dust will be provided by automated covers above and below the mirrors, and by pointing the mirrors down (-20° elevation). The first LFAST array, some 150 m in diameter, will comprise 132 mounts carrying a total of 2,640 mirrors and having $1,200 \text{ m}^2$ in collecting area. The light from all the fibers is combined at the central spectrographs, with little increase in etendue, by a 5×528 array of adjacent hexagonal lenses. A telecentric lens is used to reimage the lens array at the entrance slits of two echelle spectrographs. Together, these two cover simultaneously the full $390 \text{ nm} - 1700 \text{ nm}$ spectral range of the star being observed. The targeted cost for the installed LFAST telescope and fiber array is $\$60\text{M}$.

Photon buckets work and are cheap

29 August 2022

LFAST, the Large Fiber Array Spectroscopic Telescope

Roger Angel, Chad Bender, Joel Berkson, Nick Didato, John Ford, Peter Gray, Buell Jannuzi, Dean Ketelsen, Daewook Kim, Gilberto Chavez Lopez, Andrew Monson, Chang-Jin Oh, Jason Patrou, Matthew Rademacher, Christian Schwab, Melanie Sisco, Rich Wortley, Andrew Young

[Author Affiliations +](#)

Proceedings Volume 12182, Ground-based and Airborne Telescopes IX; 121821U (2022)

<https://doi.org/10.1117/12.2629655>

Event: [SPIE Astronomical Telescopes + Instrumentation](#), 2022, Montréal, Québec, Canada

Abstract

The LFAST concept is to use thousands of small telescopes combined by fibers for high resolution ($R=150,000$) spectroscopy, in a way that will realize large cost savings and lead to an affordable aperture as large as $20,000 \text{ m}^2$. Such large aperture is needed, for example, to make a comprehensive search for biosignatures in the atmospheres of transiting exoplanets. Each unit telescope of 0.76 m aperture (0.43 m^2) will focus the image of a single star onto a small ($17 \text{ }\mu\text{m}$ core) fiber, subtending 1.32 arcsec . Our telescope design calls for a spherical mirror, with a 4-lens assembly at prime focus that corrects not only for spherical aberration, but also for atmospheric dispersion down to 30° elevation, from $390 \text{ nm} - 1700 \text{ nm}$, and for rapid image motion caused by seeing or wind jitter. A method for rapid production of such mirrors has been tested, in which a disc of borosilicate float glass is slumped over a high-precision polished mandrel to an accuracy that greatly reduces subsequent optical finishing time. A method for active thermal control of mirror figure using Peltier devices will be incorporated. The projected cost of each unit telescope, when mass produced by the thousand, would then be approximately $\$8,000$. The telescopes will be mounted in the open in groups of 20 located 12 m apart. The mirrors will be arrayed on either side of a central, pedestal-mounted alt-az drive using commercial worm gear bearings. Protection against rain and dust will be provided by automated covers above and below the mirrors, and by pointing the mirrors down (-20° elevation). The first LFAST array, some 150 m in diameter, will comprise 132 mounts carrying a total of 2,640 mirrors and having $1,200 \text{ m}^2$ in collecting area. The light from all the fibers is combined at the central spectrographs, with little increase in etendue, by a 5×528 array of adjacent hexagonal lenses. A telecentric lens is used to reimage the lens array at the entrance slits of two echelle spectrographs. Together, these two cover simultaneously the full $390 \text{ nm} - 1700 \text{ nm}$ spectral range of the star being observed. The targeted cost for the installed LFAST telescope and fiber array is $\$60\text{M}$.

Photon buckets work and are cheap

29 August 2022

LFAST, the Large Fiber Array Spectroscopic Telescope

Roger Angel, Chad Bender, Joel Berkson, Nick Didato, John Ford, Peter Gray, Buell Jannuzi, Dean Ketelsen, Daewook Kim, Gilberto Chavez Lopez, Andrew Monson, Chang-Jin Oh, Jason Patrou, Matthew Rademacher, Christian Schwab, Melanie Sisco, Rich Wortley, Andrew Young

[Author Affiliations +](#)

Proceedings Volume 12182, Ground-based and Airborne Telescopes IX; 121821U (2022)

<https://doi.org/10.1117/12.2629655>

Event: [SPIE Astronomical Telescopes + Instrumentation](#), 2022, Montréal, Québec, Canada

Abstract

The LFAST concept is to use thousands of small telescopes combined by fibers for high resolution ($R=150,000$) spectroscopy, in a way that will realize large cost savings and lead to an affordable aperture as large as $20,000 \text{ m}^2$. Such large aperture is needed, for example, to make a comprehensive search for biosignatures in the atmospheres of transiting exoplanets. Each unit telescope of 0.76 m aperture (0.43 m^2) will focus the image of a single star onto a small ($17 \text{ }\mu\text{m}$ core) fiber, subtending 1.32 arcsec . Our telescope design calls for a spherical mirror, with a 4-lens assembly at prime focus that corrects not only for spherical aberration, but also for atmospheric dispersion down to 30° elevation, from $390 \text{ nm} - 1700 \text{ nm}$, and for rapid image motion caused by seeing or wind jitter. A method for rapid production of such mirrors has been tested, in which a disc of borosilicate float glass is slumped over a high-precision polished mandrel to an accuracy that greatly reduces subsequent optical finishing time. A method for active thermal control of mirror figure using Peltier devices will be incorporated. The projected cost of each unit telescope, when mass produced by the thousand, would then be approximately $\$8,000$. The telescopes will be mounted in the open in groups of 20 located 12 m apart. The mirrors will be arrayed on either side of a central, pedestal-mounted alt-az drive using commercial worm gear bearings. Protection against rain and dust will be provided by automated covers above and below the mirrors, and by pointing the mirrors down (-20° elevation). The first LFAST array, some 150 m in diameter, will comprise 132 mounts carrying a total of 2,640 mirrors and having $1,200 \text{ m}^2$ in collecting area. The light from all the fibers is combined at the central spectrographs, with little increase in etendue, by a 5×528 array of adjacent hexagonal lenses. A telecentric lens is used to reimage the lens array at the entrance slits of two echelle spectrographs. Together, these two cover simultaneously the full $390 \text{ nm} - 1700 \text{ nm}$ spectral range of the star being observed. The targeted cost for the installed LFAST telescope and fiber array is $\$60\text{M}$.

Photon buckets work and are cheap

29 August 2022

LFAST, the Large Fiber Array Spectroscopic Telescope

Roger Angel, Chad Bender, Joel Berkson, Nick Didato, John Ford, Peter Gray, Buell Jannuzi, Dean Ketelsen, Daewook Kim, Gilberto Chavez Lopez, Andrew Monson, Chang-Jin Oh, Jason Patrou, Matthew Rademacher, Christian Schwab, Melanie Sisco, Rich Wortley, Andrew Young

[Author Affiliations +](#)

Proceedings Volume 12182, Ground-based and Airborne Telescopes IX; 121821U (2022)

<https://doi.org/10.1117/12.2629655>

Event: [SPIE Astronomical Telescopes + Instrumentation](#), 2022, Montréal, Québec, Canada

Abstract

The LFAST concept is to use thousands of small telescopes combined by fibers for high resolution ($R=150,000$) spectroscopy, in a way that will realize large cost savings and lead to an affordable aperture as large as $20,000 \text{ m}^2$. Such large aperture is needed, for example, to make a comprehensive search for biosignatures in the atmospheres of transiting exoplanets. Each unit telescope of 0.76 m aperture (0.43 m^2) will focus the image of a single star onto a small ($17 \text{ }\mu\text{m}$ core) fiber, subtending 1.32 arcsec . Our telescope design calls for a spherical mirror, with a 4-lens assembly at prime focus that corrects not only for spherical aberration, but also for atmospheric dispersion down to 30° elevation, from $390 \text{ nm} - 1700 \text{ nm}$, and for rapid image motion caused by seeing or wind jitter. A method for rapid production of such mirrors has been tested, in which a disc of borosilicate float glass is slumped over a high-precision polished mandrel to an accuracy that greatly reduces subsequent optical finishing time. A method for active thermal control of mirror figure using Peltier devices will be incorporated. The projected cost of each unit telescope, when mass produced by the thousand, would then be approximately $\$8,000$. The telescopes will be mounted in the open in groups of 20 located 12 m apart. The mirrors will be arrayed on either side of a central, pedestal-mounted alt-az drive using commercial worm gear bearings. Protection against rain and dust will be provided by automated covers above and below the mirrors, and by pointing the mirrors down (-20° elevation). The first LFAST array, some 150 m in diameter, will comprise 132 mounts carrying a total of 2,640 mirrors and having $1,200 \text{ m}^2$ in collecting area. The light from all the fibers is combined at the central spectrographs, with little increase in etendue, by a 5×528 array of adjacent hexagonal lenses. A telecentric lens is used to reimage the lens array at the entrance slits of two echelle spectrographs. Together, these two cover simultaneously the full $390 \text{ nm} - 1700 \text{ nm}$ spectral range of the star being observed. The targeted cost for the installed LFAST telescope and fiber array is $\$60\text{M}$.

$1,200 \text{ m}^2$

Photon buckets work and are cheap

29 August 2022

LFAST, the Large Fiber Array Spectroscopic Telescope

Roger Angel, Chad Bender, Joel Berkson, Nick Didato, John Ford, Peter Gray, Buell Jannuzi, Dean Ketelsen, Daewook Kim, Gilberto Chavez Lopez, Andrew Monson, Chang-Jin Oh, Jason Patrou, Matthew Rademacher, Christian Schwab, Melanie Sisco, Rich Wortley, Andrew Young

[Author Affiliations +](#)

Proceedings Volume 12182, Ground-based and Airborne Telescopes IX; 121821U (2022)

<https://doi.org/10.1117/12.2629655>

Event: [SPIE Astronomical Telescopes + Instrumentation](#), 2022, Montréal, Québec, Canada

Abstract

The LFAST concept is to use thousands of small telescopes combined by fibers for high resolution ($R=150,000$) spectroscopy, in a way that will realize large cost savings and lead to an affordable aperture as large as $20,000 \text{ m}^2$. Such large aperture is needed, for example, to make a comprehensive search for biosignatures in the atmospheres of transiting exoplanets. Each unit telescope of 0.76 m aperture (0.43 m^2) will focus the image of a single star onto a small ($17 \text{ }\mu\text{m}$ core) fiber, subtending 1.32 arcsec . Our telescope design calls for a spherical mirror, with a 4-lens assembly at prime focus that corrects not only for spherical aberration, but also for atmospheric dispersion down to 30° elevation, from $390 \text{ nm} - 1700 \text{ nm}$, and for rapid image motion caused by seeing or wind jitter. A method for rapid production of such mirrors has been tested, in which a disc of borosilicate float glass is slumped over a high-precision polished mandrel to an accuracy that greatly reduces subsequent optical finishing time. A method for active thermal control of mirror figure using Peltier devices will be incorporated. The projected cost of each unit telescope, when mass produced by the thousand, would then be approximately $\$8,000$. The telescopes will be mounted in the open in groups of 20 located 12 m apart. The mirrors will be arrayed on either side of a central, pedestal-mounted alt-az drive using commercial worm gear bearings. Protection against rain and dust will be provided by automated covers above and below the mirrors, and by pointing the mirrors down (-20° elevation). The first LFAST array, some 150 m in diameter, will comprise 132 mounts carrying a total of 2,640 mirrors and having $1,200 \text{ m}^2$ in collecting area. The light from all the fibers is combined at the central spectrographs, with little increase in etendue, by a 5×528 array of adjacent hexagonal lenses. A telecentric lens is used to reimage the lens array at the entrance slits of two echelle spectrographs. Together, these two cover simultaneously the full $390 \text{ nm} - 1700 \text{ nm}$ spectral range of the star being observed. The targeted cost for the installed LFAST telescope and fiber array is $\$60\text{M}$.

$1,200 \text{ m}^2$

$\$60\text{M}$

Photon buckets work and are cheap

29 August 2022

LFAST, the Large Fiber Array Spectroscopic Telescope

Roger Angel, Chad Bender, Joel Berkson, Nick Didato, John Ford, Peter Gray, Buell Jannuzi, Dean Ketelsen, Daewook Kim, Gilberto Chavez Lopez, Andrew Monson, Chang-Jin Oh, Jason Patrou, Matthew Rademacher, Christian Schwab, Melanie Sisco, Rich Wortley, Andrew Young

[Author Affiliations +](#)

Proceedings Volume 12182, Ground-based and Airborne Telescopes IX; 121821U (2022)

<https://doi.org/10.1117/12.2629655>

Event: [SPIE Astronomical Telescopes + Instrumentation](#), 2022, Montréal, Québec, Canada

Abstract

The LFAST concept is to use thousands of small telescopes combined by fibers for high resolution ($R=150,000$) spectroscopy, in a way that will realize large cost savings and lead to an affordable aperture as large as $20,000 \text{ m}^2$. Such large aperture is needed, for example, to make a comprehensive search for biosignatures in the atmospheres of transiting exoplanets. Each unit telescope of 0.76 m aperture (0.43 m^2) will focus the image of a single star onto a small ($17 \text{ }\mu\text{m}$ core) fiber, subtending 1.32 arcsec . Our telescope design calls for a spherical mirror, with a 4-lens assembly at prime focus that corrects not only for spherical aberration, but also for atmospheric dispersion down to 30° elevation, from $390 \text{ nm} - 1700 \text{ nm}$, and for rapid image motion caused by seeing or wind jitter. A method for rapid production of such mirrors has been tested, in which a disc of borosilicate float glass is slumped over a high-precision polished mandrel to an accuracy that greatly reduces subsequent optical finishing time. A method for active thermal control of mirror figure using Peltier devices will be incorporated. The projected cost of each unit telescope, when mass produced by the thousand, would then be approximately $\$8,000$. The telescopes will be mounted in the open in groups of 20 located 12 m apart. The mirrors will be arrayed on either side of a central, pedestal-mounted alt-az drive using commercial worm gear bearings. Protection against rain and dust will be provided by automated covers above and below the mirrors, and by pointing the mirrors down (-20° elevation). The first LFAST array, some 150 m in diameter, will comprise 132 mounts carrying a total of 2,640 mirrors and having $1,200 \text{ m}^2$ in collecting area. The light from all the fibers is combined at the central spectrographs, with little increase in etendue, by a 5×528 array of adjacent hexagonal lenses. A telecentric lens is used to reimage the lens array at the entrance slits of two echelle spectrographs. Together, these two cover simultaneously the full $390 \text{ nm} - 1700 \text{ nm}$ spectral range of the star being observed. The targeted cost for the installed LFAST telescope and fiber array is $\$60\text{M}$.

nature astronomy

[Explore content](#) [About the journal](#) [Publish with us](#)

[nature](#) > [nature astronomy](#) > [letters](#) > [article](#)

Letter | Published: 20 July 2020

Demonstration of stellar intensity interferometry with the four VERITAS telescopes

[A. U. Abeysekara](#), [W. Benbow](#), [A. Brill](#), [J. H. Buckley](#), [J. L. Christiansen](#), [A. J. Chromey](#), [M. K. Daniel](#), [J. Davis](#), [A. Falcone](#), [Q. Feng](#), [J. P. Finley](#), [L. Fortson](#), [A. Furniss](#), [A. Gent](#), [C. Giuri](#), [O. Gueta](#), [D. Hanna](#), [T. Hassan](#), [O. Hervet](#), [J. Holder](#), [G. Hughes](#), [T. B. Humensky](#), [P. Kaaret](#), [M. Kertzman](#), ... [T. J. Williamson](#)

[+ Show authors](#)

[Nature Astronomy](#) **4**, 1164–1169 (2020) | [Cite this article](#)

1322 Accesses | **29** Citations | **73** Altmetric | [Metrics](#)

$1,200 \text{ m}^2$

$\$60\text{M}$

Photon buckets work and are cheap

29 August 2022

LFAST, the Large Fiber Array Spectroscopic Telescope

Roger Angel, Chad Bender, Joel Berkson, Nick Didato, John Ford, Peter Gray, Buell Jannuzi, Dean Ketelsen, Daewook Kim, Gilberto Chavez Lopez, Andrew Monson, Chang-Jin Oh, Jason Patrou, Matthew Rademacher, Christian Schwab, Melanie Sisco, Rich Wortley, Andrew Young

[Author Affiliations +](#)

Proceedings Volume 12182, Ground-based and Airborne Telescopes IX; 121821U (2022)

<https://doi.org/10.1117/12.2629655>

Event: [SPIE Astronomical Telescopes + Instrumentation](#), 2022, Montréal, Québec, Canada

Abstract

The LFAST concept is to use thousands of small telescopes combined by fibers for high resolution ($R=150,000$) spectroscopy, in a way that will realize large cost savings and lead to an affordable aperture as large as $20,000 \text{ m}^2$. Such large aperture is needed, for example, to make a comprehensive search for biosignatures in the atmospheres of transiting exoplanets. Each unit telescope of 0.76 m aperture (0.43 m^2) will focus the image of a single star onto a small ($17 \text{ }\mu\text{m}$ core) fiber, subtending 1.32 arcsec . Our telescope design calls for a spherical mirror, with a 4-lens assembly at prime focus that corrects not only for spherical aberration, but also for atmospheric dispersion down to 30° elevation, from $390 \text{ nm} - 1700 \text{ nm}$, and for rapid image motion caused by seeing or wind jitter. A method for rapid production of such mirrors has been tested, in which a disc of borosilicate float glass is slumped over a high-precision polished mandrel to an accuracy that greatly reduces subsequent optical finishing time. A method for active thermal control of mirror figure using Peltier devices will be incorporated. The projected cost of each unit telescope, when mass produced by the thousand, would then be approximately $\$8,000$. The telescopes will be mounted in the open in groups of 20 located 12 m apart. The mirrors will be arrayed on either side of a central, pedestal-mounted alt-az drive using commercial worm gear bearings. Protection against rain and dust will be provided by automated covers above and below the mirrors, and by pointing the mirrors down (-20° elevation). The first LFAST array, some 150 m in diameter, will comprise 132 mounts carrying a total of 2,640 mirrors and having $1,200 \text{ m}^2$ in collecting area. The light from all the fibers is combined at the central spectrographs, with little increase in etendue, by a 5×528 array of adjacent hexagonal lenses. A telecentric lens is used to reimage the lens array at the entrance slits of two echelle spectrographs. Together, these two cover simultaneously the full $390 \text{ nm} - 1700 \text{ nm}$ spectral range of the star being observed. The targeted cost for the installed LFAST telescope and fiber array is $\$60\text{M}$.

nature astronomy

[Explore content](#) [About the journal](#) [Publish with us](#)

[nature](#) > [nature astronomy](#) > [letters](#) > [article](#)

Letter | Published: 20 July 2020

Demonstration of stellar intensity interferometry with the four VERITAS telescopes

[A. U. Abeysekara](#), [W. Benbow](#), [A. Brill](#), [J. H. Buckley](#), [J. L. Christiansen](#), [A. J. Chromey](#), [M. K. Daniel](#), [J. Davis](#), [A. Falcone](#), [Q. Feng](#), [J. P. Finley](#), [L. Fortson](#), [A. Furniss](#), [A. Gent](#), [C. Giuri](#), [O. Gueta](#), [D. Hanna](#), [T. Hassan](#), [O. Hervet](#), [J. Holder](#), [G. Hughes](#), [T. B. Humensky](#), [P. Kaaret](#), [M. Kertzman](#), ... [T. J. Williamson](#)

[+ Show authors](#)

[Nature Astronomy](#) **4**, 1164–1169 (2020) | [Cite this article](#)

1322 Accesses | **29** Citations | **73** Altmetric | [Metrics](#)

Uses Chereknov array

$1,200 \text{ m}^2$

$\$60\text{M}$

Photon buckets work and are cheap

29 August 2022

LFAST, the Large Fiber Array Spectroscopic Telescope

Roger Angel, Chad Bender, Joel Berkson, Nick Didato, John Ford, Peter Gray, Buell Jannuzi, Dean Ketelsen, Daewook Kim, Gilberto Chavez Lopez, Andrew Monson, Chang-Jin Oh, Jason Patrou, Matthew Rademacher, Christian Schwab, Melanie Sisco, Rich Wortley, Andrew Young

[Author Affiliations +](#)

Proceedings Volume 12182, Ground-based and Airborne Telescopes IX; 121821U (2022)

<https://doi.org/10.1117/12.2629655>

Event: [SPIE Astronomical Telescopes + Instrumentation](#), 2022, Montréal, Québec, Canada

Abstract

The LFAST concept is to use thousands of small telescopes combined by fibers for high resolution ($R=150,000$) spectroscopy, in a way that will realize large cost savings and lead to an affordable aperture as large as $20,000 \text{ m}^2$. Such large aperture is needed, for example, to make a comprehensive search for biosignatures in the atmospheres of transiting exoplanets. Each unit telescope of 0.76 m aperture (0.43 m^2) will focus the image of a single star onto a small ($17 \text{ }\mu\text{m}$ core) fiber, subtending 1.32 arcsec . Our telescope design calls for a spherical mirror, with a 4-lens assembly at prime focus that corrects not only for spherical aberration, but also for atmospheric dispersion down to 30° elevation, from $390 \text{ nm} - 1700 \text{ nm}$, and for rapid image motion caused by seeing or wind jitter. A method for rapid production of such mirrors has been tested, in which a disc of borosilicate float glass is slumped over a high-precision polished mandrel to an accuracy that greatly reduces subsequent optical finishing time. A method for active thermal control of mirror figure using Peltier devices will be incorporated. The projected cost of each unit telescope, when mass produced by the thousand, would then be approximately $\$8,000$. The telescopes will be mounted in the open in groups of 20 located 12 m apart. The mirrors will be arrayed on either side of a central, pedestal-mounted alt-az drive using commercial worm gear bearings. Protection against rain and dust will be provided by automated covers above and below the mirrors, and by pointing the mirrors down (-20° elevation). The first LFAST array, some 150 m in diameter, will comprise 132 mounts carrying a total of 2,640 mirrors and having $1,200 \text{ m}^2$ in collecting area. The light from all the fibers is combined at the central spectrographs, with little increase in etendue, by a 5×528 array of adjacent hexagonal lenses. A telecentric lens is used to reimage the lens array at the entrance slits of two echelle spectrographs. Together, these two cover simultaneously the full $390 \text{ nm} - 1700 \text{ nm}$ spectral range of the star being observed. The targeted cost for the installed LFAST telescope and fiber array is $\$60\text{M}$.

nature astronomy

[Explore content](#) [About the journal](#) [Publish with us](#)

[nature](#) > [nature astronomy](#) > [letters](#) > [article](#)

Letter | Published: 20 July 2020

Demonstration of stellar intensity interferometry with the four VERITAS telescopes

[A. U. Abeysekara](#), [W. Benbow](#), [A. Brill](#), [J. H. Buckley](#), [J. L. Christiansen](#), [A. J. Chromey](#), [M. K. Daniel](#), [J. Davis](#), [A. Falcone](#), [Q. Feng](#), [J. P. Finley](#), [L. Fortson](#), [A. Furniss](#), [A. Gent](#), [C. Giuri](#), [O. Gueta](#), [D. Hanna](#), [T. Hassan](#), [O. Hervet](#), [J. Holder](#), [G. Hughes](#), [T. B. Humensky](#), [P. Kaaret](#), [M. Kertzman](#), ... [T. J. Williamson](#)

[+ Show authors](#)

Nature Astronomy **4**, 1164–1169 (2020) | [Cite this article](#)

1322 Accesses | 29 Citations | 73 Altmetric | [Metrics](#)

Uses Chereknov array

JOURNAL ARTICLE

Spatial intensity interferometry on three bright stars FREE

[W Guerin](#) ✉, [J-P Rivet](#) ✉, [M Fouché](#), [G Labeyrie](#), [D Vernet](#), [F Vakili](#), [R Kaiser](#)

Monthly Notices of the Royal Astronomical Society, Volume 480, Issue 1, October 2018, Pages 245–250, <https://doi.org/10.1093/mnras/sty1792>

Published: 06 July 2018 [Article history](#)

$1,200 \text{ m}^2$

$\$60\text{M}$

Photon buckets work and are cheap

29 August 2022

LFAST, the Large Fiber Array Spectroscopic Telescope

Roger Angel, Chad Bender, Joel Berkson, Nick Didato, John Ford, Peter Gray, Buell Jannuzi, Dean Ketelsen, Daewook Kim, Gilberto Chavez Lopez, Andrew Monson, Chang-Jin Oh, Jason Patrou, Matthew Rademacher, Christian Schwab, Melanie Sisco, Rich Wortley, Andrew Young

[Author Affiliations +](#)

Proceedings Volume 12182, Ground-based and Airborne Telescopes IX; 121821U (2022)

<https://doi.org/10.1117/12.2629655>

Event: [SPIE Astronomical Telescopes + Instrumentation](#), 2022, Montréal, Québec, Canada

Abstract

The LFAST concept is to use thousands of small telescopes combined by fibers for high resolution ($R=150,000$) spectroscopy, in a way that will realize large cost savings and lead to an affordable aperture as large as $20,000 \text{ m}^2$. Such large aperture is needed, for example, to make a comprehensive search for biosignatures in the atmospheres of transiting exoplanets. Each unit telescope of 0.76 m aperture (0.43 m^2) will focus the image of a single star onto a small ($17 \text{ }\mu\text{m}$ core) fiber, subtending 1.32 arcsec . Our telescope design calls for a spherical mirror, with a 4-lens assembly at prime focus that corrects not only for spherical aberration, but also for atmospheric dispersion down to 30° elevation, from $390 \text{ nm} - 1700 \text{ nm}$, and for rapid image motion caused by seeing or wind jitter. A method for rapid production of such mirrors has been tested, in which a disc of borosilicate float glass is slumped over a high-precision polished mandrel to an accuracy that greatly reduces subsequent optical finishing time. A method for active thermal control of mirror figure using Peltier devices will be incorporated. The projected cost of each unit telescope, when mass produced by the thousand, would then be approximately $\$8,000$. The telescopes will be mounted in the open in groups of 20 located 12 m apart. The mirrors will be arrayed on either side of a central, pedestal-mounted alt-az drive using commercial worm gear bearings. Protection against rain and dust will be provided by automated covers above and below the mirrors, and by pointing the mirrors down (-20° elevation). The first LFAST array, some 150 m in diameter, will comprise 132 mounts carrying a total of 2,640 mirrors and having $1,200 \text{ m}^2$ in collecting area. The light from all the fibers is combined at the central spectrographs, with little increase in etendue, by a 5×528 array of adjacent hexagonal lenses. A telecentric lens is used to reimage the lens array at the entrance slits of two echelle spectrographs. Together, these two cover simultaneously the full $390 \text{ nm} - 1700 \text{ nm}$ spectral range of the star being observed. The targeted cost for the installed LFAST telescope and fiber array is $\$60\text{M}$.

nature astronomy

[Explore content](#) [About the journal](#) [Publish with us](#)

[nature](#) > [nature astronomy](#) > [letters](#) > [article](#)

Letter | Published: 20 July 2020

Demonstration of stellar intensity interferometry with the four VERITAS telescopes

[A. U. Abeysekara](#), [W. Benbow](#), [A. Brill](#), [J. H. Buckley](#), [J. L. Christiansen](#), [A. J. Chromey](#), [M. K. Daniel](#), [J. Davis](#), [A. Falcone](#), [Q. Feng](#), [J. P. Finley](#), [L. Fortson](#), [A. Furniss](#), [A. Gent](#), [C. Giuri](#), [O. Gueta](#), [D. Hanna](#), [T. Hassan](#), [O. Hervet](#), [J. Holder](#), [G. Hughes](#), [T. B. Humensky](#), [P. Kaaret](#), [M. Kertzman](#), ... [T. J. Williamson](#)

[+ Show authors](#)

Nature Astronomy **4**, 1164–1169 (2020) | [Cite this article](#)

1322 Accesses | 29 Citations | 73 Altmetric | [Metrics](#)

Uses Chereknov array

JOURNAL ARTICLE

Spatial intensity interferometry on three bright stars FREE

[W Guerin](#) , [J-P Rivet](#) , [M Fouché](#), [G Labeyrie](#), [D Vernet](#), [F Vakili](#), [R Kaiser](#)

Monthly Notices of the Royal Astronomical Society, Volume 480, Issue 1, October 2018, Pages 245–250, <https://doi.org/10.1093/mnras/sty1792>

Published: 06 July 2018 [Article history](#)

Uses modern photodetectors

$1,200 \text{ m}^2$

$\$60\text{M}$

SPADs can be bought commercially

hamamatsu.com

HAMAMATSU PHOTON IS OUR BUSINESS

Products Applications Why Hamamatsu? Resources Support Our company Investors

USA

Product lineup Related documents

8 products

Clear all filter Column settings A A

Part no.		Data Sheet	Product Name		Wavelength type		Built-in sensor		Effective photosensitive area		Spectral response range		Output		Note		Contact
Sort	Filter		Sort	Filter	Sort	Filter	Sort	Filter	Sort	Filter	Sort	Filter	Sort	Filter	Sort	Filter	
	C11202-050		SPAD module		VIS		SPAD		φ50 μm		320 to 900 nm		Digital		--		
	C11202-100		SPAD module		VIS		SPAD		φ100 μm		320 to 900 nm		Digital		--		
	C13001-01		SPAD module		VIS		SPAD		-		370 to 900 nm		Digital		Fiber coupling type		
	C14076-01		SPAD module		VIS		SPAD		-		370 to 900 nm		Digital		Fiber coupling type		
	C16531-050GD		SPAD module		VIS to NIR		SPAD		φ50 μm		400 to 1000 nm		Digital		--		
	C16531-100GD		SPAD module		VIS to NIR		SPAD		φ100 μm		400 to 1000 nm		Digital		--		
	C16533-050GD		SPAD module		VIS to NIR		SPAD		-		400 to 1000 nm		Digital		Fiber coupling type		
	C16534-050GD		SPAD module		VIS to NIR		SPAD		-		400 to 1000 nm		Digital		Fiber coupling type		